

**NASA TECHNICAL
TRANSLATION**

NASA TT F-246



NASA TT F-246

U.S. AIR FORCE
AFHQ, WASHINGTON
D.C. 20330-5000

0068707



TECH LIBRARY KAFB, NM

ATMOSPHERIC TURBULENCE

N. Z. Pinus, Editor in Chief

*Trudy Tsentral'noy Aerologicheskoy Observatorii, No. 54,
Hydrometeorological Publishing House, Moscow, 1964.*





ATMOSPHERIC TURBULENCE

N. Z. Pinus, Editor in Chief

Translation of "Atmosfernaya turbulentnost'."
Trudy Tsentral'noy Aerologicheskoy Observatorii,
No. 54, Gidrometeorologicheskoye Izdatel'stvo, Moscow, 1964.

NATIONAL AERONAUTICS AND SPACE ADMINISTRATION

For sale by the Clearinghouse for Federal Scientific and Technical Information
Springfield, Virginia 22151 - Price \$4.00

TABLE OF CONTENTS

	Page
Some Results of the Experimental Investigations of the Atmospheric Turbulence Using Radiosondes V. P. Belyayev, T. G. Beltadze, V. P. Litovchenko, V. D. Litvinova, V. P. Lominadze, N. Z. Pinus, Ye. M. Sofiyev and G. N. Shur	1
The Turbulence in Jetstreams in the Clear Sky A. A. Reshchikova	66
Application of the Boundary Layer Method to the Determination of the Parameters of Turbulence in the Free Atmosphere V. A. Shnaydman	85
Turbulence in the Proximity of Jetstreams T. P. Krupchatnikova	95
Some Results of the Determination of Turbulence Characteristics in Jetstreams V. D. Litvinova	103
Application of a Thermoanemometer on an Aircraft N. K. Vinnichenko	109

ANNOTATION

This collection is concerned with the work conducted at the Atmospheric Dynamics Laboratory, Central Aerological Observatory, 1961-1962.

One of the articles describes the method and the apparatus for measuring the turbulence of the free atmosphere by means of radiosondes as well as the results of measurements in the troposphere and in the lower stratosphere. Three articles deal with the calculations of the turbulence in the proximity of the jetstream from the data obtained in temperature-wind probing of the atmosphere. One article is concerned with turbulence and jetstreams in the clear sky from the data of flight experiments on the TU-104 airplane equipped with special scientific apparatus. The last article deals with the methods for measuring fluctuations of the horizontal component of wind velocity by means of an airplane thermoanemometer.

This collection is designed for specialists in the physics of the atmosphere and in aerodynamics, and for persons who are associated with the organization and the performance of airplane flights.

SOME RESULTS OF THE EXPERIMENTAL INVESTIGATIONS OF THE ATMOSPHERIC TURBULENCE USING RADIOSONDES

V. P. Belyayev, T. G. Beltadze, V. P. Litovchenko, V. D. Litvinova,
V. P. Lominadze, N. Z. Pinus, Ye. M. Sofiyev and G. N. Shur

ABSTRACT

The method and the apparatus for measuring atmospheric turbulences using radiosondes are described. The results of the theoretical and of the experimental investigations of the method as well as the turbulence characteristics over Moscow, Sukhumi and Tashkent are given. From annual observations over the Moscow region, the distribution of turbulence along the altitude and its seasonal variations, the data on the thickness of the turbulent layers, and on the stability of the turbulent zone as a function of time are given. The relationship between turbulence, the vertical temperature gradients and wind velocity are considered.

Introduction

Experimental studies of turbulence in the free air are currently being conducted using various methods. The most widespread are those in which the measuring instrument is an airplane on which is mounted an accelerometer (Refs. 5, 20).

The measurements taken using this method have helped in obtaining some interesting data on the structure of atmospheric turbulence (Refs. 13, 20), specifically, on the repetition of turbulences at different altitudes, the sizes of turbulence zones, the nature of turbulence at the zone boundaries, the velocities of vertical air blasts, the energy distribution in the turbulence spectrum, etc. However, such investigations of atmospheric turbulence are expensive experiments; in addition, they are limited in altitude by the ceiling on airplane flights, and cannot provide operational accumulation of data over a large territory.

In relation to the development of aviation technology, it became necessary to obtain the turbulence data to altitudes of 25-30 km. The most appropriate method would be the construction of a turbulence--measuring radiosonde which would be applicable for use at the network points of aerological observations.

In the development of such a radiosonde, one can make use of the principles of measurement (Ref. 5). The first method is the measurement of the mean absolute and the mean relative vertical velocity of the sounding balloon in a given layer. The vector difference of these velocities gives the magnitude of the mean velocity and the direction of the vertical motion of air in that layer. This method was well-developed and was used at the Central Aerological Observatory (CAO) by P. F. Zaychikov (Refs. 4, 5). The second method, proposed by Junge (Ref. 21), consists of the measurement of the instantaneous shifts of the registering balloon when it enters the turbulent layers of the atmosphere.

In the Atmospheric Dynamics Laboratory of the Central Aerological Observatory work was conducted from 1954 to 1956, on the development of shift-measuring sounding instruments. Two types of apparatus were developed: an autonomous instrument for measuring turbulence (ZIT), and a shift-measuring attachment for the radiosonde RZ-049. Both of these instruments are accelerometers. The autonomous, turbulence-measuring instrument was developed by Ye. A. Besyadovskiy and G. N. Shur, and is described in Ref. 5. The data on the shifts of the recording balloon were transmitted on a special channel and were recorded on a motion picture film by a special radio receiver which was equipped with a panoramic attachment and a motion picture camera.

In 1956 work on these instruments was terminated because the short-wave range used for the transmission of turbulence data had by 1956 become so saturated with transmitting stations of different designations that reliable reception was limited to the low altitudes of the sounding balloon (approximately 5 km); each launching of a ZIT instrument was too expensive for obtaining only the lower troposphere data.

During that period, work on a theoretical foundation of this method was also conducted. For example, S. M. Shmeter solved the problem on the motion of a balloon in an accelerated stream of an ideal and of a real fluid (Ref. 19). It was shown that the acceleration of the sounding balloon corresponds quite well to the acceleration of the vertical air blasts.

In 1960 the Atmospheric Dynamics Laboratory renewed its work on the development of a radiosonde with an accelerometer attached. V. P. Belyayev and G. N. Shur (Ref. 2) were able to develop the apparatus for obtaining data on atmospheric turbulence using a serial production radiosonde, A-22-III, furnished with a special accelerometric attachment. The signals caused by the turbulence are transmitted continuously on the same ultrashortwave band as the code signals of the A-22-III radiosonde. They are received by the radiotheodolite "Malakhit" and are separated from the video signal of the receiver of the radiotheodolite by a specially constructed device. The radiosonde signals

of temperature, pressure and humidity of air at different altitudes are received simultaneously.

The synchronous measurement of the atmospheric turbulence with measurements of the principal atmospheric parameters--temperature, humidity, pressure, velocity and direction of wind--is an extremely important advantage of the developed method and apparatus.

It should be noted that in the United States a sounding device was also developed for measuring the atmospheric turbulence; however, it was not combined with a radiosonde and, therefore, it was incapable of giving synchronous data on the atmospheric turbulence and on the distribution of temperature and wind at high altitudes.

In 1961 work was completed on the development of terrestrial devices for receiving and recording turbulence signals from the radiosonde. At the same time, the production of accelerometer attachments to the A-22-III radiosonde was established and temporary instructions were drawn up on the observation procedure. In addition, terrestrial observation apparatus were constructed for the Transcaucasian and Mid-asiatic Hydrometeorological Scientific Research Institutes. The workers from these institutes were instructed in the preparation of radiosondes for launching, receiving, recording, and processing signals.

The Central Aerological Observatory organized the atmospheric turbulence observations in Moscow (Dolgoprudnoye), at the Transcaucasian Hydrometeorological Scientific Research Institute in Sukhumi, and at the Midasiatic Hydrometeorological Scientific Research Institute in Tashkent. In the course of 1961-62, there were 326 observations conducted in Moscow, 89 in Sukhumi, and 42 in Tashkent. More detailed information on the scope of observations is given in Chapter III.

CHAPTER I APPARATUS AND METHODS OF OBSERVATION

1. Brief Description of the Method of Measurement

When an ascending radiosonde enters the zone of perturbed air, the velocity of its ascension changes. From the accelerations of the radiosonde, it is possible to elucidate atmospheric turbulence.

The accelerometric method of measurement was used. In a normal accelerometer a weight, suspended on a spring, is displaced with respect to the body of the instrument under the influence of the acceleration. The sounding balloon, because of its small mass and large displacement, is easily carried away when it enters an accelerated airstream. At the same time the radiosonde itself is quite immovable compared to the balloon, as it has a small volume and a large mass. If a radiosonde is attached to the balloon on a spring, then when the balloon enters an accelerated airstream, the radiosonde will be displaced with respect to the balloon.

The magnitude of the initial displacement x_0 , corresponding to the stationary condition or uniform ascension of the balloon, may be determined from the following relationship:

$$kx_0 = Mg, \quad (1)$$

where k is the force constant for the spring, M is the mass of the load (radiosonde), and g is the acceleration due to gravity.

When the balloon changes its velocity, $dW/dt = a$, we have

$$M(g + a) = k(x_0 + \Delta x) \quad (2)$$

or

$$Ma = k \Delta x. \quad (3)$$

From which we obtain

$$\Delta x = \frac{M}{k} a \quad (4)$$

Thus, the displacement of the sensitive element of the shifting radiosonde, Δx , is a linear function of the acceleration, a , which acts on the balloon. Consequently, the problem is reduced to the measurement of Δx and transmission of the results of the measurements to earth. A number of difficulties arose, however, in the course of the development

of this method; it was first necessary to transmit the turbulence data and to maintain the same number of channels which serve for transmission of meteorological information; second, measurement of the acceleration and the transmission of this information to earth was required to be continuous.

The resistance of the grid leak (of a tube) in the radiosonde transmitter was chosen as a parameter whose value changed with the change of Δx . It was decided to replace the constant grid leak resistance by a potentiometer and to correlate its displacement with Δx .

In Ref. 2, the construction of the shift-measuring terrestrial devices for recording the accelerations of the balloon during ascension has been described in detail. However, in the utilization of the principle of measurement and recording of the self-modulation frequency of the transmitter there is a significant drawback. The terrestrial apparatus--the frequency detector--developed a voltage which was proportional to the frequency of the video signal. The frequency of the video signal changed not only during the shift of the balloon when it entered a blast of air, but also during the passage of code signals. During transition from a pulse to a pause, the frequency changed much more than during the entry of the balloon into a turbulent gust. In order to obtain reliable data on the turbulence, it was necessary to eliminate the pause artificially by eliminating one of the atmospheric parameters measured by the radiosonde, i.e., humidity. Consequently, it was necessary to arrange special launchings of such radiosondes, since in the operative sounding it was not possible to eliminate humidity measurement. Further development of this method required a development of a device which would be capable of receiving continuously the information on shifts of the balloon during ascension on the same channel as the code signals of the radiosonde, without exclusion of any of the usually recorded atmospheric parameters.

For this purpose, we first investigated the video signals of the radio transmitter. Various resistance values were assigned to the grid leak of the receiver, and certain parameters of the video signal were measured at the output of the radiotheodolite receiver, "Malakhit".

Figure 1 shows a graph of the dependence of video signal parameters on the change of load (change of the resistance of the grid leak). The abscissa corresponds to the load values, which are in a linear relationship to the resistance values of the grid leak. On the ordinate is represented the frequency of the video signal, f ; the period of tracking the impulse, T ; the duration of the impulse, τ ; and, the duty ratio, $S = T/\tau$.

It is apparent from the figure that during the passage of the code signals, i.e., during the passage from the signal to pause, all of the parameters of the video signal change except the duty ratio, which in

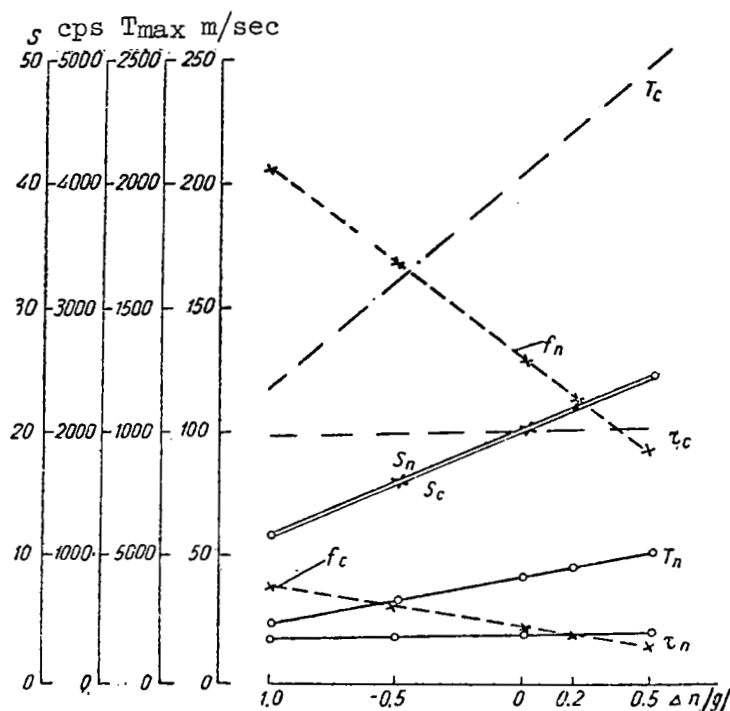


Figure 1. The graph showing the dependence of the parameters of video signals on shifts of the radiosonde

practice depends only on the change of load. The idea of the possibility of using the duty ratio was predicted by M. V. Krechmer.

If on the earth current pulses are formed in such a way that the frequency of repetition and the duration of these pulses correspond to the frequency and duration of the video signals, and the amplitude of the current remains constant, then the mean current value, measured by means of an inertia instrument, will correspond to the duty ratio of the video signal, and consequently the acceleration of the sounding balloon.

Thus, the outline of this method is reduced to the following.

- 1) Acceleration of the sounding balloon is transformed into a corresponding displacement of mass, Δx , of the sonde with respect to the mounting point.
- 2) The relative displacement, Δx , is converted into the change of the resistance of the grid leak of a transmitter tube.
- 3) The change of the resistance of the grid leak is transformed into the change of the duty ratio of the modulating impulse ΔS .

4) The radio transmitter emits the high frequency pulses of variable duty ratio.

5) The receiver of the radiotheodolite "Malakhit" emits a video signal of variable duty ratio.

6) Change of the duty ratio of the video signal is transformed into changes of the mean magnitude of current, $\Delta \bar{I}$, which in turn is recorded.

All of the apparatus used for obtaining the turbulence data may be separated into equipment for measurement and transmission of data, and the setup for receiving and recording the signals on the earth.

Figure 2 shows a block diagram of the whole apparatus. The equipment for the measurement and transmission of data consists of the shift pickup (1), the transmitter, PRB-1.5 (2), and radiosonde A-22 (3). This payload also serves the purpose of converting the shifts caused by the vertical updrafts into changes of the duty ratio of the radio frequency pulses of the transmitter, and the transmission of these data to the earth.

The terrestrial unit consists of the radiotheodolite, "Malakhit" (4), a device for measuring shifts of sonde (5), and a recorder (6). The terrestrial unit is designed for the reception of the signal of the radiosonde, for the isolation of the signals pertaining to the turbulence from the total flux of coded signals, and for the conversion of these signals and their recording on the chart of the recorder.

2. A Device for Measuring and Transmission of Data

A basic advantage of a transmitting device is the fact that through the use of a very simple and inexpensive attachment, an ordinary serial production radiosonde, A-22, becomes a shift-measuring radiosonde.

The mechanism of the shift-measuring attachment consists of a bracket, a potentiometer, a spiral spring, and a double pulley. The bracket is a duralumin plate, bent at a right angle, the lower part (the base) of which is bolted to the cover of the radiosonde. The potentiometer is mounted on the bracket. The double pulley in turn is mounted on the axis of the potentiometer. The small diameter pulley is connected with the upper end of the spiral spring, and the lower end of the spring is mounted to the base of the bracket. A rigid suspension is solidly mounted and turned several times on the large diameter pulley, and proceeds to the appendix of the balloon.

Thus, the balloon is connected to the radiosonde through the spring. The double pulley increases the sensitivity of the system to shifts, and

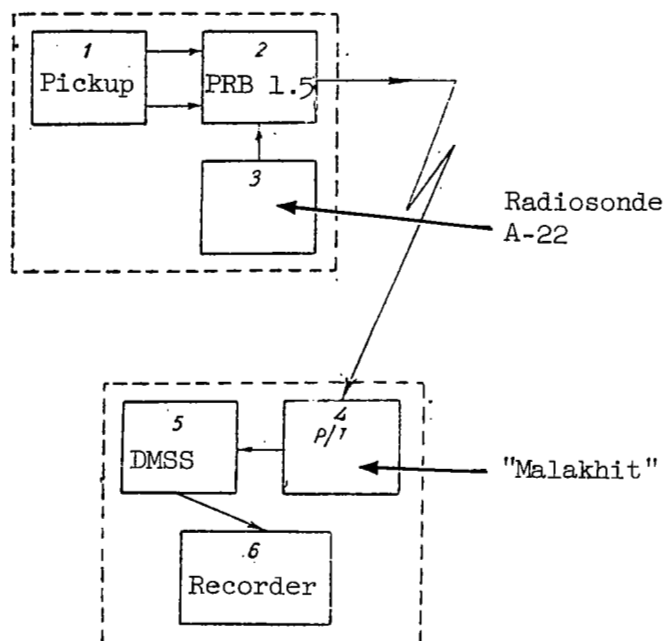


Figure 2. Block diagram of the system

the potentiometer becomes the link which converts the changes in the stretching of the spring into changes of resistance. The range of measurements of the instrument is determined by the strength of the spring and the potentiometer installation.

The potentiometer instead of the constant resistance is included in the grid leak of the radio transmitter and the sonde. It was already indicated above that changes of the resistance in the grid circuit of the transmitter lead to changes of the duty ratio of the radio frequency pulse. A detailed description of the transmitter is given in Ref. 2.

3. A Device for Receiving and Recording of Signals Due to Shifts

In order to receive radiosonde signals and in order to track the radiosonde along its angular coordinates, a "Malakhit" radiotheodolite is used. In the radiotheodolite receiver, conversion of the radio transmitter signal occurs. From the radio frequency pulse, it forms video pulses which are passed from the output of the radiotheodolite to the input of the device for measuring sonde shifts (DMSS).

Figure 3 shows a main circuit of the DMSS. A trigger with one stable state is assembled from the tube L_1 and L_2 (a dual triode 6N1P).

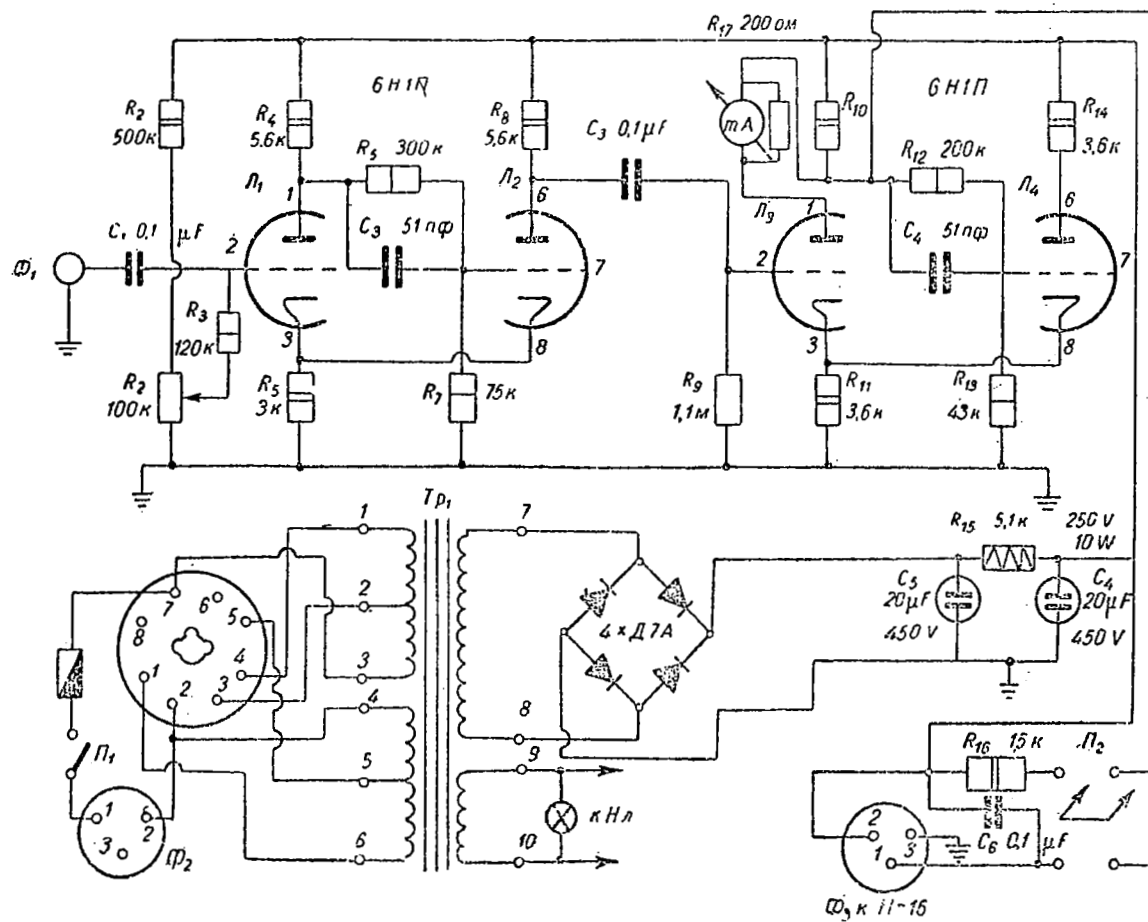


Figure 3. The principal circuit diagram of DMSS

Tube L_2 is open and carries a large current, thus producing a voltage drop across R_5 of the order of 50 v. The bias to the grid of the first tube is applied through a voltage divider R_1 and R_2 . The grid voltage of L_1 is selected to be such that it is 7-10 v lower than the unlocking threshold.

The grid voltage of L_2 is taken from the voltage dividers R_4 , R_6 and R_7 . In the absence of a signal, tube L_1 is locked, but currents flow through its plate and filament resistances. The second part of the circuit is assembled from tubes L_3 and L_4 , and is also a trigger circuit with one stable state. Contrary to the first trigger, the biasing at the input, i.e., at the grid of L_3 , is much greater than the unlocking threshold, and it comprises approximately 50 v. In addition the plate circuit of tube L_3 has a permanently installed visual indicator device, which shows the mean plate current. Since the amplitude of pulses on the grid of L_3 is constant, the mean current, which is measured by the visual instrument M-24, is proportional to the duty ratio of the input signal.

The plate circuit of tube L_3 contains some sort of recording milliammeter, such as N-16, for example, or a resistance, equal to the internal resistance of the recording instrument, connected in parallel to the resistance, R_{10} . The switching is conducted by means of a tumbler, P_2 .

The instrument is powered from a 50 cps ac line with 220, 127 and 110 v. The circuit is turned on by tumbler P_1 .

The circuit contains a power transformer, Tr_1 , and a rectifier, assembled from a two half-wave rectifier circuit from diodes D-7a.

In addition to tumblers P_1 and P_2 , the front panel of the instrument contains a signal level regulator, R_2 , a visual instrument, M-24, and a signal lamp, L_s . The back panel of the instrument contains the following jacks: F-1--input, F-2--power, and F-3--output.

Figure 4 is a diagram indicating voltages and currents at some of the points of the DMSS.

The video signal from the output of the "Malakhit" radiotheodolite is carried to jack F-1, and through capacitor C-1 to grid L_1 (on the circuit the video signal is represented as U_{imp}). If the amplitude of U_{imp} (Figure 4a) at some time, t_1 , exceeds 10-15 v, then a tube L_1 will be opened and will remain open until the grid voltage of L_1 will exceed the opening threshold-- U_{thr} . When L_1 opens, the potential on its plate

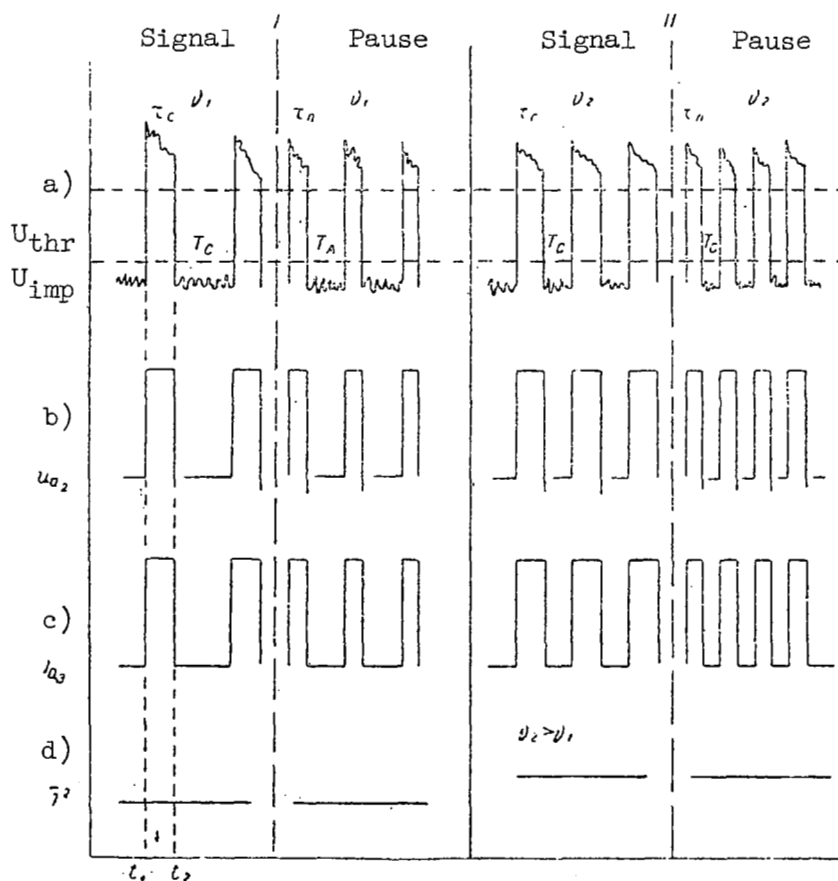


Figure 4. The diagram showing voltages and currents at some of the points of the DMSS

drops, and, consequently, the voltage drops on the grid of L_2 . Since the voltage drop across R_5 is maintained due to the plate current of R_1 , L_2 will lock and will remain locked as long as L_1 is open, i.e., until time t_2 . After the potential on the grid of the first tube U_{imp} drops below the unlocking threshold, the circuit will return to the original state until the arrival of the following video impulse. Thus, (in Figure 4b) at the output of trigger I (plate of L_2), positive voltage pulses of standard amplitude are developed (about 100 v), the frequency and the duration of which correspond to the frequency and the duration of the video signals. The second trigger, based on tubes L_3 and L_4 , operates in a similar manner.

The current pulses in the plate circuit of L_3 (Figure 4c) have the same duration and frequency as the video signals. The plate circuit of L_3 contains a visual instrument and a recorder which measure the mean³ current \bar{I} :

$$\bar{I} = kA \frac{\tau}{T} = kA \frac{1}{S} = kA \Theta, \quad (5)$$

where τ is the duration of the pulse; T is the tracking period; A is the amplitude of the current pulse; S equals T/τ is the duty ratio; Θ equals $1/S$; and, k is a constant.

During the passage of code signals, the frequency and duration of the video pulses change, but at the same time the duty ratio, as was shown in Figure 1, remains constant (Figure 4d). The indications of the visual instrument do not change and the recorder displays a straight line. If the duty ratio of the video signal changes (Figure 4II), the mean current value also changes; this change is indicated by the visual instrument and the recorder.

In our work we used N-16, N-370 and K4-51 recorders; however, any recording milliammeter may be used. The most favorable chart speed was 0.5 mm/sec. The mean output current of the DMSS did not exceed 3 ma.

The DMSS circuit was assembled for work with the N-16 recorder, the internal resistance of which is 1500 ohms.

When working with other recorders it was necessary to match their internal resistance with the mounter resistor to preserve the operating conditions with and without recording.

4. Observation Methods and Analysis of Recordings

The preparation for launch, the actual launch and reception from the shift-registering radiosonde were accomplished according to the directions for conducting radiosonde observations, with the exception that prior to launching the radiosonde into free flight, a static taring of the shift-measuring attachment was performed. The reception of signals emitted because of shifts of the sonde in flight occurred simultaneously with and independently of the reception of code signals. The altitude and the extent of perturbed zones were determined by combining in time the recording of the semiautomatic device and the DMSS.

The recording obtained from the DMSS may be subdivided into the following types (Figure 5):

(1) a nearly horizontal line with slight oscillations around the mean value;

(2) sinusoidal oscillations with slight damping and a constant period of about 3 sec;

(3) short period pulsations in the form of a series of oscillations with maximum period of about 1 sec, starting sharply and sharply dropping to zero, sometimes in the form of isolated spikes;

(4) sinusoidal oscillation with a period close to that described in type 2, but with less rigorous conservation of the constancy of the period and having high frequency, short-period pulsations riding the sinusoidal oscillations.

The recording of the first type apparently corresponds to the case in which no perturbing forces are acting on the instrument. The recording of the second type is caused by changes of the tension on the

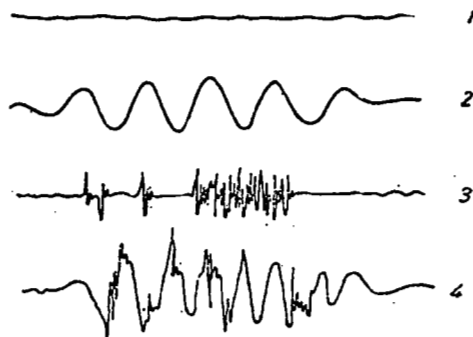


Figure 5. Types of recordings of the radiosondes with shift-measuring attachment

suspension when the instrument is rocked. These oscillations dampen very slowly and may last for quite long periods of time after the cessation of the interaction. Moreover, it will be shown later that the occurrence of such oscillations will not necessarily result from external factors; therefore, the sections with this type of recording should not be identified with perturbed zones.

A conclusion as to the presence of the external interaction on the instrument may be made only when the recording is of type 3 or 4.

Type 3 includes the case in which the turbulent waves follow one another and, therefore, the recordings of the oscillations of the tension of the suspension result from forced oscillations under the influence of the periodic perturbation forces on the free oscillations of the balloon appendix.

Type 4 results from combination of the three other types of oscillations.

Zones with type 3 and type 4 oscillations are isolated on the ascension curve. The recording chart is calibrated with respect to time, and the time of the beginning and the end of "tossing" of the radiosonde is determined. Thence, from the results of radiosonde data processing, the altitude and the thickness of the turbulent layer are determined.

The intensity of turbulence is measured on a three-division scale:

weak (δ^1)--load shifts of the order of $\Delta n \leq 0.2$ g; intermediate (δ^2)--load shifts of the order of $0.2 \text{ g} < \Delta n \leq 0.4 \text{ g}$; and, strong (δ^3)--load shifts of the order of $\Delta n > 0.4 \text{ g}$.

CHAPTER II

CHARACTERISTICS OF THE RADIOSONDE METHOD OF TURBULENCE INVESTIGATION

A freely ascending radiosonde is a system with many degrees of freedom; consequently, its behavior in flight cannot be rigorously described mathematically. Therefore, several independent problems describing the behavior of the investigated system were considered from different viewpoints. In particular, we considered the behavior of a sounding balloon in an accelerating airstream for an instantaneous change of velocity and for a periodically changing velocity of the airstream. In addition, we studied the effect of instrument rocking on the nature of recording. Naturally, with this approach, each problem is described by equations with certain constants. In order to obtain a quantitative evaluation, we conducted special experiments.

Thus, for example, the data on the period and magnitude of damping of longitudinal oscillations of the system were basically obtained by the experimental method. Certain data on the nature of the behavior of the system were extracted during the analyses of recordings of the radiosonde methods.

Unfortunately, we were unable to conduct simultaneous measurements of the turbulence in the same region by the airplane and radiosonde method, and, therefore, the comparative data which are given below may be only partially used in evaluating this method.

In addition, it is necessary to consider the fact that while the airplane may be used for the study of turbulences of the order of 50-250 m, the radiosonde reacts to perturbations which are basically from 0-10 m. In certain cases, on the basis of the existing concept regarding the turbulence spectra, and on the basis of the average data which were obtained by one method, mean values may be predicted which will be obtained by the other methods.

1. Interaction of the Sounding Balloon with Accelerated Airstream

The motion of a balloon in an accelerated airstream is described by the first order nonlinear differential equation:

$$m_1 \frac{dv}{dt} = m_2 \frac{du}{dt} + m_{\text{con}} \frac{a}{dt} (u - v) - \frac{3}{8} \frac{c_x}{r} m_2 (u - v)^2 + (m_2 - m_1) g - N, \quad (6)$$

where m_1 is the mass of the balloon; m_2 is the mass of air inside the balloon; v is the velocity of the balloon; u is the velocity of the

stream (vertical); m_{con} is the connected mass; r is the radius of the balloon; c_x is the coefficient of the aerodynamic resistance; and, N is the vertical component of the reaction of suspension when the balloon is loaded.

Equation (6) generally is not reduced to the quadratures since u , v and N are unknown time-dependent functions. Let us solve it for the case in which $N = \text{const}$ (specifically $N = 0$).

Considering the motion of the air and of the balloon in the turbulent zone (generally stabilized), we shall introduce new designations

$$\begin{aligned} u &= \bar{u} + u', \\ v &= \bar{v} + v', \end{aligned} \quad (7)$$

where \bar{u} and \bar{v} are the mean (in time) values for the velocity of the stream and the velocity of the balloon, while u' and v' are pulsating values of these velocities. Let us assume that the mean value of the pulsation velocity is equal to zero.

For the case in which the velocities u and v are constant, equation (6) will have the following form:

$$\frac{3}{8} \frac{c_x}{r} m_2 (\bar{u} - \bar{v})^2 = (m_2 - m_1) g - N. \quad (8)$$

Subtracting equation (8) from equation (6) we obtain

$$\begin{aligned} m_1 \frac{dv}{dt} &= m_2 \frac{du'}{dt} + m_{\text{con}} \frac{d}{dt} (u' - v') - \\ &- \frac{3}{8} \frac{c_x}{r} m_2 [(u - v)^2 - (\bar{u} - \bar{v})^2]. \end{aligned}$$

Assuming that the pulsations are small, we may neglect their square terms as compared with their first power terms. Thus, our equation is reduced to the first order linear differential equation with constant coefficients:

$$\begin{aligned} m_1 \frac{dv'}{dt} &= m_2 \frac{du'}{dt} + m_{\text{con}} \frac{d}{dt} (u' - v') - \\ &- \frac{6}{8} \frac{c_x}{r} m_2 (u' - v') (\bar{u} - \bar{v}). \end{aligned} \quad (9)$$

This equation may be solved in quadratures by assigning a definite form to the stream velocity.

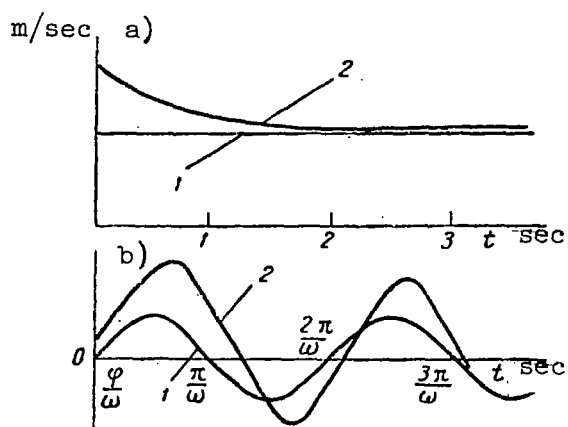


Figure 6. Functions $u'(t)$ and $v'(t)$: a) for instantaneous jump of u' ; b) for periodically changing u' . 1- u' , 2- v'

A. A balloon in a stream with a spontaneous jump of velocity

Let

$$u' = \begin{cases} 0 & \text{at } t < 0 \\ |u'| = \text{const} & \text{at } t > 0, \end{cases} \quad (10)$$

then

$$\frac{du'}{dt} = |u'| \delta(t), \quad (11)$$

where $\delta(t)$ is a delta function.

Figure 6a represents a plot of u' function.

Equation (9) may be written in the form

$$\frac{dv'}{dt} + 2b(\bar{v} - \bar{u})v' = a \frac{du'}{dt} + 2b(\bar{v} - \bar{u})u', \quad (12)$$

where

$$a = \frac{m_2 + m_{np}}{m_1 + m_{np}} = 1.715, \quad (13)$$

$$b = \frac{3}{8} \frac{c_x}{r} \frac{m_2}{m_1 + m_{np}} = 0.244.$$

con

Assuming $v'(t)$ to be integrable in the $-\infty, \infty$, interval we solve the equation by means of a Fourier transform. Considering that

$$V(\sigma) = \int_{-\infty}^{\infty} v'(t) e^{-i\sigma t} dt,$$

$$v'(t) = \frac{1}{2\pi} \int_{-\infty}^{\infty} V(\sigma) e^{i\sigma t} d\sigma$$

and, consequently, that the following relationships are true:

$$\frac{dv'(t)}{dt} = \frac{1}{2\pi} \int_{-\infty}^{\infty} i\sigma V(\sigma) e^{i\sigma t} d\sigma,$$

$$\frac{du'}{dt} = |u'| \delta(t) = \frac{|u'|}{2\pi} \int_{-\infty}^{\infty} e^{i\sigma t} d\sigma,$$

$$u'(t) = \int_{-\infty}^t \delta(t) dt = \int_{-\infty}^t \frac{1}{2\pi} \int_{-\infty}^{\infty} e^{i\sigma t} d\sigma dt = \frac{1}{2\pi} \int_{-\infty}^{\infty} \frac{e^{i\sigma t}}{i\sigma} d\sigma,$$

from equation (12), we obtain the following expression for determining the Fourier transform for the velocity and for the acceleration of the balloon:

$$i\sigma V(\sigma) + 2b(\bar{v} - \bar{u}) V(\sigma) = a|u'| + 2b(\bar{v} - \bar{u}) \frac{|u'|}{i\sigma}. \quad (14)$$

From (14) we obtain

$$V(\sigma) = |u'| \frac{a i\sigma + 2b(\bar{v} - \bar{u})}{i\sigma + 2b(\bar{v} - \bar{u})} \frac{1}{i\sigma},$$

$$i\sigma V(\sigma) = |u'| \frac{a i\sigma + 2b(\bar{v} - \bar{u})}{i\sigma + 2b(\bar{v} - \bar{u})}. \quad (15)$$

Here, by means of a reverse transformation, we obtain the pulsation velocity of the balloon

$$v'(t) = |u'| \left[1 + (a-1) e^{-2b(\bar{v} - \bar{u})t} \right], \quad (16)$$

and then the acceleration

$$\frac{dv'(t)}{dt} = |u'| \left[\delta(t) - 2b(\bar{v} - \bar{u})(a-1) e^{-2b(\bar{v} - \bar{u})t} \right] \quad (17)$$

The manner in which the pulsation velocity, v' , approaches the stream velocity, u' , is indicated in Figure 6a.

Thus, as a result of the interaction of the stream with the instantaneous velocity jump, the balloon will also change its velocity. As t is increased, the increase of the velocity of the balloon will also approach the increase of the velocity of the stream. When $t = 0$, v' is not equal to zero, but to a $|u'|$. The fact that the very same acceleration has a component of the form $\delta(t)$ may be explained by the nonrigorous starting equation.

Let us determine the time after which the difference of the pulsation of the velocity of the air and of the balloon in an updraft with an instantaneous increase of velocity comprises not more than 5 percent of the original difference of these pulsations, i.e., the time after which the pulsations of the velocity of the stream and of the balloon will essentially coincide. It is apparent from (16) that this time, t_0' , at $N = 0$ is

$$t_0' = 3\tau = \frac{3}{2b(\bar{v} - \bar{u})} = 1.14 \text{ sec}$$

and at $N = 1 \text{ kg}$

$$t_0'' = 3\tau = \frac{3}{2b(\bar{v} - \bar{u})} = 1.55 \text{ sec}$$

All of the above is applicable to the balloon which is continuously subjected to the force of suspension, i.e., to the case in which the action of a stream would result in a strictly vertical motion without any sideways oscillations of the suspension, or a motion with simultaneous rocking of the sonde in a circular pattern.

B. A balloon in a stream with periodically changing vertical velocity

Let

$$\begin{aligned} u' &= A \sin \omega t, \\ \frac{du'}{dt} &= A \omega \cos \omega t \end{aligned} \quad (18)$$

and equation (9) will become

$$\frac{dv'}{dt} + 2b(\bar{v} - \bar{u})v' = A\omega \cos \omega t + 2b(\bar{v} - \bar{u})A \sin \omega t \quad (19)$$

The solution of the homogeneous equation

$$v_1' = c e^{-2b(\bar{v} - \bar{u})t}$$

The general solution, obtained by varying the constant, has the following form

$$v'(t) = \frac{A}{\omega^2 + [2b(\bar{v} - \bar{u})]^2} \left\{ \left[(a\omega^2 + (2b(\bar{v} - \bar{u}))^2) \sin \omega t + \right. \right. \\ \left. \left. + 2b(\bar{v} - \bar{u})(a-1) \cos \omega t \right] + 2b(\bar{v} - \bar{u})\omega(a-1)e^{-2b(\bar{v} - \bar{u})t} \right\}$$

or

$$v'(t) = M \sin(\omega t + \varphi) + L e^{-2b(\bar{v} - \bar{u})t}, \quad (20)$$

where

$$M = A \sqrt{\left\{ \frac{a\omega^2 + [2b(\bar{v} - \bar{u})]^2}{\omega^2 + [2b(\bar{v} - \bar{u})]^2} \right\}^2 + \left\{ \frac{-2b(\bar{v} - \bar{u})\omega(a-1)}{\omega^2 + [2b(\bar{v} - \bar{u})]^2} \right\}^2}, \\ \varphi = \arctg \frac{2b(\bar{v} - \bar{u})\omega(a-1)}{a\omega^2 + [2b(\bar{v} - \bar{u})]^2}, \\ L = A \frac{2b(\bar{v} - \bar{u})\omega(a-1)}{\omega^2 + [2b(\bar{v} - \bar{u})]^2}; \quad (21)$$

Figure 6b shows the solution of equation (19). It is apparent from equation (20) and from the figure that the velocity of the balloon v' , in a stream with a periodically changing vertical velocity u' , will also change periodically with the same frequency as the velocity of the stream, but with some phase shift. In addition, a transition process will take place which is rapidly damped. The system will be subject only to forced oscillations resulting from the linearization of equation (6). From formulas (21) it is possible to calculate the amplification coefficient from the amplitude and the phase shift for any external harmonic interaction.

2. Rocking of the Radiosonde

The theodolite observations of a balloon with a suspended radiosonde have shown that, as a rule, the instrument, while pulling on the suspension, circumscribes trajectories resembling ellipses. If we consider the suspension to be rigid, then the instrument in its oscillatory motion is displaced along the sphere with the center in the appendix.

In order to determine the nature of the stretching of the suspension, let us examine the motion of the sounding balloon disregarding the effects of the medium on this motion. This will be an extremely approximate model giving only the conception of the degree of complexity of the trajectory as transcribed by the instrument.

Let us write equations for the moments of forces which act on the system in a rectangular coordinate system. This coordinate system is to be parallel to the coordinates of the earth. In the same coordinate system, let us write equations for the motion of the balloon, including also in the system of forces the reaction of the suspension. We shall write the equations for the motion of the instrument in a system of coordinates parallel to the coordinates of the earth, and associated with the instrument.

$$\begin{aligned}\frac{d}{dt} \frac{G}{g} (y_1 \dot{z}_1 - z_1 \dot{y}_1) &= Gl \sin \varphi \sin \psi, \\ \frac{d}{dt} \frac{G}{g} (z_1 \dot{x}_1 - x_1 \dot{z}_1) &= -Gl \sin \varphi \cos \psi, \\ \frac{d}{dt} \frac{G}{g} (x_1 \dot{y}_1 - y_1 \dot{x}_1) &= 0, \\ m_1 \ddot{x} &= -N \sin \varphi \cos \psi,\end{aligned}\tag{22}$$

$$\begin{aligned}m_1 \ddot{y} &= -N \sin \varphi \sin \psi, \\ m_1 \ddot{z} &= -m_1 g + N \cos \varphi, \\ m_b \ddot{x}_1 &= N \sin \varphi \cos \psi, \\ m_b \ddot{y}_1 &= N \sin \varphi \sin \psi; \\ m_b \ddot{z}_1 &= P - m_b g - N \cos \varphi,\end{aligned}\tag{23}$$

where m_1 is the mass of the load; m_b is the mass of the balloon; and, P is the force which is equal to the sum of the lift of the balloon and the vertical component of the updraft.

The formulas which relate these systems of coordinates have the following forms:

$$\begin{aligned}x_1 - x &= l \sin \varphi \cos \psi, \\ y_1 - y &= l \sin \varphi \sin \psi, \\ z_1 - z &= -l \cos \varphi,\end{aligned}\tag{24}$$

where φ is the angle of deviation of the suspension from the Z_1 axis (vertical), ψ is the angle between the axis x_1 and the projection of the suspension onto the plane $x_1 y_1$.

From these equations, after certain transformations, we obtain three independent differential equations for the determination of φ , ψ , N :

$$\begin{aligned}\ddot{\varphi} &= c_1^2 \frac{\cos \varphi}{\sin^3 \varphi} - \frac{G}{l} \sin \varphi, \\ \ddot{\psi} &= \frac{c_1}{\sin^2 \varphi}, \\ \ddot{N} \sin \varphi + \dot{\varphi}^2 \cos \varphi &= \frac{N}{l} \left(\frac{1}{m_b} + \frac{1}{m_l} \right) \cos \varphi - \frac{P}{lm_b}.\end{aligned}\quad (25)$$

If at time t_0 the balloon were subjected to the action of such perturbation to cause the instrument to occupy a position x_0, y_0, z_0 , and to acquire an initial velocity $(\dot{x}_0, \dot{y}_0, \dot{z}_0)$, then having solved the system of equations (25), it would be possible to obtain the value of angles and the magnitude of stretching as a function of time and initial conditions. We obtain quite a simple relationship for N :

$$\begin{aligned}N &= 3G \frac{m_b}{m_b + m_l} \cos \varphi + \left(P \frac{m_l}{m_b + m_l} - G \frac{m_b}{m_b + m_l} \right) \frac{1}{\cos \varphi} + \\ &+ \varphi_0^2 l \frac{m_b m_l}{m_b + m_l} - 2G \frac{m_b}{m_b + m_l} \cos \varphi_0 + \psi_0^2 l \frac{m_b m_l}{m_b + m_l} \sin^2 \varphi_0.\end{aligned}\quad (26)$$

From the first two equations of the system of equations (25), we may obtain, in principle, the time in which the instrument will complete its trajectory (or any part of it). This time can be temporarily called the period of the oscillatory motion of the instrument. If the instrument is in circular motion, then naturally the period will be the time of a complete revolution of the instrument, i.e., the time in which the angle ψ will change by 2π .

Analogous to the case of circular motion, the period of the instrument along a somewhat more complex trajectory may be considered the time in which the magnitude of ψ changes by 2π . In practice, however, it is not possible to obtain an analytical expression which would be usable for numerical calculation. Therefore, let us limit ourselves to consideration of certain specific cases of motion for which we shall determine the period.

It was shown in Ref. 5 that the instrument will move along the trajectories which form loops, and only in certain exclusive cases (when the circles coincide) are the trajectories closed. The period of rotation of the instrument along a circular trajectory is determined by the formula

$$\tau = 2\pi \sqrt{\frac{z_1}{g}},$$

where $z_1 = l \cos \varphi_1$ -- the distance from the center of the sphere to the plane of rotation. Stretching remains constant, i.e., rocking does not affect the nature of the recording.

In the case of the instrument rocking in one plane, the last term is dropped in formula (26), as it describes the initial conditions of motion in space. Since this term is significantly positive, then apparently in the case of plane motion the stretching will be minimal. The period of oscillations of the instrument is determined from the formula for the plane pendulum.

The radiosonde with a force measuring attachment is launched on an 8-10 m suspension. The period of the change of force during the pendulum motion of the radiosonde was determined experimentally on the ground. Figure 7 shows a section of the chart with a recording of the pendulum oscillations obtained in one of the experiments. Since the mean period of oscillations, $\bar{\tau}$, equals 3.15 sec, then

$$T_{\text{pen}} = 2\bar{\tau} = 6.3 \text{ sec},$$

which corresponds to the period of oscillations of the ideal pendulum for which $l = 10 \text{ m}$.

3. Elastic Oscillations of the System Along the Axis of Suspension

During the discussion of this method it was suggested that elastic oscillations of the system along the axis of suspension, especially the oscillations in the appendix, may cause false signals resembling turbulence. In order to study these oscillations and to evaluate their

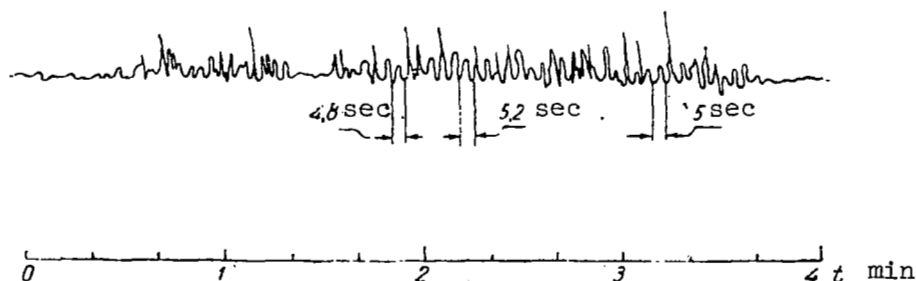


Figure 7. Recording of pendulum oscillations

nature and the nature of damping, the following experiment was conducted. On the ground at a positive temperature the instrument was suspended on a rigid support instead of on the balloon. The instrument was then displaced from the equilibrium conditions and let free. By means of the DMSS, mounted in the "Malakhit" radiotheodolite, a curve was recorded for the transition process. The experiment was then repeated; now the instrument was not mounted to the rigid support, but rather to the appendix of balloon No. 150, which was stretched on a special frame. In this case the curve for the transition process was also recorded. From these curves the frequency of the damping oscillations and quenching decrement were determined as the ratio of two consistent amplitudes. Let us designate the quantity which characterizes the rigidly suspended system by (1) and the system with the appendix by (2).

$$f^{(1)} = \frac{1}{T_1} = \frac{1}{0.3} = 3 \text{ cps}, \quad (27)$$

$$\theta^{(1)} = \ln \left(\frac{x_1}{x_2} \right) = \ln 10 = 2.03,$$

$$f^{(2)} = \frac{1}{0.53} = 1.9 \text{ cps}, \quad (28)$$

$$\theta^{(2)} = \ln 2 = 0.69.$$

Then

$$\delta = \frac{\theta}{T} = \theta f, \quad (29)$$

$$\delta^{(1)} = 6 \text{ cps} = 37.7 \text{ rad/sec},$$

$$\delta^{(2)} = 1.3 \text{ cps} = 8.16 \text{ rad/sec}. \quad (30)$$

From which

$$\begin{aligned} \omega_0^{(1)} &= \sqrt{4\pi^2 f^{(1)2} + \delta^{(1)2}} = 41.6 \text{ rad/sec}, \\ \omega_0^{(2)} &= 14.5 \text{ rad/sec}, \\ f_0^{(1)} &= 6.36 \text{ cps}, \\ f_0^{(2)} &= 2.3 \text{ cps}. \end{aligned} \quad (31)$$

Let us now evaluate the effect of the rigidity of the appendix on the period and the nature of damping of free oscillations. It is well known that

$$\omega_0 = \sqrt{\frac{c}{m}} \quad (32)$$

for the case of series connection of springs

$$c = \frac{c_a c_s}{c_a + c_s}, \quad (33)$$

where c_a is the elastic constant of the appendix and c_s is the elasticity of the spring.

$$\frac{\omega_0^{(2)}}{\omega_0^{(1)}} = \sqrt{\frac{c^{(2)}}{c^{(1)}}},$$

$$c^{(2)} = c^{(1)} \left[\frac{\omega_0^{(2)}}{\omega_0^{(1)}} \right]^2 = 0.12 c^{(1)}$$

From which

$$\frac{c_a c_s}{c_a + c_s} = 0.12 c_s \quad \text{and} \quad c_a = 0.14 c_s. \quad (34)$$

Thus, on the ground the rigidity of the appendix is about seven times lower than that of the spring. During the rise the rigidity of the spring remains constant, while the rigidity of the appendix will, generally speaking, change. On one hand the rigidity will decrease due to the increase of the diameter of the balloon and on the other hand it will increase due to the freezing of the balloon.

We later conducted an experiment for the determination of the nature of longitudinal oscillations as a result of the elasticity of the balloon and of the appendix at different altitudes. The experiment was conducted at positive temperatures in the following manner. Balloon No. 150 was filled with different volumes of air, corresponding to the volumes that this balloon has at different altitudes when it is filled with hydrogen. In the experiment, measurements were made of the vertical rigidity of the balloon-instrument system as the ratio of the load on the suspension to the vertical elongation of the system. Since, during the experiments, the balloon was suspended by its upper end, the elasticity values obtained were somewhat lower than the actual values.

In the first approximation, assuming that during ascension the elongation of the system results from the stretching of the lower

hemisphere and the appendix and, in the experiment, that this stretching is also augmented by the stretching of the upper hemisphere and the upper "appendix", and considering that the balloon is symmetrical, we obtain a transition coefficient from the elasticity, obtained in the experiment, to the actual elasticity of the system, equal to 2. Then

$$f_0 = \frac{1}{2\pi} \sqrt{\frac{2c}{m}} : \quad (35)$$

Using the well-known relationship between the altitude and the diameter of balloon No. 150, the experimentally-obtained elasticity was referred to a definite frequency. Using formula (35), the frequency of free oscillations was calculated for each altitude. Figure 8 shows a graph of elasticity and the frequency of natural oscillations of balloon No. 150 as a function of altitude.

It is seen from the graph that the elasticity and, consequently, the natural frequency of the system decreases with altitude. However, from 17 km and higher, the natural frequency of the system increases and at the altitude of 25-27 km, it exceeds the natural frequency of oscillations of this system in the near-the-ground layer.

We were not able to obtain any experimental data for low temperature conditions, but qualitative evaluation of the behavior of the system under actual conditions is possible through the following reasoning. Generally speaking, freezing of the balloon will decrease the elasticity and, consequently, it will lead to the increase of the frequency of natural oscillations. The launching of radiosondes with shift-measuring attachments was conducted in the daytime. Under such conditions, the temperature of the balloon with respect to the surrounding air, due to direct absorption of solar radiation, may exceed 20° according to the data of many investigators. Therefore, the change of frequency of the natural oscillations due to cooling of the balloon will hardly be significant.

However, we are interested not so much in the frequency of free longitudinal oscillations as in their number, i.e., the damping characteristics of the system after cessation of the external interaction. The experimental data were obtained on the ground by stretching the lower part of the balloon on a frame. Here the damping decrement was

$\delta = 1.3 \text{ sec}^{-1}$. We have no experimental data on the nature of the damping of the longitudinal oscillations of the system at high altitudes. However, considering that natural frequencies change very little (of the order of 50 percent), it is possible to assume that the damping decrement, and, consequently, the damping time will change insignifi-

cantly. Thus, for example, when $\delta = 0.5 \text{ sec}^{-1}$, the transition process in this system is damped, for all practical purposes, after 3-4 sec.

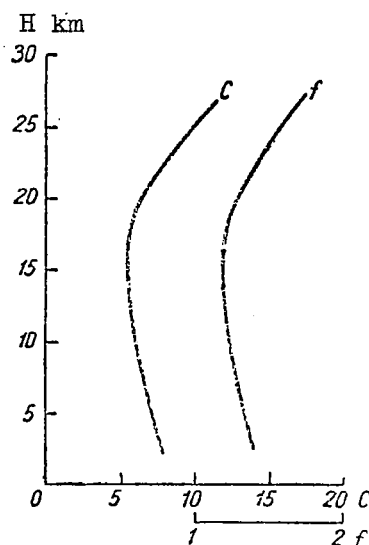


Figure 8. Rigidity and natural frequency of the balloon No. 150 as a function of altitude

This means that if a recorder chart has sections with oscillations, the frequency of which exceeds 1 cps, they correspond to perturbed layers, and that the uncertainty of the determination of the thickness of the turbulent layer, even if the velocity of the lift of the balloon is 7-8 m/sec, will not exceed 25-30 m.

Some data on the magnitude of damping may be obtained from the analysis of the recordings of the instrument directly after the start. At the start there is an instantaneous change of the tension of the suspension. With a slight damping of the oscillations of the system, caused by the starting push, these oscillations would be observed up to high altitudes. However, the analysis of recordings made after the start in 208 launchings showed that in 102 cases the first section of the recording had no shifts along the axis of suspension. This again substantiates the fact that free longitudinal oscillations of the system are very rapidly quenched. It follows that the presence of shifts on the remaining 106 recordings corresponds to the presence of perturbations in the near-the-ground layer.

4. Comparison of Radiosonde Turbulence Data with the Airplane Tossing Data

It is of practical interest to compare the simultaneous measurements of atmospheric turbulence by means of radiosondes and airplanes. This will solve the question of the possibility of using radiosonde observations for the operational servicing of airplane flights.

Unfortunately, we were unable to obtain strictly synchronous flights with the use of radar to bring the plane into the region where there was a radiosonde.

For comparison of radiosonde data we made use of flight data from airplanes from different airports in the Moscow region. In some cases airplanes were removed by as far as 200-300 km from the radiosonde. The time difference on the average did not exceed two hours. In addition, we made use of the comparison between the radiosonde data in Sukhumi and the airplane data from the same region.

In comparing the airplane and the radiosonde data it is necessary to keep in mind that in addition to the nonsynchronous time operations and different locations of measurements, these methods differ greatly in the dimensions of disturbances which they can detect.

The airplane reacts to disturbances with characteristic dimensions from several decades to several thousands of meters, while the radiosonde may record disturbances from 2 to 10 m.

Naturally, the question arises about the applicability of radiosonde data to aircraft and vice versa.

From the presently existing concepts of turbulence, the spectrum in the atmosphere is continuous, starting from the large dimensions of primary turbulent formations, of the same order as the stream as a whole, and ending with molecular size disturbances where the kinetic energy is dissipated as thermal energy.

The experimental investigations of the atmospheric turbulence spectrum by means of airplanes (Ref. 20) showed that in the cases of medium and small dimensions of disturbances, those which are less than 600 m can be determined more accurately. The energy distribution is in good agreement with the spectral law "minus five-thirds" (this refers to those cases when the characteristic size of the primary turbulent formation is sufficiently large). Knowing the energy density over 100 m distance, it is possible to determine the energy density arriving over 5 m distance. It is possible to assume that if an airplane in some layer experiences turbulence, then the shift-measuring radiosonde in the same layer (in the case of synchronous measurements) will also experience turbulence.

For the Moscow region we analyzed 288 airplane flights, approximately coinciding in time with the radiosonde launchings. In 253 cases airplane flights were quiet. Thus, the frequency of occurrence of tossing, according to the airplane data, comprised 12 percent.

In order to obtain more detailed comparative data regarding tossing of airplanes and radiosondes, we have made use of 35 almost simultaneous flights of airplanes and radiosondes in the Moscow region and eight flights in the Sukhimi region. Comparisons were conducted for each of the kilometer layers of the atmosphere up to the maximum flight altitude of the plane. There were altogether 429 pairs of comparisons, made according to the following scheme:

positive-positive (pos/pos)
 negative-negative (neg/neg)
 positive-negative (pos/neg)
 negative-positive (neg/pos)

The comparison data are given according to the scheme in Table 1.

From the data of Table 1 it is apparent that the coincidence (pos/pos, neg/neg) comprised 61 percent of all cases. However, in 49 out of 102 cases the radiosonde did not verify the airplane indications in the case of the existence of airplane tossing, and in 117 cases turbulence data of radiosondes were not supported by the airplane data.

Table 1. The Results of Comparison of Airplane and Radiosonde Data

	pos/pos	neg/neg	pos/neg	neg/pos
Airplane-radiosonde.	53	210	49	117
Total.	263 (61 percent)		166 (39 percent)	

The first form of noncoincidences could be explained by the non-synchronous observations and the somewhat different locations of observations. Within the second class of noncoincidences, in addition to the above cause, the turbulence spectrum (i.e., the turbulences to which the radiosonde reacts) may be a result of small scale turbulences.

In order to finally solve the problem of the applicability of the radiosonde data to airplanes, it is necessary to accumulate a sufficient statistical sample of the comparisons of simultaneous observations. However, on the basis of the available data on the structure of the turbulent stream in the atmosphere, obtained by independent methods, we believe that the reverse argument about the applicability of radiosonde data to airplanes is also valid.

To verify this assumption it is necessary to conduct experimental flights of airplanes for measuring the turbulence and launching of shift-measuring radiosondes, and make their time and location coincide closely.

CHAPTER III FREE AIR TURBULENCE FROM RADIOSONDE DATA

1. Organization of Radiosonde Observations and the Characteristic of Measurement Data

It was already mentioned that the launchings of A-22-111 radiosondes with shift-measuring attachment were organized by the Central Aerological Observatory in Moscow (Dolgoprudnoye), the Transcaucasian Scientific Research Hydrometeorological Institute in Sukhumi (on the Black Sea shore of the Caucasus), and the Central Asiatic Scientific Research Institute in Tashkent. From July, 1961, until October, 1962, there were only 457 radiosonde launchings, 326 in Moscow, 89 in Sukhumi, and 42 in Tashkent. The monthly distribution of the launchings is given in Table 2.

From the data of Table 2 it is apparent that in Moscow, starting with October, 1961, in the course of the whole year, observations were carried out quite regularly. Radiosondes with shift-measuring attachment were launched in the course of a nine-hour operative period of aerological observations. In addition, in October, 1961, five series of more frequent observations were carried out in order to determine the temporary variability of the state of the atmosphere. Each such series of more frequent observations consisted of four to six consecutive launchings of radiosondes with a shift-measuring attachment conducted with approximately a 1.5 hour time interval.

In Sukhumi the launchings were established at the end of November, 1961, and continued until the end of March, 1962. Launchings here were also conducted in the course of a nine-hour operative period of aerological observations.

In Tashkent measurements of atmospheric turbulence began in January, 1962, and were conducted almost regularly until the beginning of April.

Table 2. The Data on the Number of Radiosonde Observations
of the Atmospheric Turbulence

Name of the point	1961						1962									Total num- ber of launchings
	VII	VIII	IX	X	XI	XII	I	II	III	IV	V	VI	VII	VIII	IX	
Moscow	16	7	7	39	22	23	24	22	25	23	22	25	22	25	24	326
Sukhumi	-	-	-	-	3	20	19	12	15	-	-	-	-	20	-	89
Tashkent	-	-	-	-	-	-	15	8	16	3	-	-	-	-	-	42

Thus, the period from December to March (the winter season) was well investigated at the above three points. One hundred percent of all launched balloons in all three locations reached altitudes of the order of 12-13 km. Seventy-five percent of all launched balloons in Moscow and Tashkent reached the altitude of 20 km, and in Tashkent 87-88 percent of all launchings reached that altitude. Thirty-kilometer heights and above were reached by 25-27 percent of the radiosondes sent up in Tashkent, and only 5-7 percent in Sukhumi and Dolgoprudnoye. These data give a good idea of the statistical reliability of those scientific results which shall be presented in the following sections of this article.

During the analysis of observation data, we used for comparison the results of atmospheric turbulence measurements over the United States (Ref. 22). One thing which should be kept in mind is the fact that measurements in the United States were conducted with shift-measuring instruments connected by means of suspension to a falling parachute. Thus, the measuring element was a parachute and not a balloon.

2. The Frequency of the Occurrence of Turbulence at High Altitudes. Seasonal and Yearly Changes.

At the present time we have access to a sufficient number of data on the distribution and the frequency of the occurrence of turbulence, which results in the tossing of airplanes, up to the altitude of 10-12 km (Ref. 13). Turbulence is most frequently observed in the atmospheric layer up to 1-2 km in altitude, and then the frequency of occurrence decreases, reaching a minimum at an altitude of 6-7 km. At high altitudes the recurrence of turbulence increases with altitude, reaching a maximum at 10-12 km.

Therefore, it is natural to first consider the frequency of occurrence of turbulence, measured by means of radiosondes, and to compare these data with the data on the distribution of airplane tossing.

The frequency of the occurrence of turbulence was calculated by us from the number of cases for each kilometer layer. A given kilometer layer of the atmosphere was considered turbulent if there existed in it a turbulent layer greater than 50 m in thickness.

The results of the calculations are shown in Figure 9. This figure illustrates the vertical distribution of the frequency of occurrence of turbulence over Moscow, Sukhumi, and Tashkent.

In Figure 9a, curve 1 characterizes the mean annual vertical distribution of the frequency of occurrence of turbulence over Moscow. The same figure shows the curves for the turbulences which cause airplane

tossing (borrowed from Ref. 13). Curve 2 characterizes the frequency of the occurrence of the airplane tossing from the data of vertical airplane probing in the southern regions of the USSR, and curve 3 shows the recurrence of turbulence over the United States, which was obtained from the data of shift-measuring instruments descended by parachutes (Ref. 22). The same figure shows the data (curve 4) of Hyde (Ref. 25) for London-Far East and London-North Africa routes, as well as the data for the mean latitudes of the territory of the USSR (curve 5).

From the comparison of the curves in Figure 9a, it is apparent that the frequency of occurrence of turbulence, measured by means of radio-sondes, is much greater than the frequency of occurrence of airplane tossing. However, there is a resemblance in its variation with altitude.

Figure 9a shows that the frequency of occurrence of turbulence decreases with altitude, especially in the atmospheric layer up to 2 km, reaching a minimum (27 percent) on the average at an altitude of 11.5 km. We then note a sharp increase in the frequency of occurrence of turbulence up to an altitude of 12.5 km (50 percent), following which it slowly decreases. At an altitude of 27-33 km the frequency of the occurrence of turbulence varies in the proximity of 5 percent.

Figure 9a shows that the lower part of the stratosphere is sufficiently turbulent. This structural characteristic of the stratosphere

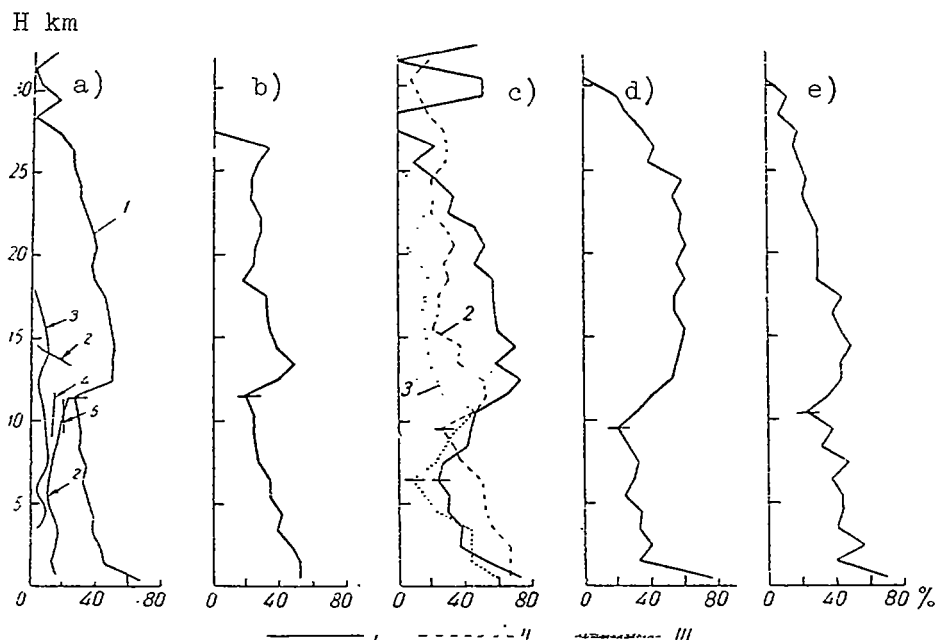


Figure 9. The altitude distribution of the frequency of occurrence of turbulence; a) annual, b) autumn, c) winter, d) spring, e) summer; I-Moscow, II-Tashkent, III-Sukhumi

is seen even more clearly in Figure 9b-e, which show the vertical distribution of frequency of the occurrence of turbulence for all seasons of the year over Moscow and for winter over Sukhumi and Tashkent (Figure 9c).

The analyses of the curves in Figure 9b-e show that there exist seasonal differences in the altitude distribution of the turbulence, although the general appearance of these curves is sufficiently similar. First, the altitude of the tropospheric maximum of the frequency of occurrence of turbulence over Moscow is greatest in the autumn (11.5 km), and lowest in the winter (7.5 km). Second, the greatest frequency of occurrence of turbulence in the middle and the upper troposphere is observed in the summer; and in the stratosphere, on the contrary, it is observed in the winter and especially in the spring.

It is interesting that the general distribution of the frequency of occurrence of turbulence in the winter is sufficiently similar in Moscow, Sukhumi, and Tashkent; but it differs in the altitude of the pronounced tropospheric minimum of the occurrence of turbulence. Over Moscow and Sukhumi it is at an altitude of 6-7 km, but in Tashkent it is at an altitude of 9.5 km. In addition, the frequency of the occurrence of turbulence in the lower stratosphere over Moscow reaches 70-80 percent, over Tashkent 30-50 percent, and over Sukhumi about 20 percent.

Let us now consider the annual change of the frequency of occurrence of turbulence, taking into account its intensity over Moscow, where we have an almost complete yearly cycle of observations. Let us remember that the intensity of the turbulence of the atmosphere is determined, as it was stated in Chapter I, on the three-point scale: weak, medium, and strong.

Figures 10-12 (in which the isolines of the same frequency of occurrence have been drawn) show the annual change of the frequency of the occurrence of turbulence over Moscow. It can be seen from these figures that the distribution has the nature of spots with areas of high (H) and low (L) frequency of occurrence of turbulence. Figure 10 shows that the frequency of occurrence of weak turbulence in the atmospheric layer to an altitude of 2-3 km is sufficiently high during all months, reaching as high as 50-70 percent. In the middle troposphere the frequency of the occurrence is somewhat lower, and for the upper troposphere the summer months are characterized by frequently occurring, strongly developed convection processes with characteristic convective clouds. The frequency of the occurrence of weak turbulence in the stratosphere during the summer months is relatively low. In the autumn, and especially in the winter months, one observes areas of high frequency of

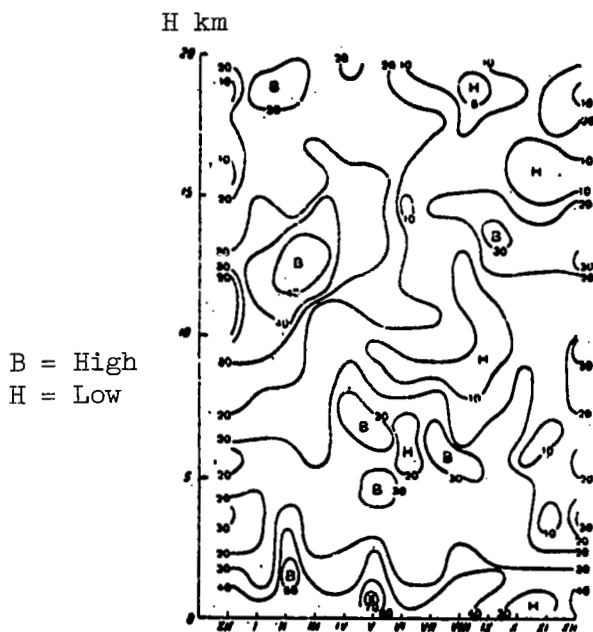


Figure 10. Yearly changes of the frequency of occurrence (in percent) of weak turbulence at high altitudes (Moscow)

occurrence of turbulence (over 40 percent) (in the winter these areas occur at 10-15 km and 18-20 km altitudes).¹

A characteristic feature of the annual change of the distribution of medium-strength turbulence, as seen in Figure 11, is its low frequency of occurrence in the middle and the upper troposphere in the cold seasons, and the high frequency of occurrence in the summer. In the winter and spring there is a high frequency of occurrence of medium strength turbulences (up to 40-50 percent) at 14-17 km altitudes. An analogous picture is seen in the case of annual change of strong turbulence (Figure 12).

Figure 13 gives an idea of the frequency of the occurrence of weak, medium, and strong turbulence over Sukhumi in the winter. Here, in general, the frequency of occurrence of turbulence at all altitudes is

¹According to the data of D. Coloson (Ref. 24), who combined the data of many visual observations of intermediate and strong airplane tossing at high altitudes over the United States. His data were collected in the winter months of 1961-62. A significant turbulence was noted above 12 km and to altitudes of 21-22 km.

H km

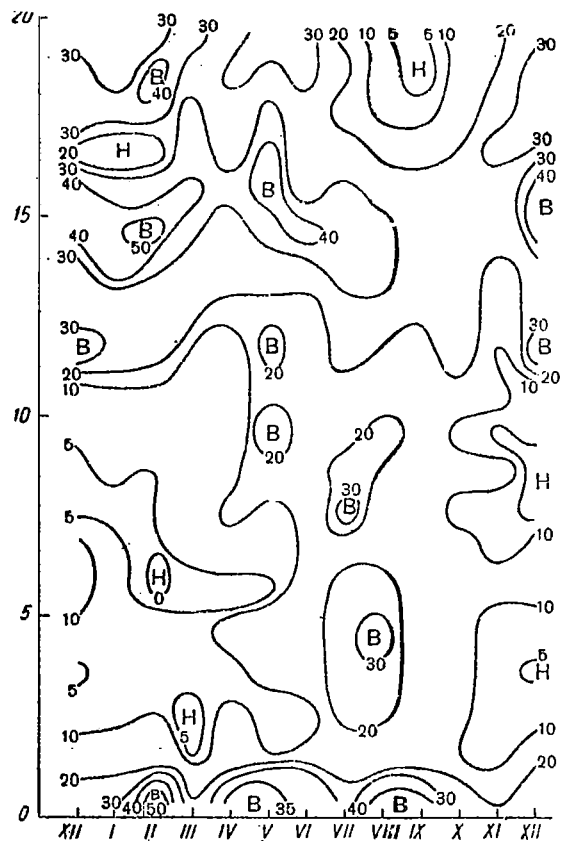


Figure 11. Yearly changes of the frequency of occurrence (in percent) of medium turbulence at high altitudes (Moscow)

H km

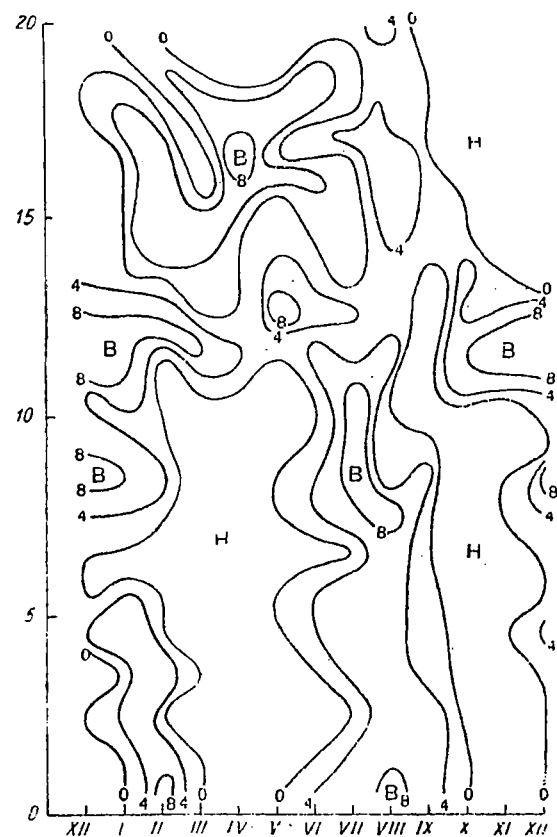


Figure 12. Yearly changes of the frequency of occurrence (in percent) of strong turbulence at high altitudes (Moscow)

B = High
H = Low

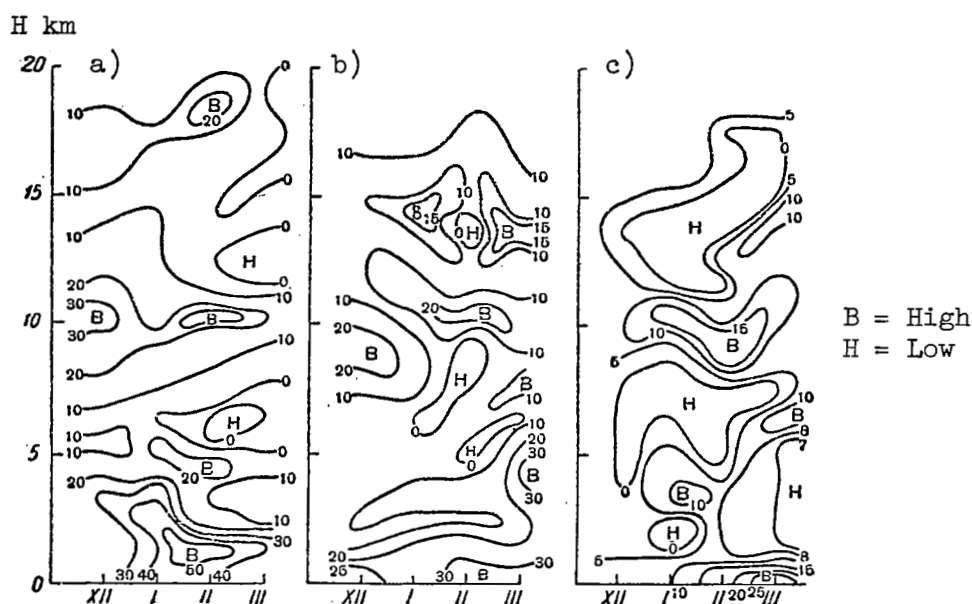


Figure 13. The frequency of occurrence of weak (a) medium, (b) and strong, (c) turbulence in the winter over Sukhumi

lower than over Moscow. The greatest frequency of occurrence of turbulence, just as for Moscow, was observed in the lower half of the troposphere. The middle and the upper troposphere are most frequently unperturbed. The recurrence maxima of weak as well as of medium and strong turbulence are observed in the tropopause region and in the stratosphere.

3. The Thickness of the Turbulent Layers and Its Relationship to the Intensity of Turbulence

Let us now consider another extremely important parameter of atmospheric turbulence--the thickness of turbulent layers. Let us remember that the minimum thickness of the turbulent layer which may be reliably detected by the radiosonde is approximately 50 m. Furthermore, the error in the determination of the thickness of the turbulent layer due to the rocking of the instruments along the suspension to the balloon does not exceed 30 m. Naturally the greater the thickness of the layer, the smaller is the relative error which is introduced by this factor.

It is of great interest to consider the relationship between the thickness of the perturbed layers and the turbulence intensity. Airplane studies lead to contradictory conclusions; some investigators believe that on the average the medium and strong turbulences which bring about airplane tossing are observed in much thicker layers than

the weak turbulences (Ref. 13), while other investigators, on the contrary, conclude that the more intense the turbulence, the smaller the thickness of the turbulent layer (Ref. 18).

In connection with this, the reproducibility of the thickness of turbulent layers is viewed, taking into account the intensity of the turbulence. The reproducibility was calculated for layers of 50-100 m, 100-200 m, etc., up to 1000 m. In addition, all of the data for thicknesses greater than 1000 m were combined into one group. The frequency of the recurrence distribution is given for larger layers of the atmosphere: 0-2, 2-5, 5-8, 8-12, 12-16, 16-20, and 20-24 km.

Figure 14 shows the curves for the integral frequency of the recurrence of the thickness of turbulent layers over Moscow, Sukhumi, and Tashkent (not considering the intensity of the turbulence). From the analysis of the curves in Figure 14, it is apparent that the largest thickness of turbulent layers was observed over Tashkent, where on practically all altitudes one observes thicker turbulent layers than over Sukhumi, and, especially, over Moscow.

The difference in the position of curves of the integral recurrence of the thickness of turbulent layers for Moscow and Sukhumi is not large, although, in general, the curves for Sukhumi lie more to the right (except for the 5-8 km layer) than do curves for Moscow. Above these regions the thickness of turbulent layers in 70 percent of all cases does not exceed 200-300 m.

It was already indicated that over Tashkent the frequency of the recurrence of large thickness of turbulent layers is relatively large. Thus, for example, in the atmospheric layer up to 2 km above the surface of the earth in 40 percent of all cases the thickness of turbulent layers was larger than 1000 m. At other altitudes in 70 percent of all cases the thickness of turbulent layers did not exceed 400-500 m. It should be remembered that the data for Tashkent refer to winter.

For comparison let us note that in the troposphere over Moscow (326 launchings of radiosondes) only in six cases were layers observed with a thickness exceeding 2 km (maximum thickness 3.4 km). Also, there were six cases in the stratosphere (maximum thickness 6.5 km) with a thickness exceeding 2 km. At the same time, in the troposphere over Tashkent (42 launchings of radiosondes) there were 13 cases in which the thickness was greater than 2 km (maximum thickness 5.9 km), and in the stratosphere there were ten such cases (maximum thickness about 13 km).

Let us now compare the data on the thickness of turbulent layers, obtained by us for Moscow and Sukhumi, with the data of Anderson (Ref. 22) for the United States. The results of such comparisons are given

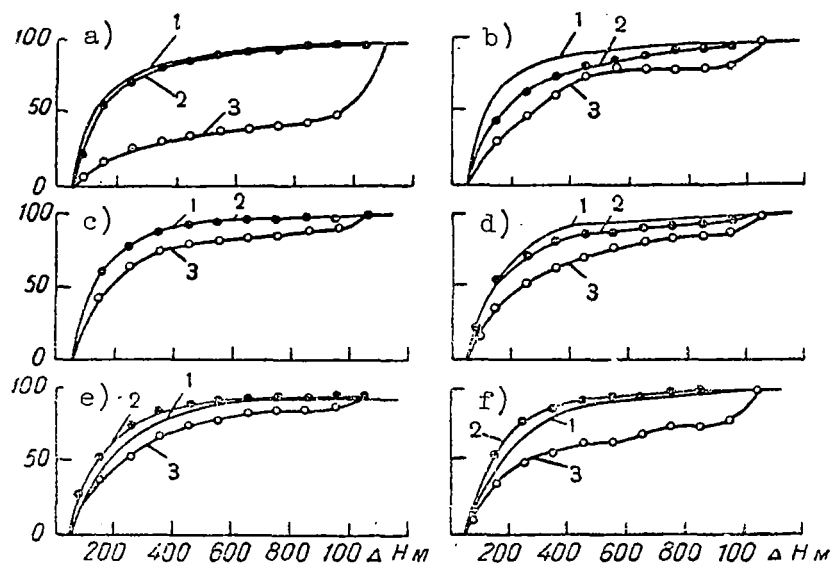


Figure 14. The integral recurrence of the thickness of turbulent layers over Moscow (1), Sukhumi (2), Tashkent (3); a, 0-2 km; b, 2-5 km; c, 5-8 km; d, 8-12 km; e, 12-16 km; f, 16-20 km

in Table 3. It is clear from the data of this table that the distribution of data for these regions is in good agreement. Here the recurrence maxima falls on the thick layer 150 m.

The airplane investigations have shown that with the decrease of the latitude of the locality the recurrence of the large thickness turbulent layers also increases. At high and medium latitudes the frequency of the occurrence of turbulent layers thicker than 1000 m is 10-15 percent, while in the lower latitudes it is 30 percent. In northern and intermediate latitudes the recurrence of the maximum occurs in turbulent layers 300-600 m thick, and in southern latitudes it occurs in 400-800 m layers.

The comparison of these data with the data of Figure 14 and Table 3 show that on the average the thickness of the turbulent layers detected by the radionsondes is approximately two to three times less than the turbulent layers detected by airplanes. The thin structure of layers, in which one finds the turbulence, of the same dimensions as the dimensions of the sounding balloon, is an extremely important factor which must be taken into account when use is made of the radiosonde data.

As we indicated above, the relationship between the thickness of the perturbed layer of the atmosphere and the intensity of the turbulence is of great interest. One obtains this relationship from the analysis of the integral reproducibility of the thickness of the

Table 3. The Frequency of Occurrence of a Given Thickness of the Turbulent Layer (in percent)

Region	Thickness (in m)			
	150	250	350	550
Moscow	33	19	9	3
Sukhumi.	35	19	10	3
United States.	33	19	10	3

turbulent layers as a function of the intensity of turbulence for Moscow (for the whole year, for summer and for the winter), Sukhumi (for the winter) and Tashkent (for the winter).

In the summer in the troposphere of mean latitudes (Moscow), medium and strong turbulence occurs in the thicker layers than the weak turbulence. In the winter, on the contrary, the curves of integral frequency of the occurrence of layers for medium and strong turbulence lie to the left of curves with weak turbulence. This is particularly well expressed for the middle and the upper troposphere.

Approximately the same situation is observed over Sukhumi. In Tashkent it occurs only in the upper troposphere. In the lower and the middle troposphere the winter curves for the integral recurrence of the thickness of layers with medium and strong turbulence lie significantly more to the right of curves for layers with weak turbulence.

In the stratosphere, at altitudes of 12-20 km, less distinct differences are found, except for curves of the Tashkent region, where winter curves for the integral recurrence of the thickness of layers with medium and strong turbulence lie to the left of curves for layers with weak turbulence.

The quantitative picture of this is given in Table 4, which shows the thickness of turbulent layers with 85 percent integral frequency of recurrence.

The indicated relationship, which has a unique seasonal variation, may be explained by the fact that in the summer the development of the intense turbulence results predominantly from thermal instability, encompassing relatively large thicknesses of layers. In the winter, on the contrary, when the thermal instability is expressed weakly, dynamic factors begin to play a relatively important role (shift of the wind, etc.) encompassing, generally, the thin layers. In addition, an important factor may be the interlayer diffusion of the intensity of turbulence (due to convection).

Table 4. The Thickness of Turbulent Layers (in m) with
85 Percent Integral Frequency of Occurrence

Altitude in km	Moscow								Sukhumi		Tashkent	
	Spring		Summer		Autumn		Winter		Winter		Winter	
	1	2	1	2	1	2	1	2	1	2	1	2
0-2	260	360	320	600	480	500	300	280	400	330	1090	1040
2-5	280	340	250	330	400	450	300	180	500	210	990	1020
5-8	340	280	210	550	300	400	360	200	350	330	720	390
8-12	350	480	320	380	360	360	360	320	350	270	720	320
12-16	440	440	440	460	480	600	360	450	490	670	940	530
16-20	620	630	400	450	680	460	340	380	240	360	1030	680

4. Stability and Preservation of Turbulent Layers

The next problem, which is an extremely important characteristic of turbulence which we attempted to clarify by radiosonde observations, is the degree of stability and preservation of turbulent layers in the atmosphere. For this purpose, as was indicated before, we organized a series of frequent launchings of A-22-111 radiosondes, equipped with shift-measuring attachments. In 1961 five series of such experiments were conducted with four to five launchings in each series with the time interval between them of the order of 1.0, 1.5, or 2.0 hours.

The preservation of turbulent layers at different altitudes was determined according to the following scheme:

positive/positive
positive/negative (disappeared)
negative/positive (arose or appeared)
negative/negative

For the convenience of subsequent analysis we combined into one group pos/pos and neg/neg, and into the second group cases with neg/pos and pos/neg. Then we calculated the probability (in percent) of the preservation of the state of the atmosphere for 60, 90, 180, 270, 360 and 450 min. The results of such calculations are given in Table 5.

From the data of Table 5, it can be seen that preservation of a given state of the atmosphere for an hour has a probability of the order of 80-90 percent. In the case of 1.5-6.0 hours this probability in the middle and the upper troposphere is, in general, equal to 60-75 percent (up to the altitudes of 8-12 km), while at higher altitudes it becomes smaller or close to 50 percent. For a time exceeding 6 hours the

Table 5. The Probability of the Preservation of the Turbulence or Its Absence (in percent)

H in km	Time (in Min)					
	0-60	60-90	90-180	180-270	270-360	360-450
0-2	81	55	66	57	62	47
2-5	92	62	65	61	54	63
5-8	79	69	59	76	64	48
8-12	78	59	67	68	64	70
12-16	-	57	52	52	44	50
16-20	-	63	59	52	43	40

probability at almost all levels is less than or close to 50 percent. The stable nature of the preservation of turbulence in the 8-12 km layer may be explained, apparently, by the fact that here the turbulence is determined by such relatively constant factors as the effect of the tropopause and the maximum wind level.

In order to determine the stability of turbulent zones and their relationship to the temperature and the wind propagation at different altitudes under definite synoptic conditions, let us consider the vertical time cross section of the atmosphere, constructed from the observation data of October 27, 1961.

During a more frequent series of observations, the region of observations (at Dolgoprudnaya) was to the northwest of the periphery of an anticyclone, the center of which was north of the Caspian Sea. There was a stationary front, 300-350 km from Moscow, oriented along the latitudinal circle.

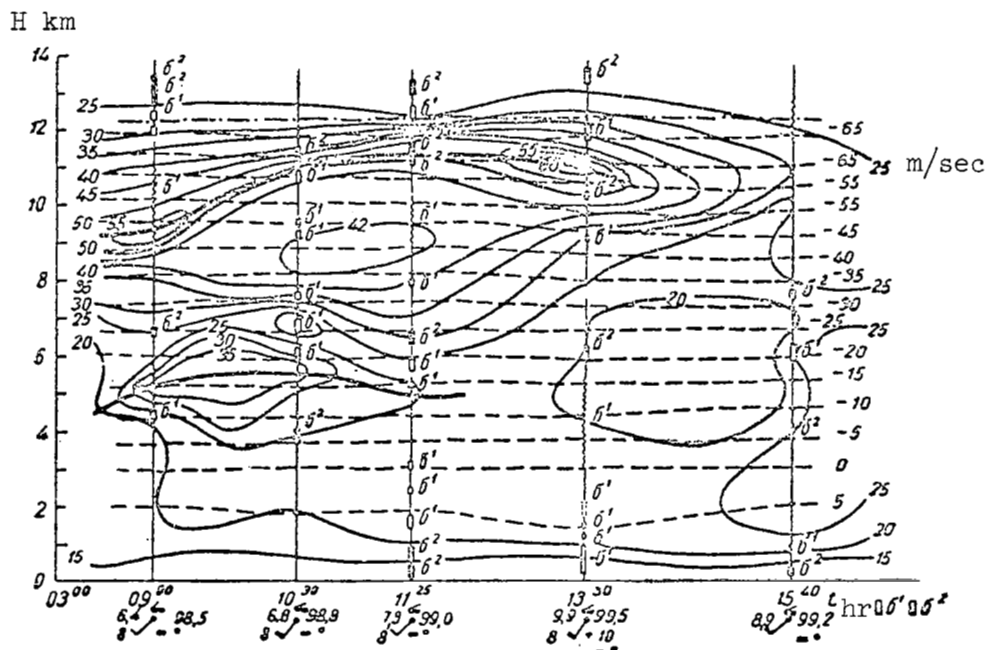
On the AT_{200} and AT_{300} maps for the Moscow region one could see westerly flows with a velocity of 40-60 m/sec. The jetstream axis passed from the south of Scandinavia to the Gulf of Riga in the Rybinsk region. From there one branch of the stream passed to the Kotlas-Syktvykar region and then south of Omsk, while the other branch went to Kazan' and northern Kazakhstan. The maximum wind velocity in the stream was about 80 m/sec. Moscow was in the southern part of the stream and the wind velocity here was 40-60 m/sec. In the Moscow region we observed a solid overcast at the intermediate level (alto-cumulus).

The launchings of A-22 radionsondes with shift-measuring attachments were done on this day from 0900 until 1600, with one and a half hour intervals. There were five launchings.

Using the data of frequent radiosonde launchings and also the data of operational launching at 0300 and 2100 hours, a vertical cross section of the atmosphere was constructed for the Moscow region. This cross section is shown in Figure 15.

The analysis of the temperature field at different altitudes shows that, disregarding the daily variation of the $+5^{\circ}\text{C}$ isotherm, the temperature at the remaining altitudes did not have any significant changes. The tropopause was located at 12,100-12,600 m altitude. The front, located to the north of Moscow, had no apparent effect on the temperature field, with the exception of bringing in cloudiness.

In the wind field one can clearly see two wind velocity maxima. The first of these maxima (37 m/sec) at 5-6 km altitude, was observed in the morning and the second maximum (62 m/sec) at 9-12 km altitude. The latter is associated with the jetstream, the axis of which was located at 10.5-11.0 km altitude.



From the analysis of the cross section it appears necessary to divide the atmosphere over Moscow into several layers. In the first layer, extending from the earth's surface to the altitude of 4 km, during experiments the diurnal variation of the turbulence of the atmosphere was well observable. In the morning the atmosphere in this layer was quiet. The turbulence began to develop after 1030 and by 1130 it occupied the layer up to 3 km altitude. The most intense turbulence was observed in the lower kilometer layer. The intensity weakened with altitude. As a whole the distribution of turbulence was stratified. Unfortunately, it was not possible to launch a radiosonde between 1145 and 1330, consequently it is not possible to trace the development of turbulence in the considered layer. However, at 1330, as may be seen on the cross section, the weak turbulence encompasses a layer up to 2-3 km. Later it weakens and at 1615 it is observed only in the lower layer of the atmosphere.

In the middle and the upper troposphere the turbulent state was determined by the nature of the vertical temperature and wind distribution. The distribution of turbulence in the morning in the layer from 7 to 9 km altitude was characterized by the presence of a nucleus with high wind velocities. It is possible to note two turbulent layers with respect to this nucleus: one above the maximum wind level and the second below it. This characteristic is observed during three periods of observation: 0900, 1030 and 1145.

In the upper troposphere and tropopause, atmospheric turbulence was observed at all times. Just as in the middle troposphere, in the morning in the upper troposphere two turbulent layers were observed with respect to the maximum wind, one above the maximum wind level and the second below it. The most intense turbulence was observed in the layer with large vertical wind gradients. At the maximum wind level the atmosphere was quiet. The distribution of turbulence with respect to the tropopause, as may be seen from the time cross section, is complex in nature. It is almost always observed below the tropopause, but in some cases it is observed in the tropopause layer itself.

Thus, from the analysis of the time cross section of the atmosphere it is possible to make the following conclusions:

(a) Distribution of turbulence along the altitude is complex in nature.

(b) In the lower 1-3 km layer the development of turbulence proceeds according to the diurnal cycle with maximum intensity occurring during the day.

(c) In the upper and the middle troposphere the presence of turbulence is associated with the vertical temperature distribution and the

vertical distribution of wind velocities as well as with the formation of maximum wind velocity levels; two turbulent layers are formed with respect to these levels (one above and one below the maximum wind level); at the maximum wind level the atmosphere is generally quiet.

(d) The turbulence is observed not only below the tropopause, but frequently in the tropopause itself.

(e) The preservation of turbulent layers depends on the degree of preservation of characteristic temperature and wind fields over a given location.

The obtained results, which characterize the turbulence distribution in the free atmosphere from the radiosonde observations, are in good agreement with the results of the airplane investigations (Ref. 13).

5. Turbulence Near the Maximum Wind Level

From the analysis of the time vertical cross section of the atmosphere over Moscow, constructed according to the data from observations conducted on October 27, 1961 (Figure 15), one can observe the characteristics of the distribution of turbulence with respect to the maximum wind level. The distribution of turbulence with respect to the maximum wind level may be pictured as a two-layer model: one layer below the maximum wind level and the second layer above it.

On the basis of theoretical considerations (Ref. 8) it is seen that at the maximum wind level the atmosphere must be quiescent. The presence of turbulence at this level may result only from the diffusion of turbulence from the turbulent layers located above and below the maximum wind level.

The intensity of turbulence in the maximum wind level depends on the location of this level with respect to the altitude of the tropopause, considering that under the tropopause, as a rule, favorable conditions exist for the development of turbulence.

We shall return to this question in Section 7.

Figure 16 shows the distribution of the recurrence of turbulence along the altitude with respect to the maximum wind velocity level over Moscow, Sukhumi, and Tashkent. The recurrence was calculated from the number of cases in 500 m thick layers for the altitude from 0-2.5 km above and below the maximum wind velocity level.

From the analysis of Figure 16, which shows the curves for the vertical distribution of only medium and strong turbulence with respect to

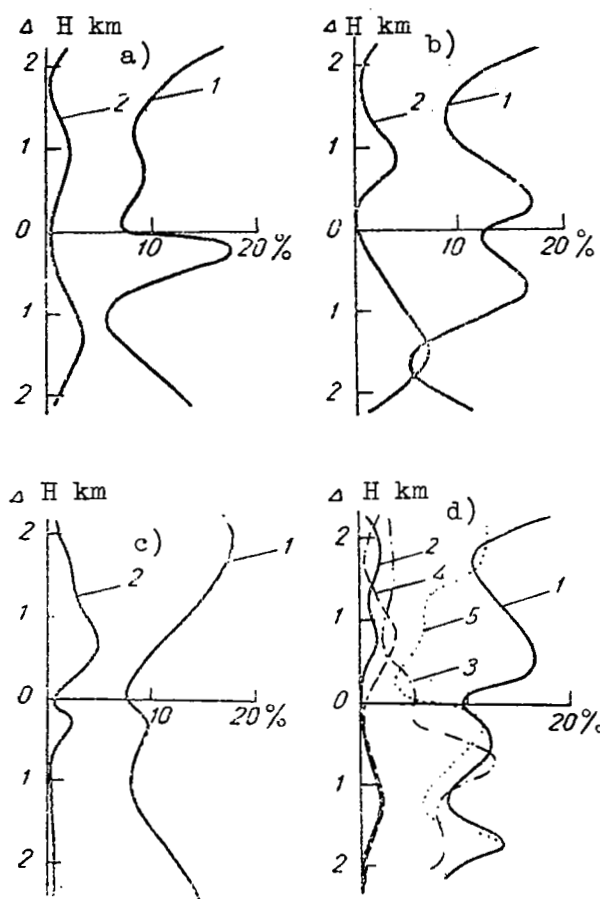


Figure 16. The distribution of the frequency of the occurrence of intermediate (1) and strong (2) turbulence in the maximum wind velocity zone over Moscow, intermediate (3) and strong (4) turbulence over Sukhumi and the intermediate turbulence (5) over Tashkent; a. spring, b. summer, c. autumn and d. winter

the maximum wind velocity level over Moscow, it can be seen that the layers with maximum frequency of occurrence of turbulence above and below the maximum wind velocity level are clearly expressed for all four seasons of the year. Table 6 shows the altitudes of the relative level of the maximum wind velocity, at which the recurrence of turbulence is greatest (including the weak turbulence).

It is apparent from Figure 16 and from the data of Table 6 that in some seasons one may observe not one maximum above and one below the

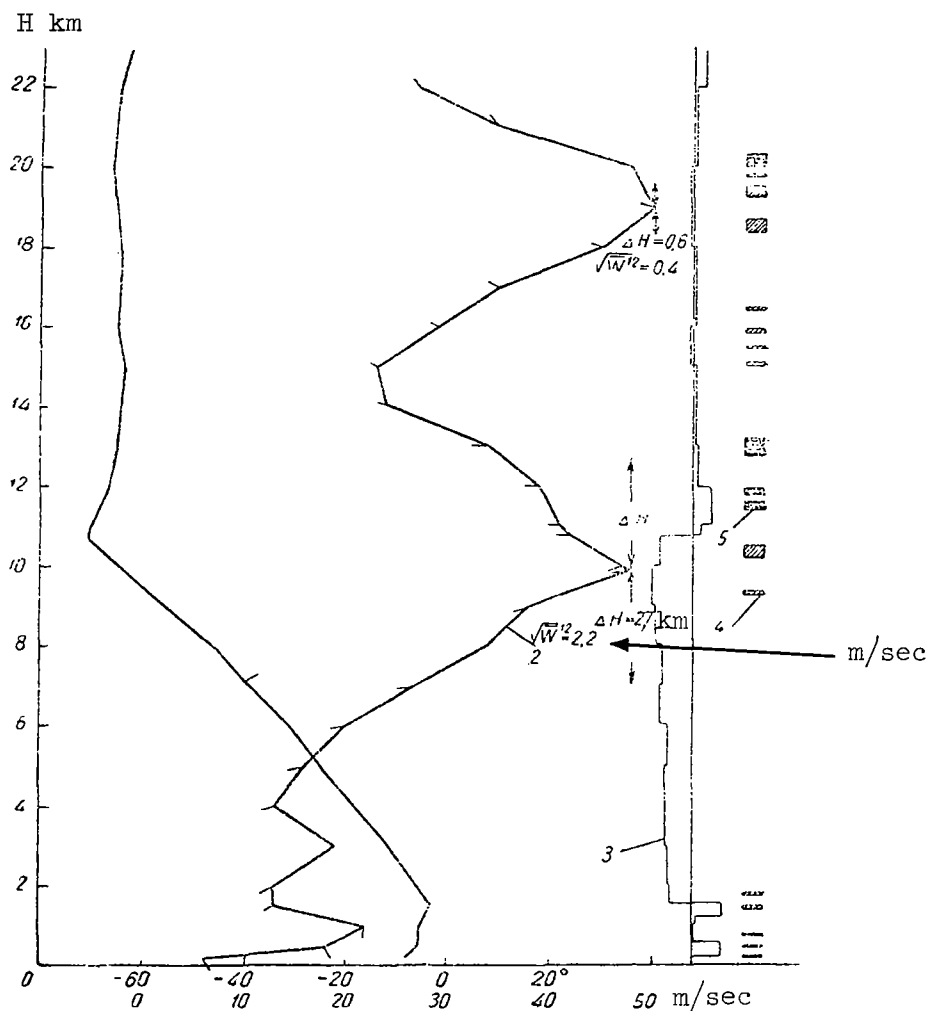


Figure 17. The temperature profile (1) and wind profile (2) over Moscow from the data of radiosonde observations on January 23, 1962; (3) temperature gradient, (4) weak turbulence, (5) intermediate and strong turbulence

maximum wind velocity level, but two above and two below it. In addition, after the maximum recurrence of turbulence above the maximum wind velocity level, almost all recurrence curves show a tendency to increase with altitude.

The distribution of the recurrence with respect to the maximum wind velocity level over Sukhumi and Tashkent is given in Figure 16 and the distribution of altitude with maximum recurrence is given in Table 7.

Table 6. The Maximum Frequency of the Occurrence of Turbulence with Respect to the Maximum Wind Velocity Level (Moscow)

Intensity	Above and below the level	Spring	Summer	Autumn	Winter
δ^1	above	1250	250(1750)	750	1250
	below	750	750	1500	250(1250)
δ^2	above	750	250	1750	500
	below	250	750	250	500(1750)
δ^3	above	1000	750	750	750(1750)
	below	1250	1500	250	1250
$\bar{\delta}$	above	1250	250	1250	750
	below	250	750	250	2000

Note: The altitudes of the second maximum are given in parentheses.

Table 7. The Maximum Frequency of the Occurrence of Turbulence with Respect to the Maximum Wind Velocity Level (Winter)

Intensity	Above and below the level	Sukhumi	Tashkent
δ^1	above	750	750
	below	250	1250
δ^2	above	250(1250)	750(1750)
	below	750(1750)	250
δ^3	above	750	-
	below	1250	-
$\bar{\delta}$	above	750	750
	below	750	1750

The described nature of the distribution of turbulence with respect to the maximum wind velocity level is observed not only in the troposphere, but also in the stratosphere. For illustration we show in Figure 17 the results of radiosonde measurements of the atmospheric turbulence conducted on January 23, 1962. On this day a characteristic wind velocity distribution was observed for the winter season--westerly wind to very high altitude, maximum wind velocity near the upper boundary of the troposphere, and the second wind velocity maximum in the stratosphere at an altitude of approximately 19 km. This figure shows a two-layer distribution of turbulence with respect to the maximum wind velocity in the troposphere as well as in the stratosphere. It is interesting to note that the same distribution of the turbulent layer is observed in the stratosphere also with respect to the minimum wind velocity level, but with much greater stratification.

6. Comparison of Observations of Turbulence with Calculated Data for Jetstreams

In 1960 D. L. Laykhtman and V. A. Shnaydman (Refs. 7, 8) developed a theoretical calculation method for the parameters of atmospheric turbulence in jetstreams (in the maximum wind velocity region knowing the experimental values of the vertical temperature and wind velocity distribution). In deriving the calculation formulas it was assumed that in the jetstream zones smoothing of the geostrophic wind profile occurred, produced by the large horizontal temperature gradients. The degree of smoothing of the geostrophic wind shows the degree of the perturbation of the atmosphere. In addition it is assumed that the profile of the windstream is symmetrical with respect to its axis, the horizontal velocity gradients of geostrophic wind are equal to 0 and the turbulence is isotropic in nature.

The investigations of Laykhtman and Shnaydman enable us to calculate from the known true temperature and wind velocity distribution the value of the turbulence coefficient, the thickness of the turbulent layer as well as the root-mean-square value for the pulsation of the velocity of the wind (gustiness) for the region in the proximity of the jetstream. The method for such calculation has been described in Refs. 1 and 8, from which it is apparent that the calculation method may be used only when the wind velocity difference at the maximum and at its periphery is not less than 15-18 m/sec.

The data of 326 radiosonde launchings, conducted in Moscow, were utilized by us for calculations of the presence of the turbulence in jetstream zones and were compared with indications of shift-measuring attachments of the radiosondes.

For calculations we use only those cases in which the velocity drop was not less than 16 m/sec. There were 72 such cases from July, 1961, until September, 1962, i.e., only 22 percent of all launched radiosondes.

Figure 17 shows the results of calculations of turbulence for one specific case of tropospheric and stratospheric maxima of wind velocity.

The results of calculations of the gustiness of the wind, w' , are compared in Table 8 with turbulence data from the radiosonde measurements.

In this table for all cases of the jetstream the data are given on the presence (pos) and the absence (neg) of turbulence from the indications of the radiosonde measurements depending on the calculated values of the gustiness of the wind. From the data of Table 8 it is apparent that when the values of w' are ≤ 1 m/sec the turbulence was recorded by the radiosonde only once. When the values of $w' > 1$ m/sec and

Table 8. The Presence of Turbulence for Different Values of w' (in m/sec) from the Radiosonde Data

Presence of turbulence	$w' \leq 1$	$1 \leq w' \leq 2$	$w' > 2$
Positive.	1	13	16
Negative.	10	20	12

$w' > 2$ m/sec, the turbulence was recorded by the radiosondes in 13 out of 33 cases (39 percent) and in 16 out of 28 cases (57 percent), respectively. Thus, with an increase of the vertical velocity of wind gusts the probability of agreement between the calculated data and the indications of the radiosonde increases.

In addition, we made comparisons between the calculated values of w' and the intensity of turbulence from the radiosonde data. These comparisons showed that the turbulence observed is weak when the values of w' exceed 1.9 m/sec, medium when w' exceeds 2.3 m/sec and strong when w' exceeds 2.1 m/sec. However, the scattering around these mean values is very great. For example, the weak turbulence from the indications of radiosondes was observed at values from 1.1 to 3.4 m/sec, intermediate from 1.2 to 3.1 m/sec and strong from 1.5 to 3.1 m/sec. In addition, in 31 cases in which w' was greater than 1 m/sec, the radiosondes showed no turbulence.

Thus, it was not yet possible to find a reliable relationship between the intensity of turbulence from radiosonde data and the calculated data. At the same time, let us note that the comparison of the calculated data on the gustiness of the wind with the intensity of tossing of the TU-104 and IL-28 airplanes showed that weak tossing would be expected when the values of w' are ≥ 1 m/sec, intermediate tossing when $w' \geq 3$ m/sec, and in this case a large scattering of values of w' is also found at a given intensity of airplane tossing (Ref. 13).

7. Turbulence Distribution in the Tropopause Region

Let us pause now on the characteristics of the distribution of the recurrence of turbulence in the tropopause zone, taking into account its intensity. The presence or the absence of turbulence was determined by us separately for layers lying above and below the tropopause. The following layers were considered: 0-500, 500-1000, 1000-1500, 1500-2000 and 2000-2500 m.

Theoretical (Refs. 3, 8, 9) and experimental (Ref. 13) investigations have shown that in the tropopause region one may observe turbulence. The occurrence of turbulence is most frequently associated with the

formation of short gravitational waves, on such interfacial surface as the tropopause, and the loss of stability by these waves. The analysis of airplane investigation data have shown (Ref. 13) that the turbulence distribution in the tropopause zone depends on the type of tropopause. In the inversion tropopause the turbulence is sharply lowered at the lower tropopause boundary, and approximately 500-1000 m above and below it on the distribution curve maxima of recurrence and the intensity are observed. In the inversion tropopause the greatest turbulence was observed above the tropopause and in the tropopause itself. The turbulence decreased with altitude.

Let us note that from the data of many years, over Moscow in 23 percent of the cases one observes the first type of tropopause (direct transition into the stratospheric isothermality), in 64 percent of the cases the inversion type and in 13 percent of the cases a tropopause with a reduced type of temperature gradient. Thus, most frequently one finds the inversion type of tropopause.

The distribution of turbulence in the tropopause zone depends, to a certain extent, on the relationship between the altitude of the tropopause and the altitude of the maximum wind. In this connection one may picture the following three models for the distribution of turbulence with respect to the tropopause: single layer, double layer and triple layer (Figure 18).

The single-layer model of the distribution of the recurrence of turbulence is observed in the case when there are weak winds in the tropopause region with which one observes almost no pronounced tropopause maxima of the wind velocity. In such a case the maximum of the frequency of recurrence of turbulence and the intensity maximum of turbulence are observed in the form of one layer (Figure 18a) just below the tropopause.

The two-layer model was observed when the altitude of the tropopause and the level of the maximum wind velocity almost coincide (Figure 18b), or when the tropopause is above the maximum wind velocity level (Figure 18c). In the first case one may observe one turbulence layer below the tropopause, strengthened by the effect of the jetstream (maximum wind), and the second turbulence layer in the tropopause, resulting from the effect of the jetstream.

In the second case (Figure 18c) we may observe two turbulent layers under the tropopause where the turbulence layer directly under the tropopause is strengthened by the effect of the jetstream.

The three-layer model for the distribution of the recurrence of turbulence in the tropopause zone may be observed when the level of the maximum wind velocity is located above the tropopause (Figure 18d). In

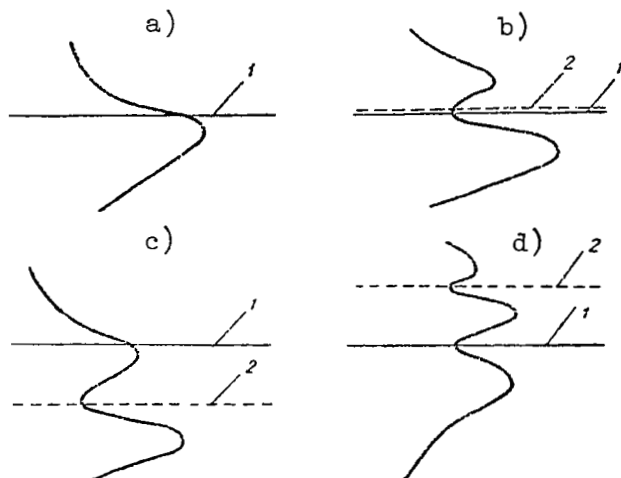


Figure 18. Schemes of the distribution of turbulence in the tropopause region; 1 - tropopause level, 2 - maximum wind velocity level

this case the two turbulent layers are located above the tropopause and one layer is located below it. The upper two layers result from the effect of the jetstream (maximum wind).

Let us note that the three-layer model of the turbulence distribution in the tropopause region is most frequently observed in the cyclonic part of the jetstream, where generally the maximum wind level is located above the tropopause, and the two-layer model, shown in Figure 18b, in the anticyclonic part of the jetstream.

Naturally, models c and d (Figure 18) may be observed with relatively small differences of altitudes between the tropopause and the maximum wind level.

Table 9 shows the frequency of recurrence of the difference between the altitude of the tropopause and the altitude of the maximum wind velocity over Moscow for all four seasons of the year. This data was obtained from many years of observations (Ref. 3). In Table 9, $\Delta_1 z$ is

the thickness of the layer below the tropopause and $\Delta_2 z$ is the thickness of the layer above it.

From the data of this table it is apparent that in the spring and summer in 33-34 percent of the cases the tropopause over Moscow lies below the maximum wind level; in the autumn this occurs in 39 percent of all cases, and in the winter in 54 percent of the cases. It follows that

Table 9. The Frequency of Recurrence (in percent) of Differences between the Altitude of the Tropopause and the Altitude of the Maximum Wind Velocity Level

Seasons	$\Delta z > 0$	$\Delta z < 0$	$\Delta_1 z \leq 3 \text{ km}$	$\Delta_2 z \leq 3 \text{ km}$	$ \Delta z \leq 3 \text{ km}$
Spring.	67	33	54	20	74
Summer.	66	34	53	29	82
Autumn.	61	39	48	28	76
Winter.	46	54	36	18	54

in the autumn and especially in the winter over Moscow one should observe a three-layer model for the distribution of turbulence in the tropopause zone. This is in good agreement with the data of Table 6.

The described schemes for the distribution of turbulent layers in the tropopause region could not be completely verified by the airplane data on turbulence at high altitudes due to the relatively low ceiling for the airplane flights (10-12 km). The radiosonde observations, reaching the altitudes of 25-30 km, helped to fill this gap.

From the analysis of data from the radiosonde observations of the atmospheric turbulence over Moscow, it was possible to establish that the frequency of occurrence of the single layer turbulence (a) comprises 31 percent, the double layer turbulence (b) comprises 39 percent, the double layer turbulence (c) comprises 19 percent, and the triple layer turbulence (d) comprises 11 percent. At the same time in approximately 30 percent of the cases the atmosphere in the tropopause region was quiescent--primarily when the single-layer conditions prevailed.

The results of calculations of turbulence distribution in the tropopause zone, taking into account the intensity, for all four seasons over the Moscow zone, and for winter over Sukhumi and Tashkent, are given in Figure 19. In this figure the dotted line indicates the most frequently occurring thickness of the tropopause layer (500-1000 m).

This figure first shows that below the tropopause in all seasons of the year one observes one maximum of the recurrence of turbulence. Second, it shows that in the autumn and winter two maxima are observed above the tropopause with higher frequencies of turbulence occurrence. In addition, Figure 19a and especially 19b show that under the layer with increased turbulence, located under the tropopause, there is pronounced minimum of the turbulence recurrence from which, down to the middle troposphere, an increase of the frequency of turbulence occurrence takes place. Such a shape of the frequency of turbulence occurrence curves is associated with the fact that in the troposphere in the spring and particularly in the summer one observes an increased turbulence

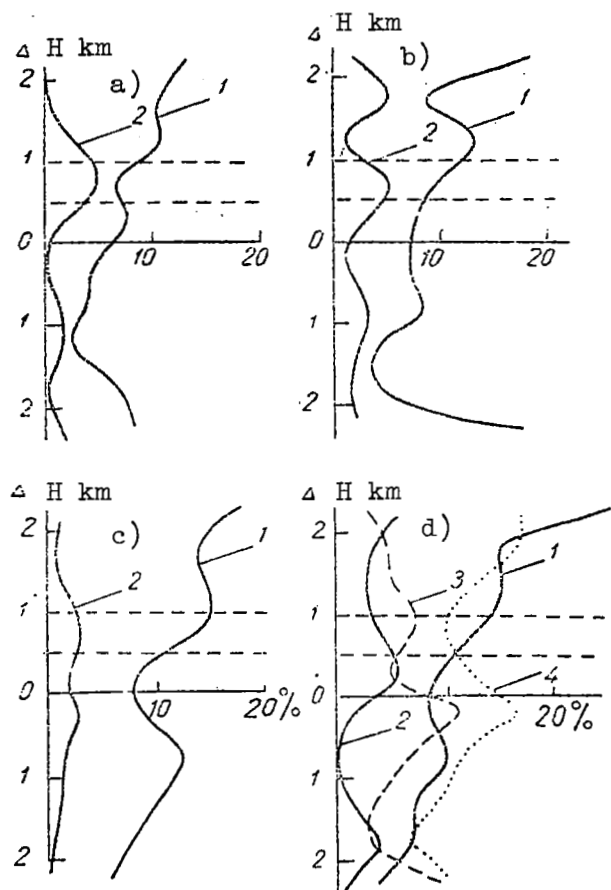


Figure 19. The distribution of the frequency of the occurrence of intermediate (1) and strong (2) turbulence in the tropopause zone over Moscow, intermediate turbulence over Sukhumi (3) and Tashkent (4).
 a. spring, b. summer, c. autumn, d. winter

resulting from the thermal instability of the atmosphere and the development of strong convective cloudiness (Figures 10-12).

In Tables 10 and 11 the altitude is given for the maximum recurrence of turbulence with respect to the altitude of the tropopause, including weak turbulences. The analyses of the data in Table 10 show that in the spring the weak turbulence is distributed with respect to the tropopause in the form of a two-layer model according to Figure 18c; the medium turbulence is distributed according to the three-layer model of Figure 18d; and, strong turbulence is distributed according to the two-layer model in Figure 18b.

Table 10. The Altitude (in m) with Maximum Frequency of Occurrence of Turbulence with Respect to the Tropopause (Moscow)

Intensity	Above and below the tropopause	Spring	Summer	Autumn	Winter
δ^1	above	1250	250	750	250
	below	250(1250)	750	1750	1250
δ^2	above	250(1250)	1250	750	1250
	below	500	750	750	750(1750)
δ^3	above	750	750(1750)	750	250
	below	1000	1000	250	1750
$\bar{\delta}$	above	1250	1250	750(1750)	250
	below	-	750	1750	1000

Table 11. The Altitude (in m) with Maximum Frequency of Occurrence of Turbulence with Respect to the Tropopause (Winter)

Intensity	Above and below the tropopause	Sukhumi	Tashkent
δ^1	above	750	750
	below	250(1750)	1250
δ^2	above	200	750(1750)
	below	750(1750)	250
δ^3	above	750	-
	below	1250	-
$\bar{\delta}$	above	750	750
	below	750	1750

In the summer weak and intermediate turbulence is distributed with respect to the tropopause in the form of a two-layer model of the scheme in Figure 18b, while the strong turbulence is distributed according to the three-layer model.

In the winter the weak turbulence is distributed according to the three-layer scheme, intermediate turbulence according to the two-layer scheme (c) and strong turbulence according to the two-layer scheme (b).

During the analyses of the data of Table 11, it is necessary to keep in mind the relatively small number of observations which were conducted in the winter in Tashkent (23 observations). Taking this into account the distribution of the strong and intermediate turbulence with respect to the tropopause over Sukhumi (as can be seen from the table) coincides with the distribution over Moscow (the strong turbulence according to the scheme b and the intermediate turbulence according to c).

The discrepancy occurs only in the distribution of the weak turbulence, which over Sukhumi proceeds according to the two-layer scheme c; over Tashkent according to the two-layer scheme b; and over Moscow it is distributed according to the three-layer scheme d.

8. Turbulence and the Vertical Distribution of Wind and Temperature in the Atmosphere

Above we have considered certain conditions for the development of turbulence in the atmosphere. Specifically, we have seen that turbulence could be observed in the tropopause zone as well as in tropospheric and stratospheric regions of the maximum wind velocity. The distribution and nature of turbulent layers in the upper troposphere depend significantly on the mutual distribution and altitude differences between the tropopause and the maximum wind velocity level.

Turbulence may be observed not only in the maximum wind velocity region, but also in the region of the minimum wind velocity. The regions with extreme wind velocities are regions with sharp discontinuities in the vertical wind profile, where, as it follows from the investigations of Rayleigh, for the uniform temperature medium, favorable conditions prevail for the disturbance of the stability of the stream and the development of turbulence.

Under the real atmospheric conditions, where an important role is played by the thermal stratification, the discontinuities in the wind velocity profile may lead to the disturbance of the dynamic stability of the atmosphere. However, the extent of the disturbance of the stability may be either increased or weakened by the thermal stratification. In this connection it is of interest to consider the distributions of the vertical temperature gradients and vertical wind velocity gradients in turbulent layers, as detected by the radiosondes. It should be stressed again that turbulence data, vertical temperature gradients, and vertical wind velocity gradients are synchronous and refer to the same layer of the atmosphere.

Figure 20 shows curves for the distribution of the frequency of occurrence of vertical temperature gradients and mean wind velocity in the turbulent layers at the following altitudes: 0-2, 2-5, 5-8, 8-12, 12-16, 16-20 and those above 20 km. It is seen from this figure that in the 0-2 km atmospheric layer the turbulence is observed in a broad range of values of the vertical temperature gradient, from -2.5°C to $+2.5^{\circ}\text{C}/100\text{ m}$, i.e., in the inversion layers as well as in layers with superadiabatic temperature gradients. The recurrence of superadiabatic temperature gradient for weak turbulence comprises 14.2 percent and for intermediate and strong turbulences comprises 15.5 percent.

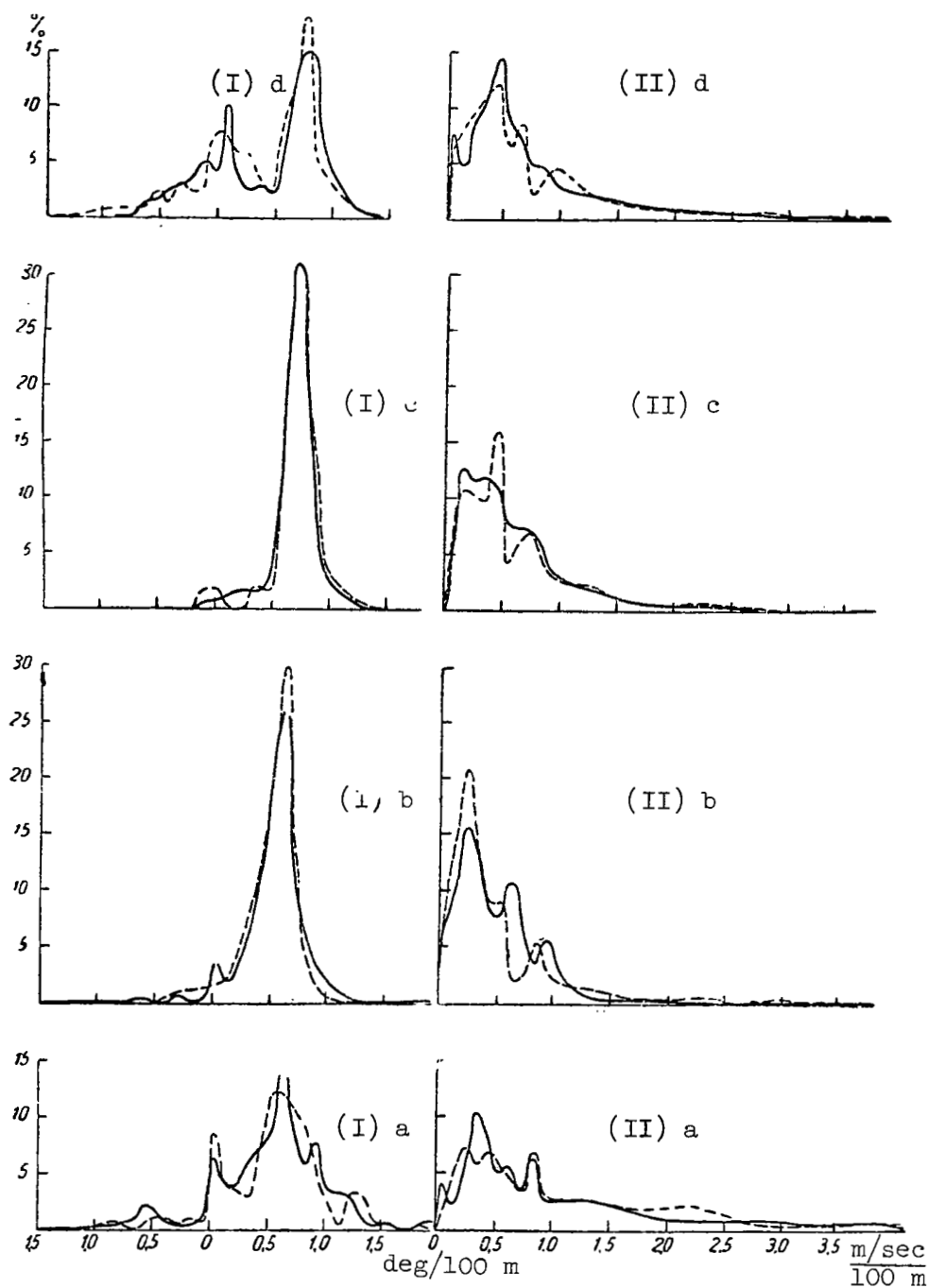


Figure 20. Curves for the recurrence of vertical gradients (I) and wind velocity gradients (II) in the turbulent atmospheric layers for weak (1) and intermediate and strong (2) turbulences. a - 0-2 km, b - 2-5 km, c - 5-8 km, d - 8-12 km, e - 12-16 km, f - 16-20 km, g - over 20 km

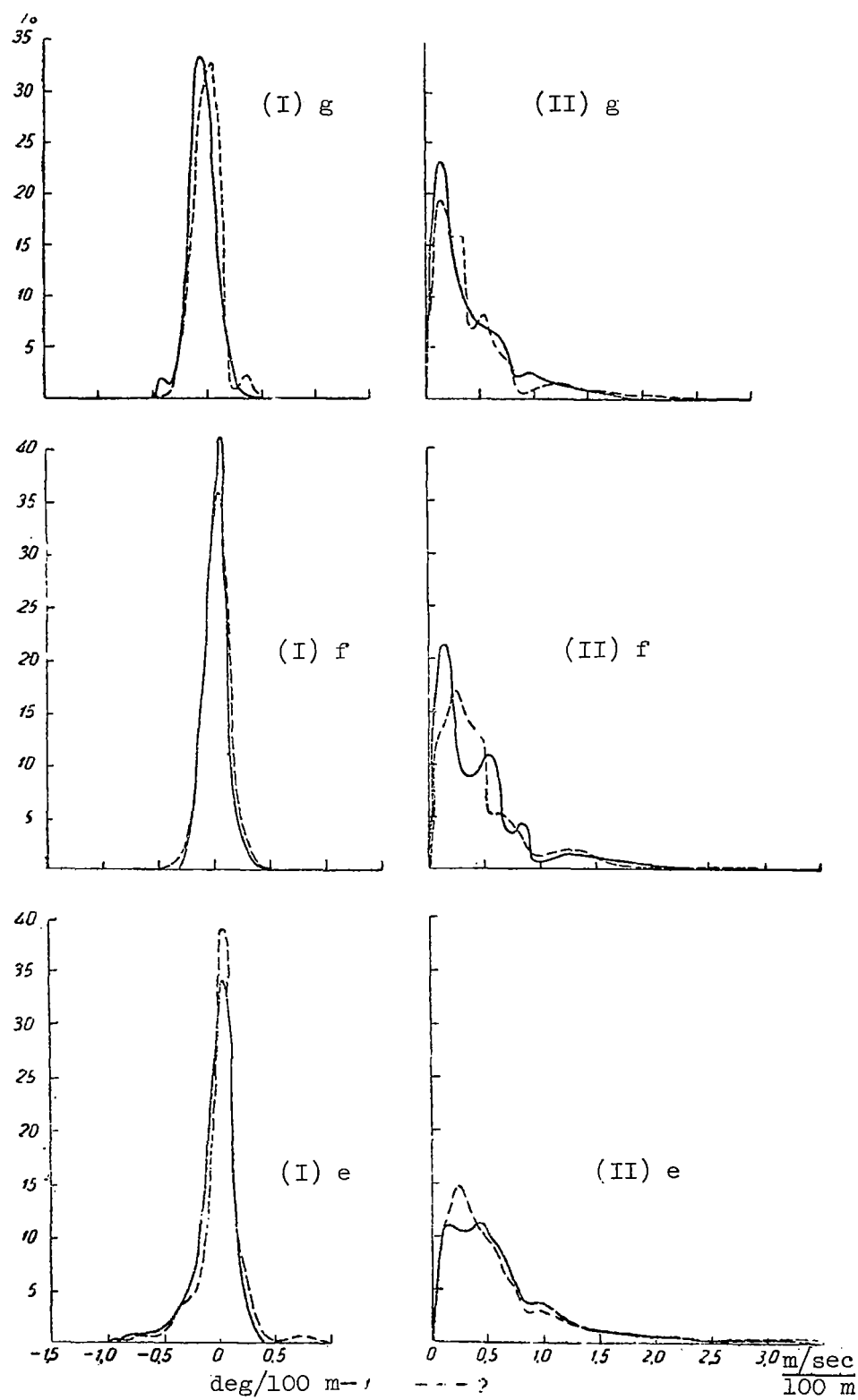


Figure 20. Continued

The main recurrence maximum on the distribution curve falls on the values of temperature gradients of the order of $0.6-0.7^{\circ}\text{C}/100\text{ m}$, and the secondary maximum occurred where the gradients were $0.0-0.1^{\circ}/100\text{ m}$. The distribution curve of the vertical temperature gradient for medium turbulence almost traces the curve for the weak turbulence. The difference lies only in that the principal maximum of the recurrence is not sharp.

It was shown in Ref. 15 that the turbulence which causes airplane tossing in the lower part of the troposphere over Moscow is also frequently observed in the presence of isothermality or the inversion of temperature.

In considering the distribution curves for the recurrence of the vertical gradients of wind velocity in the 0-2 km layer it is apparent that these curves are characterized by a "long band" of large values of the vertical gradients, reaching $6-8\text{ m/sec}/100\text{ m}$ of altitude. It is characteristic that the recurrence of vertical wind velocity gradients exceeding 1 m/sec comprises about 40 percent for the weak turbulence and for the medium and strong turbulence about 50 percent, although the recurrence maximum falls on values of the order of $0.4-0.5\text{ m/sec}/100\text{ m}$. Thus, turbulent layers as a whole in the lower 2 km layer are characterized by large wind velocity gradients.

Let us now consider the distribution of gradients in the 2-5 km layer of the atmosphere, i.e., in the middle troposphere. Figure 20 shows that distribution curves of the vertical temperature gradient are characterized by a sharp recurrence maximum for the gradients of the order of $0.6-0.7^{\circ}\text{C}/100\text{ m}$ of altitude. At this altitude one observes in turbulent layers the negative (for weak turbulence 3.5 percent, for intermediate and strong turbulence 1.8 percent, as well as superadiabatic vertical temperature gradients (1.2 and 0.6 percent, respectively). The secondary recurrence maximum is preserved only for the weak turbulence. As far as the distribution of the vertical wind velocity gradients is concerned, the band with gradients greater than $1\text{ m/sec}/100\text{ m}$ comprises 11 percent for weak turbulence and 11.9 percent for intermediate and strong turbulence. In addition, more pronounced secondary maxima occur for the wind velocity gradients lying within $0.5-1.0\text{ m/sec}/100\text{ m}$ limits.

In the upper troposphere at 5-8 km altitudes, the recurrence curves of the vertical temperature gradients have a sharp maximum for the values of $0.6-0.8^{\circ}/100\text{ m}$. The recurrence of superadiabatic gradients comprises about 1-2 percent, the negative temperature gradients about 1.5 percent for weak turbulence, and 3.5 percent for intermediate and strong turbulence. The wind velocity gradients of $0.1-0.4$ for weak turbulence and $0.4-0.5$ for intermediate and strong turbulence are most frequent. The vertical gradients exceeding $1\text{ m/sec}/100\text{ m}$ recur to the extent of 17.7 percent for weak turbulences and 20.3 percent for intermediate and strong turbulences. Thus, in the upper troposphere (as compared with the middle

troposphere) one observes most frequently in turbulent layers the temperature gradients which are close to the adiabatic and relatively large vertical wind velocity gradients.

The effect of the tropopause on the distribution of vertical temperature gradients in turbulent layers is generally apparent at 8-12 km altitudes. It can be seen from the curves in Figure 20 that the recurrence has two maxima: the principal maximum is in the region of temperature gradients from 0.7 to $0.8^{\circ}/100$ m of altitude, and the second maximum is in the region of -0.1 to $+0.1^{\circ}/100$ m of altitude. The turbulence is rather frequently observed in the case of negative temperature gradients in the tropopause (to the extent of 23-24 percent). The large temperature gradients (greater than $1^{\circ}/100$ m) are observed for weak turbulence in 2.6 percent of all cases, and for the intermediate and strong turbulence in 3.5 percent of all cases. At these altitudes weak turbulence is observed in 24.7 percent of all cases, when the wind velocity gradients are greater than 1 m/sec/100 m, and intermediate and strong turbulence is observed in 27.7 percent of all cases.

In the stratosphere (as may be seen from Figure 20), the vertical temperature gradients lie within -0.5 to $+0.5^{\circ}/100$ m of the altitude. Only at 12-16 km altitudes was intermediate and strong turbulence observed in 0.3-0.4 percent of the cases when the temperature gradients were from 0.5 to $1^{\circ}/100$ m and in 2-3 percent of all cases when the gradients were -0.5 to $-1.0^{\circ}/100$ m. The curves for the recurrence of the vertical wind velocity gradients in the stratosphere generally have broad maxima occurring at 0.2 - 0.5 m/sec/100 m gradients. The vertical wind velocity gradients which exceed 1 m/sec/100 m are found at altitudes of 12-16 km for the weak turbulence in 18.4 percent of all cases, and for intermediate and high turbulence in 19.3 percent of all cases. At 16-20 km altitudes these occur in 12.6 percent and 11.7 percent of all cases, respectively; above 20 km the recurrence is 9.3 percent and 14.2 percent, respectively. It can be seen that in the stratosphere an important role is played by the relatively large values of the vertical wind velocity gradients.

In order to evaluate the dynamic and thermodynamic conditions for the development of turbulence, use is made, as is well known, of the Richardson number:

$$Ri = \frac{g}{T} \frac{\gamma_a - \gamma}{\beta^2}, \quad (36)$$

where γ_a is the vertical adiabatic temperature gradient; γ is the observed temperature gradient; β is the vertical gradient of the mean wind velocity; T is the mean air temperature in the given layer; and, g is the acceleration due to the force of gravity.

Table 12. The Recurrence of the Values of Ri (in percent) in Turbulent Layers (over Moscow)

H (in km)	$Ri \leq 0.5$	$0.5 < Ri \leq 1.0$	$1 \leq Ri \leq 4$	$4 < Ri \leq 10$	$Ri > 10$
0-2	46	10	14	12	18
2-5	15	5	27	18	35
5-8	11	10	25	19	25
8-12	13	9	20	19	40
12-16	5	2	13	15	65
16-20	0.2	0.8	7	13	79
>20	-	1	9	8	82

For the water-vapor-saturated air and for clouds, instead of γ_a , the humid adiabatic temperature gradient (γ_{ha}) is used. In our calculations, for the atmosphere an altitude of 5 km, we used γ_{ha} equal to $0.8^\circ\text{C}/100 \text{ m}$. The recurrence of the Ri value for the turbulent layers, detected by means of radiosondes, is given in Table 12.

From the data of this table it is apparent that with values of $Ri \leq 1$ in the 0-2 km layer of the atmosphere, turbulence was observed in 56 percent of all cases; in the 2-5 km layer in 20 percent of all cases; in the 5-8 km layer in 21 percent of all cases; in the 8-12 km layer in 22 percent of all cases; in 12-16 km layer in 7 percent of all cases; and, above 16 km the turbulence was observed in 1 percent of the cases.

The increase of the recurrence of $Ri > 10$ with the increase of altitude is associated with the decrease of the role of thermal stratification, and due to the increase of the role of vertical wind velocity gradients. However, in using the Richardson number it is necessary to recall that turbulent layers are arranged in a definite manner with respect to the maximum wind velocity level in the presence of discontinuities in the vertical wind profiles. This is extremely important in the consideration of the conditions for the development of turbulence in the stratosphere.

Conclusions

A. Methods and Apparatus for Measurement of Atmospheric Turbulence by Means of Radiosondes

1. In 1960-1961 a device was developed and tested at the Central Aerological Observatory, which enabled the authors to obtain (using a

serial production A-22-III radiosonde) and to record on the earth data on the acceleration of the radiosonde in flight.

2. A special attachment to the radiosonde converts the changes of tension on the suspension into the change of the duty ratio of the radio frequency pulse. The measurement of the duty ratio of the video signal at the output of the "Malakhit" radiotheodolite enabled the authors to obtain, continuously in the course of the whole flight, information on the shifts of the radiosonde, and to transmit it on the same channel which is being used for the transmission of information on the distribution of meteorological parameters in the atmosphere.

3. In 1961-1962 there were 457 launchings of radiosondes equipped with shift-measuring attachments. Of these, 326 were launched in Moscow (Dolgoprudnoye), 89 in Sukhumi, and 42 in Tashkent.

4. The theoretical and experimental investigations of the behavior of the shift-measuring radiosonde in flight enabled the authors to establish the following.

a) During the entry into an accelerated airstream, the acceleration of the balloon tends to become equal to that of the stream. The time constant of the sounding balloon does not exceed 1 sec.

b) The presence of slowly damped oscillations on the recording with a period of the order of 3 sec may be explained by the rocking of the instrument in flight.

c) The system may display longitudinal oscillations which are determined by the spring constant of the instrument and by the elasticity of the balloon and its appendix. However, the free oscillations of the system, after cessation of the external interaction, stop in 2-3 sec. Thus, the recorded sections with short-period oscillations are associated with the interaction of turbulent pulsations of the air velocity. Considering the rapid damping of free oscillations in the system, it may be considered that the error in the determination of the thickness of the turbulent layer, even at the rate of lift of the order of 8 m/sec does not exceed 25-30 m.

d) The dimensions of turbulent formations in the atmosphere to which the shift-measuring radiosonde reacts are of several meters.

5. The comparison of the radiosonde and the airplane data on the turbulence in the kilometer thick layers showed that in 61 percent of the cases the data obtained by means of radiosondes and airplanes are in qualitative agreement. It is necessary to note that the investigations by means of airplanes and radiosondes were not quite synchronous, and that the regions of investigations also did not coincide. For the final

solution of the question on the applicability of the radiosonde data to the evaluation of the probability and the intensity of airplane tossing, it is necessary to conduct experimental flights of airplanes and to make, as much as possible, the region and the time of measurement coincide with the launching of the shift-measuring radiosondes.

B. Characteristics of the Atmospheric Turbulence According to the Data from Radiosonde Observations

1. The distribution of the frequency of the occurrence of turbulence along the altitude, measured by means of radiosondes, is characteristic in nature. The greatest frequency of occurrence is in the atmospheric layer from the surface of the earth to an altitude of 2-3 km. In the middle troposphere the frequency of occurrence is lowest; it increases toward the upper boundary of the troposphere. Similar results were obtained from the data from airplane observations.

2. During all seasons, especially in winter, turbulence is frequently observed in the stratosphere, where the frequency of its occurrence slowly decreases with altitude.

3. The annual change of the frequency of the occurrence of turbulence in the stratosphere is such that the areas with maximum or minimum recurrence in the cold seasons up to an altitude of 20 km result in the formation of two maxima: one at 12-14 km altitude, with the frequency of occurrence equal to approximately 45-50 percent, and the second at 18-19 km altitude with the frequency of occurrence of the order of 30-35 percent. In the stratosphere, during the warm half of the year, the frequency of occurrence is the lowest; in general, it does not exceed 10-20 percent.

4. The thickness of turbulent layers over Moscow and Sukhumi rarely exceeds 200-400 m. Only in the atmospheric layer to 5-7 km over Tashkent may it exceed 1000 m.

5. At the mean latitudes in the winter, the mean thickness of layers with medium and strong turbulence is less than the thickness of the layers with weak turbulence, to an altitude of 8-10 km. In the summer, on the contrary, the thickness of layers with medium and strong turbulence is greater than the thickness of layers with weak turbulence. For the stratosphere the curves of the integral frequency of recurrence of a given thickness of the turbulent layers show that they are, in general, independent of the intensity of turbulence.

6. The turbulent zones over the point of observation are preserved for 1-2 hours with the probability of 75-80 percent, and for 6 hours with the probability of 40-50 percent. In the upper troposphere

and in the stratosphere, the probability of the preservation of turbulent zones for 1-6 hours does not exceed 40-50 percent.

7. There are two turbulent layers observed with respect to the maximum wind velocity level (axis of jetstream): one below this level and one above it. This is in a good agreement with theoretical investigations, and is verified by the airplane investigation data. Turbulence is minimum at the maximum wind level.

8. The distribution of turbulence with respect to the tropopause depends on the relationship between the altitude of the tropopause and the altitude of the maximum wind velocity.

a) In the case of small winds in the upper troposphere one turbulent layer under the tropopause is observed.

b) If the maximum wind velocity level coincides with the altitude of the tropopause, then a strong turbulence layer below the tropopause and a layer of relatively weak turbulence above the tropopause level are observed.

c) If the maximum wind level is located below the altitude of the tropopause, then two turbulent layers are observed; one below the maximum wind level, and the second between the maximum wind velocity level and the tropopause.

d) If the maximum wind velocity level is located above the tropopause, then three turbulent layers are observed: one below the tropopause, the second between the tropopause and the maximum wind velocity level, and the third above the maximum wind velocity level.

9. Atmospheric turbulence is a function of thermal and dynamic stratification of the atmosphere. In the troposphere turbulence is observed most frequently at relatively large vertical temperatures and wind velocity gradients. In the atmospheric layer between the surface of the earth and the 2-3 km altitude, turbulence is frequently observed under conditions of superadiabatic temperature gradients (14-15 percent), as well as in the isothermal inversion layers. In the stratosphere turbulence development is determined primarily by the wind velocity profile (by the presence of discontinuities in the profile and relatively large wind velocity gradients).

References

1. Ariyel', N. Z. and Byutner, E. K. Metodika opredeleniya kharakteristik turbulentnosti v struynykh techeniyakh (Methods for Determining Turbulence Characteristics in Jetstreams). Meteorologiya i gidrologiya, No. 11, 1962.

2. Belyayev, V. P. and Shur, G. N. Izmereniye turbulentnosti na vysotakh s pomoshchyu sharov-zondov (Measurement of the Upper Atmosphere Turbulence by Means of Sounding Balloons). Trudy TsAO, No. 43, 1962.
3. Gandi, L. S. Ob obrazovanii turbulentnykh dvizheniy na frontakh (The Formation of Turbulent Motion at the Fronts). Trudy GGO, No. 76, 1958.
4. Zaychikov, P. F. K voprosu ob izmerenii vertikal'nykh dvizhrniy vozdukha v svobodnoy atmosfere s pomoshchyu grebenchtogo radiozonda (Measurements of the Vertical Motion of Air in the Free Atmosphere by Means of Pectinated Radiosonde). Trudy TsAO, No. 10, 1953.
5. Kalinovskiy, A. B. and Pinus, N. Z. Aerologiya (Aerology). Part I, Leningrad, Gidrometeoizdat, 1961.
6. Krylov, A. N. Lektsii o priblizhennykh vychisleniyakh (Lectures on Approximate Calculations), Moscow, Gostekhizdat, 1954.
7. Laykhtman, D. L. and Shnaydman, V. A. Kriteriy ustanovivsheysya turbulentnosti v struynykh techeniyakh (Criterion for Stabilized Turbulences in Jetstreams). Meteorologiya i gidrologiya, No. 12, 1960.
8. --- K voprosu o turbulentnosti na tropopauze i v struynykh techeniyakh. Nauchnaya konferentsiya po voprosam aviatsionnoy meyeorologii (Turbulence in the Tropopause and in Jetstreams. Scientific Conference on Problems of Aviation Meteorology), Moscow, Gidro-meteoizdat, 1960.
9. Laykhtman, D. L. O volnovykh dvizheniyakh po poverkhnosti razdela v atmosfere (Wave Motion Along the Boundary Surface in the Atmosphere). Trudy GGO, No. 2, 47, 1947.
10. Loytsyanskiy, A. G. and Lur'ye, A. I. Kurs teoreticheskoy mekhaniki (Theoretical Mechanics Course). GTTM, 1954.
11. L'vov, G. M. Teoreticheskiye issledovaniya dvizheniya svobodnogo tela v neustanovivshemsya potoke (Theoretical Investigations of the Motion of Free Body in an Unestablished Stream). Trudy TsAO, No. 22, 1957.
12. Landau, L. D. and Lifshits, Ye. M. Mekhanika (Mechanics). Moscow, Fizmatgiz, 1958.
13. Pinus, N. Z. and Shmeter, S. M. Atmosfernaya turbulentnost', vliyayushchaya na polet samoletov (Atmospheric Turbulence Which Affects the Airplane Flights). Moscow, Gidrometeoizdat, 1962.
14. Pinus, N. A. Tropopaza i uroven' s maksimal'noy skorost'yu vetra (The Tropopause and the Maximum Wind Velocity Level). Meteorologiya i gidrologiya, No. 3, 1961.
15. --- Issledovaniya poryvistosti vozdukhnykh potokov v svobodnoy atmosfere (Study of Wind Gusts in the Free Atmosphere). Meteorologiya i gidrologiya, No. 4, 1946.
16. Prandtl', L. Gidroaeromekhanika (Hydroaeromechanics). IIL, 1949.
17. Riman, I. S. and Kreps, R. L. Obshchiye svedeniya o prisoyedenennykh massakh tverdogo tela v bezgranichnoy zhidkosti (General Information on United Masses of Solids in Unbounded Fluid). Trudy TsAGI, 635, 1947.

18. Shmeter, S. M. Ob obtekanii gornykh prepyadstviy vozdushnymi potokani (Flow of Airstreams Past Mountainous Obstacles). Trudy TsAO, No. 24, 1958.
19. --- Dvizheniye shara-zonda v uskorennom vozdushnom potoke (Motion of a Sounding Balloon in an Accelerated Airstream). Trudy TsAO, No. 22, 1957.
20. Shur, G. N. Eksperimental'nyye issledovaniya energeticheskogo spektra atmosfernoy turbylentnosti (Experimental Studies of the Energy Spectrum of Atmospheric Turbulence). Trudy TsAO, No. 43, 1962.
21. Junge, C. Turbulenzmessungen in den hohoren Atmospharenschichten (Measurements of Turbulence in the Upper Atmospheric Layers). Ann. d. Hydrogr. und Marit. Met. L. XVI H III, 1938.
22. Anderson, A. D. Free-air turbulence. Journal of Meteorology, Vol. 14, 6, 1957.
23. Clodman, I. High level turbulence. Meteor. Branch, Dept. of Transport, Toronto, TEC. Cir. 2332, 160, 1953.
24. Coloson, D. Summary of high-level turbulence over the United States, 1961-1962 (Abstracts). Bull. Am. Meteorol. Soc., Vol. 43, 12, 1962.
25. Hyde, E. A. Air turbulence at high altitudes. A report by Short, Bres, and Harland, test pilots. London, Sidney Barton, Ltd., 1954.

THE TURBULENCE IN JETSTREAMS IN THE CLEAR SKY

A. A. Reshchikova

ABSTRACT

From the measurements of tossing in jetstreams made from the airborne laboratory on the TU-104 aircraft, data were obtained on the probability of occurrence of turbulence as a function of the type of high altitude pressure field, the curvature of isohypses, the horizontal temperature gradients, wind, etc. The article also considers the vertical distribution of turbulent zones with respect to the axis of the jetstream and tropopause.

Introduction

Many investigators have been concerned with the study of clear-air turbulence or the turbulence in jetstreams (Refs. 2, 3, 4, 5). However, in a number of cases the work did not go any further than the pilot reports or, in more sophisticated cases, it proceeded as far as weather forecasters' reports from the aircraft. Such information often was not specific as to locality and often did not have observations of the temperature, the altitude and wind; in addition, aircraft tossing was determined visually.

In this work, use is made of observations taken in the course of 55 special flights of the laboratory planes in 1960-1962. In these flights, the locality was known within an accuracy of 15-20 km, and the temperature as well as pressure and tossing were continuously and synchronously recorded after every 15 seconds. The velocity and the direction of the wind was determined by means of an airborne Doppler unit.

The method of investigating jetstreams in all flights was the same, i.e., at each altitude two to four passes 200-300 km long were made. These passes were made in such a way as to insure the crossing of the stream at different altitudes. In the case of a broad stream, passes were made either in the cyclonic section of the stream or in the anticyclonic section. Several flights were made along the jetstream. Altogether there were approximately 100 passes made in the jetstream. The maximum wind velocity from these sections varied from 100-250 km/hr. Unfortunately, in the intense streams at 200-250 km/hr, there were only seven passes made. Flights were conducted primarily over the European territory of the USSR, and several flights were conducted in the Khabarovsk region.

From the data of these flights, we considered all cases of turbulence under a clear sky at the altitudes of 7-11 km with maximum shifts of tossing indicated by more than ± 0.2 g.

Section 1. The Frequency of Tossing as a Function of the Nature of the High Altitude Pressure Field

Let us consider the frequency of occurrence of turbulence as a function of aerosynoptic conditions, i.e., first of all as a function of the type of pressure field. The type of pressure field is determined from the pressure topography maps for the levels which are the closest to the flight altitude.

Figure 1 shows a map compiled for all flights in the course of 1961-1962 on which each pass over a given form of pressure field is plotted. On the basis of this map, one may form a general conclusion that the areas in which the turbulence is observed most often belong to the leading part of the trough (the trailing side of the anticyclone) during divergent isohypses. This is also supported by the data of Table 1, in which a more detailed distribution of the occurrence of turbulence is given as a function of the type of pressure field. In compilation of this and of subsequent tables, one case of turbulence is taken as one passage

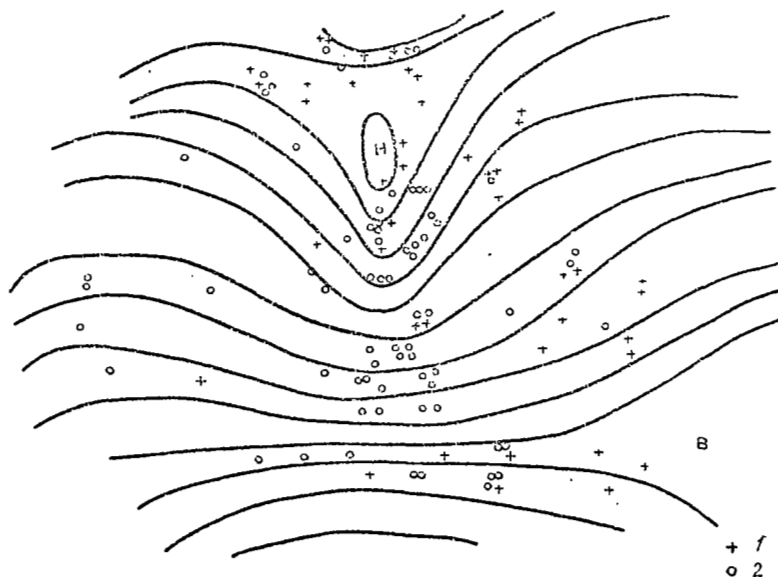


Figure 1. An accumulative map which indicates the distribution of cases (1) with and (2) without tossing from the data of 1961-1962

Table 1. Distribution of the Number of Cases (1961-1962) with Tossing as a Function of the Type of Pressure Field

	Cyclones, troughs				Anticyclones, crests				Saddle-point pressure
	Leading edge	Axis	Trailing edge	Southern periphery	Leading edge	Axis	Trailing edge	Northern periphery	
Total number of passages	20	15	6	29	9	5	12	21	7
Number of passages with aircraft tossing	9	2	1	8	2	-	5	8	6
Frequency of occurrence of aircraft tossing (in percent)	45.0	6.7	13.3	27.5	22.2	-	41.5	38.0	86.0

Tossing in cyclones 28.6 percent

Tossing in anticyclones 31.9 percent

over a definite type of pressure field, where the tossing indication was greater than 0.2 g on at least a small section of the pass.

It is apparent from the data of this table that the greatest recurrence of turbulence was observed in the leading part of a cyclone and in the trailing side of an anticyclone, i.e., in the regions of divergent streams. The frequency of occurrence of turbulence was also significant in the center of the pressure zone.

If one considers the frequency of occurrence of turbulence on one hand for anticyclones and pressure crests and on the other hand for cyclones and low pressure troughs, one may say that the occurrence of turbulence at 7-11 km altitudes is equally probable in cyclones and in anticyclones. This conclusion coincides with data of I. G. Pchelko (Ref. 4), who, on the basis of pilot reports, noted the frequency of the occurrence of turbulence in the high pressure crests and anticyclones to

be equal to or even slightly more than in high altitude cyclones. It is somewhat premature to conclude that the frequency of occurrence of tossing in the trailing side of a high altitude cyclone is insignificant since we have an insufficient number of flights in this region.

Section 2. The Frequency of Occurrence of Tossing as a Function of Curvature of Isohypsers and the Converging of the Flow in Jetstreams

The frequency of occurrence of tossing as a function of the curvature of isohypsers and the verging of the flow was considered for all the flights in jetstreams. During the determination of the curvature of isohypsers, consideration was given to the fact that in some cases it is not possible to identify the direction of the curvature of the isohypsers with any definite pressure field. For example, a trough does not necessarily mean a cyclonic curvature, and a crest does not mean anticyclonic curvature, since on the real forecast maps, other cases are possible. For example, on March 9, 1962, on the Gor'kiy-Kazan' route according to the map AT₃₀₀, at 1500 hours, the flight took place in the

leading part of a high altitude trough while the nature of isohypse curvature was definitely anticyclonic (Figure 2).

It is apparent from the data of Table 2 that the frequency of occurrence of tossing during divergence of isohypsers is significantly greater than during convergence, regardless of the direction of the curvature of isohypsers. In the case of parallel isohypsers, again regardless of the direction of their curvature, tossing is found less frequently than during divergence and convergence of the stream.

Considering all flights which involve more than one passage in the regions with the verging of the flow, it was found that in 9 out of 17

Table 2. Distribution of the Number of Cases of Tossing (1961-1962) during Convergence and Divergence of Isohypsers

	Cyclonic curvature			Anticyclonic curvature		
	Divergence	Parallel	Convergence	Divergence	Parallel	Convergence
Total number of cases	18	33	16	16	21	20
Number of cases with tossing	13	4	5	8	5	6
Same in percent	72.2	12.1	31.1	50.0	23.8	28.4

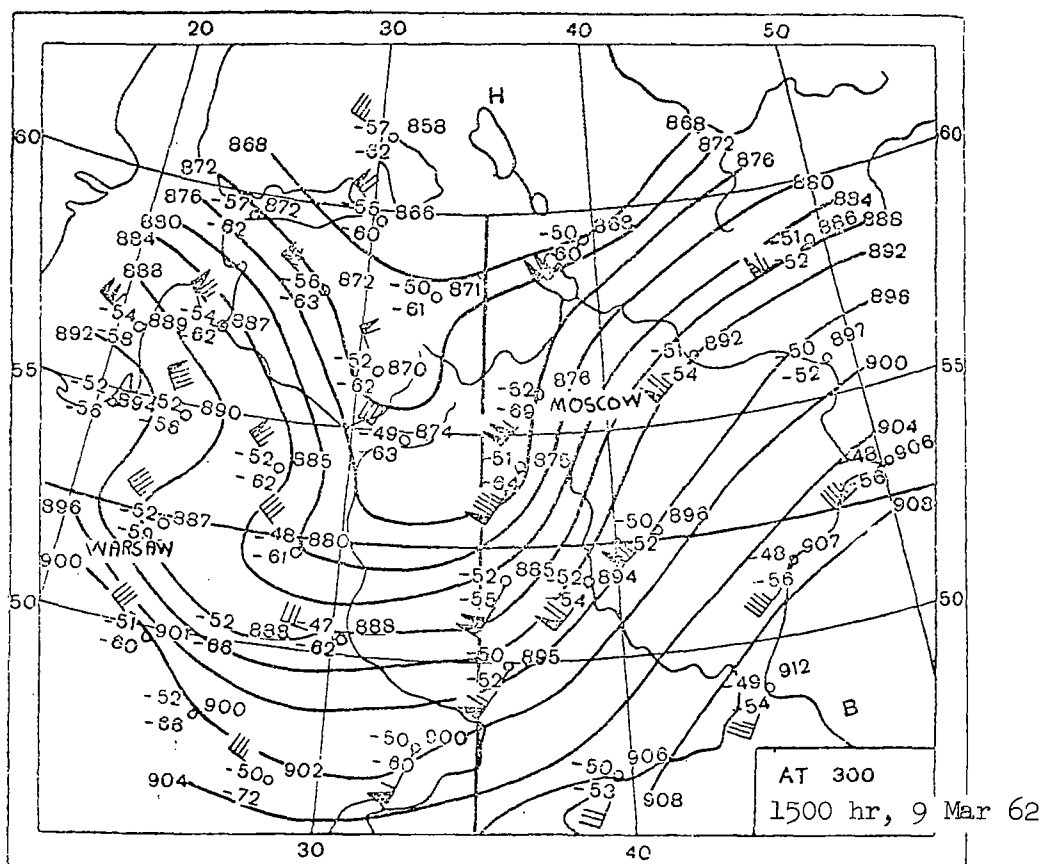


Figure 2

flights during divergence of the stream, tossing was observed during two or more passes (i.e., at two or more altitudes). In the case of convergence of the stream, the multilayer turbulence was observed only in two cases. This fact indicates that during divergence of the stream either multilayer turbulence occurs or that turbulent layers of great strength (of the order of 1.5-2 km) are formed. The latter assumption is less probable, since turbulent layers of such great strength are found infrequently.

The predominant formation of turbulence during divergence is in a good agreement with the data of I. G. Pchelko (Ref. 4), obtained by him from extensive investigations. However, from our data on sections with parallel isohypses, the probability of the occurrence of tossing is significantly less than from his data. According to the data of N. Z. Pinus, and I. A. Klemin (Ref. 1), obtained in 1954, the predominant occurrence of tossing is associated with cyclonic curvature of isohypses and convergence of the stream. It is possible that this is explained

by their method of data treatment. In their treatment, the nature of isohypses and verging of the stream were determined not for the same level, as was done by us and by Pchelko, but for the 3-8 km layer and for the 8-14 km layer for each of which a map was taken of the pressure topography close to the middle of the layer.

The recurrence of turbulent zones on the cyclonic and the anticyclonic sides of the jetstream was also considered as a function of the stream verging. The determination of the cyclonic and anticyclonic side of the jetstream was done from the maximum wind charts. By this method, quite often cases were found in which the cyclonic part of the stream had anticyclonic curvature of isohypses and vice versa. It is apparent from the data of Table 3 that the occurrence of turbulence is most probable on the cyclonic side of the jetstream in the delta of the upper air frontal zone or local divergence. The frequency of occurrence of turbulence on the anticyclonic side is somewhat greater than was indicated by other authors. However, it should be noted here that in 70 percent of the cases tossing on the anticyclonic side of the jetstream is observed in the presence of divergent isohypses.

In addition, our data contained many flights in the anticyclonic side of the stream, above its axis. However, from the data of 1961-1962 flights, the probability of tossing on the anticyclonic side of the stream in the case of divergent flow was 42 percent, and after excluding all passes above the axis of the stream, it did not exceed 21 percent. Thus, according to our data tossing should be expected on the cyclonic side of the stream primarily in the delta of the upper air frontal zone. Tossing is observed less frequently on the anticyclonic side of the stream and even then only in the case of divergence of the streams.

Section 3. The Turbulent Zone Distribution as Functions of the Level of Maximum Wind and the Altitude of the Lower Boundary of the Tropopause

At 7-10 km altitudes, the presence of turbulent layers is often associated with the tropopause and with jetstreams. We considered 133 passes above and below the stream axis during the winter and the spring. Figure 3, curve 1, shows the frequency of occurrence of tossing at different altitudes with respect to the axis of the jetstream. The graph was constructed on the basis of special flight data. It is apparent from the figure that the data form a bimodal curve above as well as below the stream axis. Above the axis of the jetstream there are two maxima (at the altitudes of 0.25 and 1.25 km). Above 2 km, the frequency of occurrence of tossing is again increased. However, we have very few measurements at these altitudes. Below the stream axis, there are also two maxima (at 0.75 and 1.75 km).

Table 3. Distribution of the Number of Cases with Tossing (1960-1962) on Cyclonic and Anticyclonic Sides in the Case of Divergence and Convergence of the Stream

	Cyclonic side of the stream			Anticyclonic side of the stream		
	Divergence	Parallel	Convergence	Divergence	Parallel	Convergence
Total number of cases	40	38	28	21	21	14
Number of cases with tossing	23	8	11	8	2	1
Same in percent	57.5	21	39.3	38.2	9.5	7.1

Curve 2 in Figure 3 was obtained from the measurement data of radiosondes, each with an attachment for measuring turbulence. Such measurements are done by a completely independent method, capable of detecting a much smaller extent of turbulence. This method also indicated that for the winter-spring season, the curve for the frequency of occurrence of turbulence with respect to the maximum wind was approximately of the same shape as curve 1 below the stream axis. Above the axis, curve 2 does not have a second maximum for the recurrence of tossing.

The quantitative results of these two methods are certainly different. Our flights were conducted in those situations under which tossing is most probable and therefore the probability of tossing here is greatly increased. The radiosonde observations were conducted every day and the quantitative results here are closer to reality (within the scale of the sensitivity of the instrument).

The probability maximum of tossing which is found at 1.25 km above the stream axis (curve 1, Figure 3) is apparently associated with the tropopause. The mean altitude of the tropopause, calculated from the data of the radiosonde was 1.63 km above the axis of the jetstream. The three remaining maxima are possibly associated with the increase and the decrease of the wind during entry and departure from jetstreams.

If we consider the curves which represent the probability of occurrence of tossing separately for conditions of the cyclonic and anticyclonic sides of the stream, then it is found that on the cyclonic side of the stream, one observes only two maxima: one above and one below the axis. The maximum above the stream axis is apparently associated with

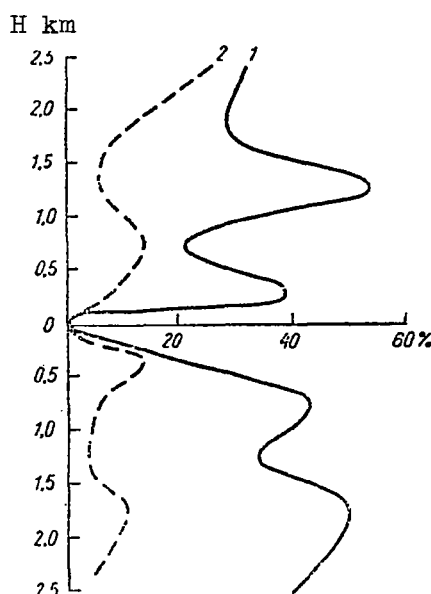


Figure 3. Curves which show frequency of occurrence of tossing with respect to the axis of the jetstream. 1. frequency curve of occurrence of an intermediate strength tossing from the aircraft data; 2. frequency curve of occurrence of intermediate and strong tossing from radiosonde measurements with turbulence measuring attachment for the winter and spring seasons

the tropopause and it is found at the same altitude as the maximum in curve 1, Figure 3. Below the stream axis, the maximum corresponds to the nearest maximum to the axis on the same curve and it is probably associated directly with the jetstream. The curve which represents the probability of occurrence of tossing above the stream axis, analogous to the probability curve 1 of Figure 3 below the axis, displays a maximum only for the anticyclonic part of the jetstream. This maximum corresponds to the farthest removed maximum from curve 1. Thus, on the cyclonic side of the jetstream, the maximum of the probability of occurrence of tossing is apparently obtained in the increased wind zone in the jetstream; on the anticyclonic side, it is principally formed in the zone of weakened wind. However, in individual cases it also occurs with the increase of wind. The latter on the anticyclonic side of the jetstream is observed somewhat further from the stream axis than on the cyclonic side. In reality, an examination of the available aerological cross sections of jetstreams indicates the lowering of the altitude of the stream on its anticyclonic side. All of these considerations are preliminary in nature since there is an insufficient amount of data. When a large amount of data becomes available, it would

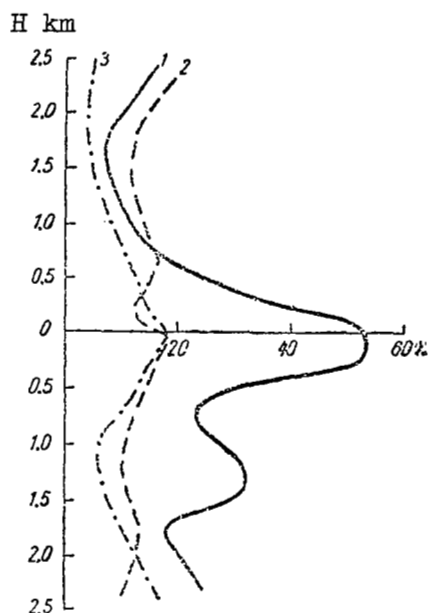


Figure 4. Curves which show frequency of occurrence of tossing with respect to the lower boundary of the tropopause. 1. frequency curve of occurrence of intermediate and severe tossing from the aircraft data; 2. frequency curve of occurrence of intermediate and severe tossing from radiosonde data with turbulence measuring attachment in the winter and spring season; 3. distribution curve of number of cases of severe turbulence according to the data of Briggs

be interesting to obtain the distribution of turbulent layers with respect to the stream axis for different seasons, since the relationship of the altitude of the axis of the stream and the tropopause change is a function of the season.

It is apparent from Table 4 that turbulence is most often observed on the cyclonic side of the jetstream, below the stream axis (41.5 percent). The frequency of occurrence is somewhat higher also on the anticyclonic side of the stream above its axis.

Briggs in Ref. 5 considered the distribution of 73 cases of strong turbulence with respect to the axis of the jetstream (Table 5). From these data, the greatest number of cases with strong tossing was noted below the axis in the cyclonic side of the stream; also a somewhat high frequency of occurrence of turbulence was observed above the axis on the anticyclonic side of the stream. However, since it is not known

Table 4. Distribution of Frequency of Occurrence of Turbulence with Respect to Axis of Jetstream (in percent)

	Cyclonic side of stream	Anticyclonic side of stream
Above axis. . . .	30	33
Below axis. . . .	41.5	15

Table 5. Distribution of Turbulence (number of cases) with Respect to Axis of Jetstream (according to data of Briggs)

	Cyclonic side of stream	Anticyclonic side of stream
Above axis. . . .	10	15
Below axis. . . .	46	2

how many flights were made under an analogous situation, when there was no tossing, these data are difficult to compare with those of Table 4.

The frequency of occurrence of turbulence with respect to the tropopause indicates the existence of a well developed maximum near its lower boundary, a small maximum 1.25 km below the tropopause, and the increase of the frequency of occurrence of the tossing from the altitude of 1.75 km also below its lower boundary. Above the lower boundary of the tropopause up to an altitude of 2 km above it, the occurrence of tossing is continuously decreasing and only above a 2 km altitude may one observe a somewhat greater frequency of occurrence. The latter fact is apparently associated with the upper boundary of the tropopause, which, according to our data, exists at a mean altitude of 2.5 km above its lower boundary. The maximum occurrence of tossing in the tropopause zone is apparently associated with the wave motion on its lower boundary and the two maxima below this boundary are associated with the jetstream, as was indicated above.

The work of Briggs (Ref. 5) shows the distribution of 105 turbulent layers with respect to the tropopause. It is apparent from Figure 4 (curve 3), from the data of Briggs, who considered the distribution of turbulence zones in more energetic layers, that the picture is more smoothed out. It does not have maximum at 1.25 km below the tropopause, yet one observes a continuous increase of the number of cases of tossing 1-3 km below the tropopause. From the data obtained with radiosondes with turbulence measuring attachments (curve 2) there is no sharp decrease of the occurrence of turbulence which was, however, obtained on the basis of the data of our flights. On the contrary, in the radiosonde

cases a weak maximum is observed at an altitude of 0.75 km. It is possible that this is associated with the nature of the tropopause layer itself and the very different altitude of its upper boundary. In the course of our flights the magnitude of the tropopause layer was on the average of 2.5 km and the tropopause layers themselves were characterized in the majority of cases by a slower temperature drop and poor definition. Apparently, this is responsible for the decrease of the occurrence of tossing above the tropopause as compared with that observed by us.

Section 4. Tossing as a Function of Horizontal Wind Gradient

Wind measurements by means of an airborne Doppler system enabled the calculations of the horizontal wind velocity gradients in the region of the intersection of the jetstreams.

This allowed the verification of the belief of some authors (Refs. 4, 5) that dangerous turbulence must originate in the sharp transition zones from the region of weak winds to strong winds and vice versa.

In order to determine the horizontal wind gradients, a graph was constructed for each horizontal section indicating the distribution of all the obtained wind velocity values as a function of time, velocity, and direction. These graphs were smoothed graphically and from them

the "mean" wind¹ was determined with respect to the speed and direction and then the points with sharp changes of the wind were marked. Between these points, the vectorial horizontal wind gradient was determined. The sections, for which the horizontal wind gradient were determined, were 20-70 km long, i.e., these sections were comparable to the mean size of the turbulent sections. Thus, the horizontal gradients were calculated for the 1962 expedition and for the flights which took place in the Khabarovsk region conducted in 1960. Later, turbulence was observed much more frequently, and was more intense than during the 1962 expedition.

Table 6 shows the distribution of the horizontal wind gradients for the jetstreams over the European territory of the USSR and in the Far East.

A fact which attracts attention is that in the Far East, the relative number of cases in which the horizontal gradient exceeded 100 km/hr per 100 km was found to be much greater than over the European territory of the USSR.

¹

Measurements of the wind were conducted every 12 seconds of the flight.

All of the cases for which a horizontal gradient was calculated were compared with the synchronous recordings of the shift of weight. Here the turbulence of any intensity was taken into account.

Table 7 shows the distribution of tossing under different values of the horizontal wind gradient. When the horizontal wind gradients were less than or equal to 60 km/hr per 100 km, tossing was observed in about 5 percent of the cases. When the horizontal gradients were greater than 60 km/hr per 100 km, then the frequency of occurrence of tossing was about 75 percent.

These results are in good agreement with those of Pchelko. If the gradient of the "mean" wind in jetstreams exceeds 50 km/hr per 100 km over a small section, then one should expect medium or strong tossing. However, our data show that the intensity of turbulence may also be small in this case.

In the majority of cases, the turbulent sections are observed directly in the zone of large wind gradients. However, quite often one finds turbulence in zones with a slight horizontal wind gradient (in the strong wind zone) in close proximity to the sections with a large gradient. Such cases were considered by us as well as the cases with a large wind gradient. For example on May 25, 1960 a jetstream was observed at an altitude of 9 km on the Iman-Khabarovsk section. The wind velocity at that time was as high as 200 km/hr. However, the increase of wind velocity in this section occurred gradually and no tossing was observed. At a 7-8 km altitude, the wind velocity was 60-80 km/hr, but in the proximity of jetstreams, an increase of up to 170 km/hr was observed and the horizontal gradients were as high as 230 km/hr per 100 km. However, tossing was observed even when the horizontal wind velocity gradients were 60 km/hr per 40 km close to the zone of strong winds.

Briggs also noted the association of turbulent zones with the horizontal wind gradient; from his data, one can also see the increase of the number of cases of turbulence when the horizontal wind gradients are large. In his case, however, this correlation is much weaker. This is explained by the fact that Briggs determined the horizontal wind gradients from radio probing data, i.e., for large distances, and, therefore, his data are greatly averaged and incomparable with turbulent zones. Therefore, from the atmospheric pressure topographic maps, it is sometimes difficult to predict the occurrence of turbulence from the horizontal wind gradients. For example, on February 21, 1962, at 1500 hours one would expect from the AT₃₀₀ map tossing on the Moscow-Gor'kiy section, where the wind was changing from northeasterly (10 km/hr) to southwesterly (160 km/hr). However, according to our data, tossing was observed in the Kanash region where the horizontal wind gradients were 144 km/hr, while according to the AT₃₀₀ map, sharp changes of wind were absent in this region.

Table 6. Horizontal Gradient Distribution (km/hr per 100 km)
for the European Territory of USSR and for Khabarovsk
Region

Horizontal wind velocity gradients	0-10	10-20	20-30	30-40	40-50	50-60	60-70	70-80	80-90	90-100	> 100
European territory of USSR	24	18	21	20	16	12	6	6	-	5	8
Khabarovsk region	2	5	6	8	9	4	4	1	-	4	17

Table 7. Distribution of Frequency of Occurrence of Tossing
under Different Horizontal Wind Velocity Gradients

Horizontal wind velocity gradients (in km/hr per 100 km)	0-10	10-20	20-30	30-40	40-50	50-60	60-70	70-80	80-90	90-100	> 100
Total number of cases.	29	28	30	23	24	11	9	8	2	5	12
Number of cases of tossing . .	1	-	1	3	2	1	6	4	2	3	12
Frequency of oc- currence (in percent) . . .	3.4	-	3.3	13.0	8.4	9.1	66.6	50.0	100.0	60.0	100.0

If one were to consider the distribution of the horizontal wind gradient separately for the cyclonic and anticyclonic part of the stream, then one would find that large horizontal wind gradients are most often observed in the cyclonic side of the jetstream. Table 8 gives the distribution of the horizontal wind gradient along the cyclonic and anticyclonic sides of the stream. From the data of the table, it is apparent that the horizontal gradients are greater than 60 km/hr per 100 km, i.e. the gradients for which the probability of tossing is very significant are found on the cyclonic side of the stream almost 2.5 times more frequently than on the anticyclonic side.

Section 5. Relationship between the Turbulent State of the Atmosphere, Horizontal Temperature Gradient, and the Richardson Number

From the data of all flights which were conducted in a direction across the jetstream, Richardson numbers were calculated in the majority of cases by the following formula:

$$Ri = \frac{l^2 T (\gamma_a - \gamma)}{g \left(\frac{\Delta T}{\Delta n} \right)^2},$$

where $\Delta T/\Delta n$ is the horizontal temperature gradient, γ is the vertical temperature gradient, $l = 2\omega \sin \phi$, ϕ is the latitude of the location and ω is the angular velocity of the rotation of the earth.

The horizontal temperature gradients were determined for all passes which were approximately as long as the extent of the turbulent zones. For the purpose of calculation the mean horizontal temperature gradient was taken in the layer for which the value of Ri was to be calculated. The extent of the layers, for which the Richardson numbers were calculated, rarely exceeded 1 km. According to such a method of calculation, the data from which we determined the horizontal and the vertical temperature gradients differed in time by 1 hr on the average.

The results of the calculations are shown on the demarcated graph (Figure 5) and in Table 9. It is apparent from the data of Table 9 that at $Ri < 1$, tossing was observed in 70 percent of all cases which fall within this gradation. The troposphere was practically calm when values $Ri < 10$.

Many investigators who look for the relationship between the values of Ri and the frequency of occurrence of turbulence give different limiting values for this criterion, and some of the authors completely reject the correlation between Ri and turbulence.

Table 8. Horizontal Wind Velocity Gradient Distributions on the Cyclonic and Anticyclonic Sides of the Stream

Horizontal wind velocity gradients (in km/hr per 100 km)	0-10	10-20	20-30	30-40	40-50	50-60	60-70	70-80	80-90	90-100	> 100
Cyclonic side of stream.	8	8	15	12	13	14	6	4	-	4	21
Anticyclonic side of stream.	19	13	15	12	10	4	3	2	-	4	3

Table 9. Frequency of Occurrence of Tossing under Different Ranges of Richardson's Number

Richardson's number ranges	<0.5	0.5-1.0	1.0-4.0	4.0-10	>10
Frequency of occurrence of tossing (in percent).	76	63	39	26	13

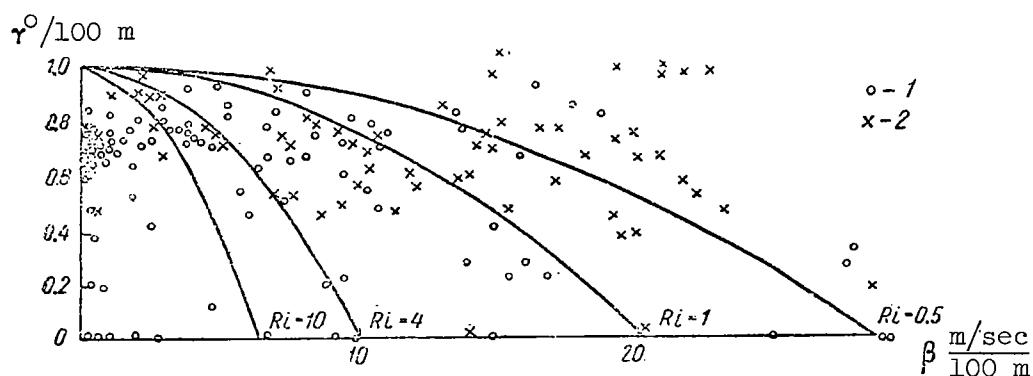


Figure 5. Demarcation from data of the 1960 expedition.
1. cases without tossing; 2. cases with tossing

In Table 10 which was taken from Ref. 3, the occurrence is shown as a function of the Richardson number from the data of different authors.

It is apparent from the data of Table 10 that conclusions regarding the use of Ri as a turbulence criterion are contradictory. This is explained mainly by the fact that Ri is not a unique factor which determines the atmospheric turbulence. It is not possible, for example to use Richardson's numbers when considering the turbulence in the tropopause layer and in the lower troposphere, where the vertical stability must play a significantly lesser role. The method of calculation also plays an important role.

From our data, in which a good correlation was found with values of Ri , the latter were calculated in the majority of cases from the horizontal temperature gradients; i.e., the calculation was made from the element which measured with greater accuracy than the present day wind velocity measurements. The measurements of temperature and turbulence were conducted on one and the same thing, while the majority of authors calculated Richardson's numbers from radiosonde data and the turbulence from aircraft data. In the latter case, in addition to asynchronous readings, which in our case were synchronous, there was also a change in the location of the plane and the radiosonde as well as various errors which are associated with different methods of calculation.

For those cases in which Ri were calculated from the vertical wind gradients, the errors which are associated with weak winds were excluded by us since we considered only the cases with jetstreams.

A good correlation between tossing and the Richardson numbers may also be connected with our method of data processing. The flight in turbulent atmosphere was characterized by two Ri numbers, calculated for layers above and below this flight. For construction of graphs, that Ri number was selected whose value was smaller.

Richardson numbers plotted against the cross section of the jet-stream sometimes help to isolate the zones with stable and unstable atmospheric conditions from the magnitudes of Ri .

However, in zones with an unstable atmospheric state as well as in the stable zones, one may find isolated values for Ri which do not correspond to the overall picture. On some cross sections, one may find zones with small values of Ri (although they are not very long) in which tossing is absent. In zones with $Ri > 10$, such cases are almost nonexistent.

Despite the fact that according to our data we find a good correlation between the Richardson numbers and turbulence, the prediction of turbulence from Ri numbers, calculated at some point, is not possible since Ri is variable in time and in space. The use of maps with Ri isolines may not give satisfactory results either, since the length of zones with small Ri numbers may be significantly less than the distance between the radio-probing points. In addition, the prediction of tossing from Ri numbers is made difficult by the fact that, as was stated above, Ri is not the only factor which determines atmospheric turbulence.

Let us now consider the relationship between the turbulence which causes aircraft tossing and the horizontal temperature gradient. The comparison results for the upper troposphere are shown in Table 11.

From the data of this table it is apparent that when the horizontal temperature gradients are greater than 6° per 100 km, aircraft tossing was observed in 86 percent of all cases, and when the temperature gradient was $4-6^{\circ}$ per 100 km, tossing was observed in 65 percent of all cases. When the horizontal temperature gradients were less than 2° per 100 km, tossing was practically not observed. Thus, according to data on temperature change in a course of horizontal flight, indicated by the aircraft thermometer, it is possible to evaluate the probability of tossing of the aircraft.

In the tropopause and in the lower stratosphere layers with horizontal temperature gradients of the order of $8-10^{\circ}$ per 100 km, one may not observe even weak tossing. For example, on May 12, 1960, when the

Table 10

Author	Richardson's number			
	< 0.5	0.5-4.0	< 10	< 10
Klemin, I. A. and Pinus, N. Z. (1953).	80-90	50	-	-
Kurilova, Yu. V. (1958)	-	-	79	30
Pchelko, I. G. (1960)	-	-	31	12
Verle, Ye. K. (1960).	74	36	-	26
Zavarina, M. V. (1960).	Coefficient of justification according to Obukhov was 0.75			
Berniger and Hysat.	75-90	-	-	-
Reshchikova, A. A. (1963)	76	56	-	13

Table 11. Distribution of Number of Cases of Tossing at Different Horizontal Temperature Gradients

Horizontal temperature gradients (in deg. per 100 km)	0-2	2-4	4-6	6-8	8-10	10-12	>12
Total number of cases.	65	32	23	8	4	4	5
Number of cases of tossing . . .	6	15	15	7	3	4	4
Frequency of occurrence of tossing (in percent)	9.0	46.8	65.0	87.5	75.0	100.0	80.0

aircraft took off at 0440, at 9 and 10 km altitudes in the area of Iman-Spassk-Dal'niy the horizontal temperature gradients were in some sections 11-13° per 100 km and were accompanied by an average to strong tossing. At an altitude of 11.25 km above the tropopause, despite the fact that the horizontal temperature gradient was as high as 14.3° per 100 km, aircraft tossing was absent.

All of the above refers to the horizontal temperature gradients, calculated for 20-70 km long sections.

The horizontal gradients taken from the pressure topography maps will not have such a definite relationship to the turbulence, due to the fact that they are greatly averaged.

Conclusions

Studies of aircraft turbulence (tossing) in jetstreams indicated the following:

1) the greatest frequency of occurrence of tossing takes place below the axis of jetstream on the cyclonic side;

2) on the anticyclonic side of the stream, below its axis, tossing rarely occurs and then primarily during divergence of the stream;

3) in the divergence region a plane may find turbulence somewhat more frequently than in the case of convergence, since in diverging streams the probability is greater for multilayer turbulence;

4) the tossing of aircraft at 7-10 km altitudes in the case of cyclonic and anticyclonic curvatures of isohypses is of equal probability;

5) the greatest probability of occurrence of tossing occurs during flights in a pressure trough with indefinite curvature of isohypses;

6) in the case of horizontal temperature gradients, calculated for sections of 20-70 km in length (at altitudes of 7-10 km), greater than 6° per 100 km (outside of tropopause and lower troposphere zone), the frequency of occurrence of tossing is as high as 85 percent;

7) the distribution of turbulent layers with respect to the axis of jetstream and the lower boundary of the tropopause depends greatly on the ratio of altitudes of these levels and on the nature of the tropopause; for the winter-spring season, two maxima are observed above and below the stream axis at altitudes 0.25, 1.25 km and at 0.75, 1.75 km;

8) during crossing of the jetstreams, the horizontal gradients of wind velocity, calculated for 20-70 km sections, correlate well with the turbulent zones. When the horizontal gradients are greater than 60 km/hr per 100 km, the probability of tossing is as high as 75 percent.

References

1. Klemin, I. A. and Pinus, N. Z. Metodichesmiye ukazaniya k diagnozu i prognozu atmosfernoy turbulentnosti, vyzyvayushchey boltanku skorostnykh samoletov (Directions for Methods of Diagnoses and Forecasting of Atmospheric Turbulences Which Cause Tossing of High-Speed Aircraft). Gidrometeoizdat, 1954.

2. Metodicheskiye ukazaniya (Directions for Methods). No. 40, Gidrometeoizdat, 1961.
3. Pinus, N. Z. and Shmeter, S. M. Atmosfernaya turbulentnost', vyzyvayushchaya boltanku samoletov (Atmospheric Turbulence Which Causes Aircraft Tossing). Moscow, Gidrometeoizdat, 1962.
4. Pchelko, I. G. Aerosinopticheskiye usloviya boltanki samoletov v verkhnikh sloyakh troposfery i nizhney stratosfery (Aerosynoptic Conditions for Aircraft Tossing in the Upper Layers of the Troposphere and in the Lower Stratosphere). Moscow, Gidrometeoizdat, 1962.
5. Briggs, B. A. Severe Clear Air Turbulence Near the British Isles. Met. Mag, Vol. 90, 1961.

APPLICATION OF THE BOUNDARY LAYER METHOD TO THE DETERMINATION
OF THE PARAMETERS OF TURBULENCE IN THE FREE ATMOSPHERE

V. A. Shnaydman

ABSTRACT

The solution of the problem for the maximum wind velocity in the case of asymmetrical wind velocity distribution along the altitude is presented. It is shown that diffusion of the energy of turbulence through the maximum velocity surface is small. It is also shown that separate solutions may be found for closed systems of equations of motion and of energy balance of the turbulence in the lower and upper parts of the turbulent layer (with respect to the maximum wind velocity). The author expresses some opinions regarding the possibility of evaluation of the diffusion of the energy of turbulence and the determination of turbulence characteristics in any layer of the free atmosphere.

In recent years a number of works have appeared in domestic and in foreign literature dealing with investigations of the turbulence in free atmosphere, and particularly in jetstreams. On the basis of theoretical and experimental data, a number of authors have shown that in proximity to the jetstream, one observes well-defined pulsation maxima of wind velocity above and below the axis of jetstreaming, while on the axis itself these pulsations are either extremely small or nonexistent. In Ref. 5, the problem of determining quantitative characteristics of turbulence in the jetstream region was solved for the case in which the wind distribution above and below the maximum level is symmetrical. That problem was reduced to the determination of the mean characteristics of turbulence in the turbulent layer with similar wind velocity profile.

However, the investigations of N. Z. Pinus (Ref. 4) as well as the results of data processing conducted under the direction of the author have shown that the wind velocity profile in the turbulent layer of the maximum wind velocity region is asymmetrical. In the upper part of the stream is observed a more drastic decrease of the wind velocity with increase of the distance from the axis of the stream. Therefore, it is of interest to determine separately the quantitative characteristics of turbulence in the upper and in the lower parts of the stream, and to evaluate the magnitude of diffusion of the energy of turbulence through the layer boundaries.

Let us consider a solution of a steady-state problem for a single layer (e.g., for the upper part of the jetstream). Let us direct the

Z-axis vertically upward, and the X-axis in the direction of the geostrophic wind. Then the equation of motion and the energy balance equation of turbulence will acquire the following form:

$$K \frac{d^2 u}{dz^2} + 2\omega_z v = 0,$$

$$K \frac{d^2 v}{dz^2} - 2\omega_z (u - u_g) = 0, \quad (1)$$

$$\int_0^H \left[\left(\frac{du}{dz} \right)^2 + \left(\frac{dv}{dz} \right)^2 \right] dz - \int_0^H \frac{g}{T} (\gamma_a - \gamma) dz + \frac{1}{K} \int_0^H D dz = 0, \quad (2)$$

$$v|_{z=H} = 0, \quad (3)$$

where u , v are velocity components of the real wind; u_g is the velocity of the geostrophic wind; K is the mean turbulence coefficient along the turbulent layer; H is the thickness of the turbulent layer; T is the temperature; $dT/dz = -\gamma$ is the vertical temperature gradient; γ_a is the dry adiabatic gradient; and, D is the magnitude of diffusion of the energy of turbulence.

Equation (3) is a condition for the determination of the thickness of the turbulent layer. The system of equations (1)-(3) is solved with the following boundary conditions:

$$u|_{z \rightarrow \infty} \neq \infty, \quad v|_{z \rightarrow \infty} \neq \infty; \quad (4)$$

$$\frac{du}{dz} \Big|_{z=0} = 0, \quad \frac{dv}{dz} \Big|_{z=0} = 0. \quad (5)$$

The given system of equations (1)-(3) in the case of boundary conditions (4) and (5) is a closed system from which it is possible to determine the quantities u , v , K and H under the condition that the velocity of geostrophic wind and the magnitude of diffusion of the energy of turbulence are known.

As indicated in Ref. 5, an exponential profile is a good approximation for the profile of geostrophic wind in the jetstream region:

$$u_g(z) = (u_m - u_1) e^{-\gamma z} + u_1, \quad (6)$$

where u_m is the velocity of geostrophic wind on the stream axis, and u_1 is the velocity of geostrophic wind outside the turbulent air, where it is equal to the velocity of real wind.

According to A. S. Monin (Ref. 3), let us assign a value to the quantity D by the following method:

$$D = \frac{d}{dz} \left[\alpha K \frac{dE_T}{dz} \right], \quad (7)$$

where $E_T = \frac{c'^2}{2}$, the kinetic energy of the turbulence (c' is the pulsation or gust of wind), and α is some parameter which in the future we shall call the diffusion parameter of the energy of turbulence.

Taking into account equation (7), the integral equation for the energy balance of the turbulence will acquire the following form

$$\begin{aligned} & \int_0^H \left[\left(\frac{du}{dz} \right)^2 + \left(\frac{dv}{dz} \right)^2 \right] dz - \int_0^H \frac{g}{T} (\gamma_a - \gamma) dz + \\ & + \alpha \left[\frac{d}{dz} \left(\frac{c'^2}{2} \right) \right]_{z=H} - \frac{d}{dz} \left(\frac{c'^2}{2} \right) \Big|_{z=0} = 0. \end{aligned} \quad (8)$$

The term which determines the diffusion of the energy of turbulence through the upper boundary of the turbulent layer ($z = H$), may be neglected as it is negligible in comparison with the other terms of the equation. It is difficult to say anything ahead of time regarding the term which determines the diffusion of the energy of turbulence through the surface $z = 0$. It must be determined from the solution of the problem.

Taking into account the above stated facts, the equation for the energy balance of turbulence may be written as follows:

$$\int_0^H \left[\left(\frac{du}{dz} \right)^2 + \left(\frac{dv}{dz} \right)^2 \right] dz - \int_0^H \frac{g}{T} (\gamma_a - \gamma) dz - \alpha \frac{d}{dz} \left(\frac{c'^2}{2} \right) \Big|_{z=0} = 0. \quad (9)$$

Having determined the velocity components of the real wind and their derivatives, it is easy to find the magnitude of gusts of wind from the following relationships:

$$c' = l \frac{dc}{dz} + \frac{l^2}{2} \frac{d^2 c}{dz^2} + \dots \quad (9a)$$

Then

$$c'^2 = K \sqrt{\left(\frac{du}{dz}\right)^2 + \left(\frac{dv}{dz}\right)^2} \quad (z \neq 0),$$

$$c'^2 = (u_m - u_1) \frac{\omega_z \sqrt{2n}}{a \sqrt{n^2 + 1}} \sqrt{e^{-2az} + e^{-2a\sqrt{2n}z} - 2e^{-a(1+\sqrt{2n})z} \cos az} \quad (z \neq 0),$$
(10)

where

$$n = \frac{K \gamma^2}{2 \omega_z}, \quad a = \sqrt{\frac{\omega_z}{K}}$$

When $z = 0$, then $dc/dz = 0$; it is necessary to take into account other terms in the formula 9a.

From the magnitude of c'^2 it is possible to find the last term in equation (9), $\propto \frac{d}{dz} (c'^2/2)$. It is not difficult to show that when $z = 0$,

this term is equal to zero, i.e., the diffusion of the energy of turbulence through the maximum wind velocity surface ($z = 0$) is absent. An analogous result may be obtained for the turbulent layer below the stream axis.

Thus, the intensity of the turbulent mixing above and below the stream axis is determined by the vertical gradients of wind velocities in these same layers.

A specific example of the above solution is the case of a symmetrical stream which was considered in Ref. 5.

The results which were obtained in Ref. 5 may be utilized for the determination of quantitative turbulent characteristics in the turbulent layers above and below the axis of the jetstream. Here, for the determination of the turbulence coefficient, the wind turbulence and the thickness of the turbulent layer, it is necessary to make use of the input parameters which are taken from the profiles of real winds and the temperature in that turbulent layer for which these characteristics are to be calculated.

For calculation of turbulence characteristics, the input parameters are as follows:

1) the difference of velocities of real wind along the jetstream axis and outside the turbulent layer ($c_m - c_1$);

2) the thickness of the layer of the greatest wind velocity gradients (\tilde{z}); \tilde{z} is that distance from the stream axis at which the velocity drops tenfold, i.e.,

$$\frac{c(\tilde{z}) - c_1}{c_m - c_1} = 0.1;$$

3) the mean vertical temperature gradient ($\bar{\gamma}$) and the mean temperature (\bar{T}) in the turbulent layer.

In such a case, K and H for a given latitude are uniquely defined by the following quantities:

$$M = \frac{g}{T} \frac{\gamma_a - \bar{\gamma}}{(c_m - c_1)^2} \text{ and } \tilde{z}.$$

From nomograms¹ it is easy to find $\log \frac{K}{\omega_z}$ and H if $\log M = A$ and z are known.

From formula (10) it is possible to calculate the profile of the wind turbulence. Its characteristic profile is shown in Figure 1. It is evident from this profile that the magnitude of the wind turbulence is quite significant. It is easily determined from the following formula

$$c'^2 = K \sqrt{\frac{g}{T} (\gamma_a - \bar{\gamma})}. \quad (11)$$

Our calculations have shown that the turbulence parameters in the jetstream regions vary within quite broad limits. However, if one selects for the critical quantity a quantity in which in 75 percent of all cases the considered characteristic is less or equal to this quantity, then the critical values of the parameters will be

- 1) 500 m²/sec as the turbulence coefficient;
- 2) 2.5 m/sec as the wind turbulence; and,
- 3) 2 km as the thickness of the turbulent layer.

The maximum magnitudes of the turbulence parameters in the cases considered by us were $K = 1,060 \text{ m}^2/\text{sec}$, $c' = 4.4 \text{ m/sec}$ and $H = 3 \text{ km}$

1

See the article by V. D. Litvinova in this collection.

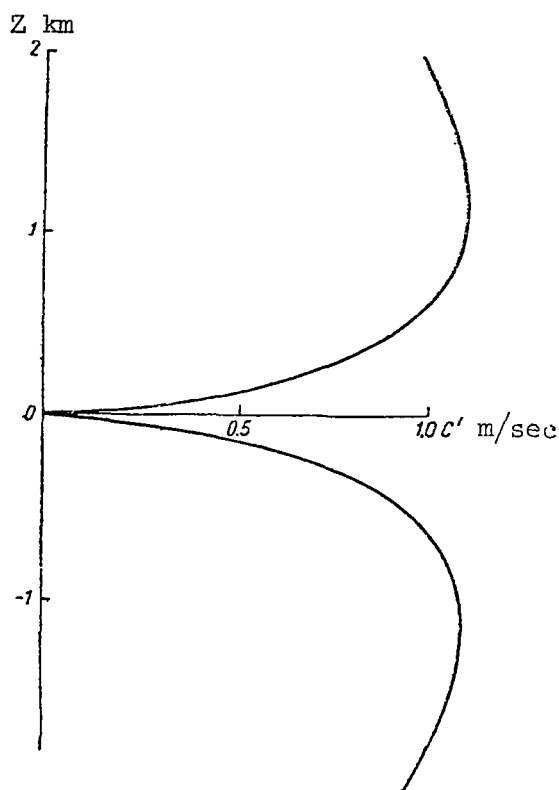


Figure 1. Distribution of air velocity turbulence c' in jetstreams

(this case was observed near Tashkent on July 18, 1960, and the sounding IL-28 aircraft in this layer recorded a strong turbulence).

Many authors investigated the relationship between the turbulence of the wind and the meteorological factors. Thus, for example, A. P. Yurgensin (Ref. 6) found a static relationship between the magnitude of turbulence and the vertical temperature gradient. Andersen (Ref. 7) insists that the principal factor which affects the formation of turbulence in the free air is the vertical wind velocity gradient. According to the data of M. V. Zavarina (Ref. 1), there is a good correlation between the turbulence in the free air and the maximum wind velocity as well as between the Ri number and the turbulence in the free air. The same conclusions follow from the work of L. T. Matveyev (Ref. 2).

Since the meteorological parameters (vertical temperature gradients and wind velocity, wind velocity gradient, the thickness of the layer, etc.) combine in a complex fashion, it is extremely difficult to evaluate theoretically the contributions of each of these factors separately in the course of formation of turbulence in the free air.

Consequently, we attempted to find the relationship between the wind turbulence and each of the indicated parameters on the basis of the observed data. Naturally, the quantitative characteristics of turbulence cannot be uniquely determined by the degree of thermal stability or by the vertical gradients of wind velocity. However, such an approach enables the evaluation of the contribution of the indicated characteristic towards the formation of turbulence of some specific intensity.

Our investigations have shown that at the very same level of thermal stability, one may observe turbulences of completely different intensities. The relationship between c' and the vertical wind velocity gradient was also found to be weak. However, it was still possible to obtain some limiting curve for the dependence of c' on $\frac{\Delta c}{\Delta z}$, i.e., at a certain given

value of the vertical wind velocity gradient, the turbulence cannot exceed a certain limiting value and as $\frac{\Delta c}{\Delta z}$ increases, this limit also in-

creases. The obtained relationship enables one to conclude that the vertical wind velocity gradients apparently play a more important role in the formation of turbulence than does thermal stability. However, it was possible to establish a relatively high correlation between the wind velocity along the stream axis and the velocity gradient in the lower kilometer layer. Consequently, there is a high correlation between c' , averaged along the turbulent layer, and the maximum wind velocity (Figure 2). The fact that the correlation is much stronger between c' and

c_m than between c' and $\frac{\Delta c}{\Delta z}$ is apparently associated with the random

choice of the thickness of the layer and the altitude with respect to the maximum wind level for calculation of the vertical wind velocity gradients.

The relationship between the wind turbulence and the Ri number is also expressed in the form of some limiting curve; this supports the conclusion that the Ri number is a necessary, but not sufficient, characteristic of the intensity of turbulence. It is interesting to note that while at low values of Ri (Ri less than 4) it is possible to find turbulence of practically any intensity, at large values of Ri the probability of intense turbulence is very low.

The above proposed method is useful only for the determination of turbulence characteristics in turbulent layers. In order to determine these characteristics in any layer in the free air it is necessary to evaluate the magnitude of diffusion of turbulent energy in the following equation

$$K \left[\left(\frac{du}{dz} \right)^2 + \left(\frac{dv}{dz} \right)^2 \right] dz - K \frac{g}{T} (\gamma_a - \gamma) = - \frac{d}{dz} \left[\alpha K \frac{d}{dz} \left(\frac{c'^2}{2} \right) \right] \quad (12)$$

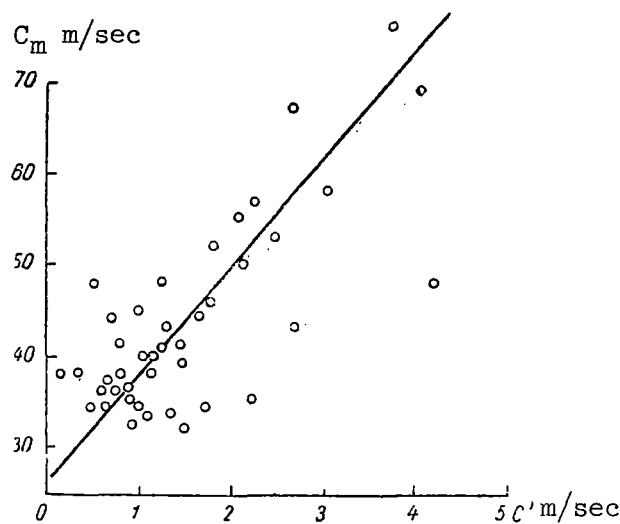


Figure 2. Air velocity turbulence c' as a function of the wind velocity along the stream axis c_m

Integrating equation (12) from 0 to z we obtain:

$$\begin{aligned} \int_0^z K \left[\left(\frac{du}{dz} \right)^2 + \left(\frac{dv}{dz} \right)^2 \right] dz - \int_0^z K \frac{g}{T} (\gamma_a - \gamma) dz = \\ = \alpha K \frac{d}{dz} \left(\frac{c'^2}{2} \right) \Big|_{z=0} - \alpha K \frac{d}{dz} \left(\frac{c'^2}{2} \right) \Big|_{z=z} \end{aligned} \quad (13)$$

Assuming that the coefficient of turbulence is very slightly dependent on the altitude, and for the level where the wind velocity reaches maximum ($z = 0$),

$$\frac{d}{dz} \left(\frac{c'^2}{2} \right) \Big|_{z=0} = 0,$$

we obtain

$$\begin{aligned} \alpha = \frac{\int_0^z \left[\left(\frac{du}{dz} \right)^2 + \left(\frac{dv}{dz} \right)^2 \right] dz - \int_0^z \frac{g}{T} (\gamma_a - \gamma) dz}{\frac{d}{dz} \left(\frac{c'^2}{2} \right)} = \\ = \frac{\frac{\omega_z (c_m - c_1)^2 2n}{K(1+n-\sqrt{2n})} \int_0^z \left(e^{-2az} + e^{-2a\sqrt{2n}z} - 2e^{-a(1+\sqrt{2n})z} \cos az \right) dz - \int_0^z \frac{g}{T} (\gamma_a - \gamma) dz}{\frac{\omega_z (c_m - c_1) \sqrt{2n}}{2a \sqrt{1+n-\sqrt{2n}}} \frac{d}{dz} \left(\sqrt{e^{-2az} + e^{-2a\sqrt{2n}z} - 2e^{-a(1+\sqrt{2n})z} \cos az} \right)} \end{aligned} \quad (14)$$

If the turbulent layer is separated in the region of maximum wind velocity into separate sublayers (beginning from the maximum wind velocity), and since the mean turbulence coefficient in all of the layer is known to us, formula (4) enables the evaluation of the diffusion of turbulent energy across the boundaries of such sublayers.

In addition to the 0 diffusion layers, $z = 0$ (maximum wind velocity level) and $z = H$ (the boundary of the turbulent layer), there is one more level inside the turbulent layer where the diffusion is equal to zero. This is the level of the maximum wind turbulence. The presence of such a level is associated with the change of the direction of diffusion flow of turbulent energy. Below the level where $c'(z) = c'_{\max}$, the flow of

turbulent energy is directed away from the considered sublayer. Above this level the diffusion flow is directed into this layer. This is supported also by the relationship of the inflow and outflow of turbulence energy in these layers. Since the vertical temperature gradients are approximately the same throughout the whole turbulence layer, this relationship is determined by the vertical wind velocity gradient. For the case of large gradients, the associated energy flow is from the considered layer; for the case of small gradients, on the other hand, the flow is into a given layer.

Calculations of the quantity α from formula (14) for the average conditions, when $\bar{T} = 0.6^\circ/100 \text{ m}$, $\bar{T} = 230^\circ$, $\bar{z} = 5 \text{ km}$, $c_m - c_l = 30 \text{ m/sec}$,

$\omega_z = 0.5 \cdot 10^{-4} \text{ 1/sec}$, $K = 100 \text{ m}^2/\text{sec}$ and $z = 0.5 \text{ km}$, give the value,

$\alpha = -0.2$.

In the future it is planned to conduct calculations of α for different magnitudes of input parameters and to consider the problem of the relationship of α with meteorological element fields.

At the present time it is possible to calculate the turbulence characteristics for any free air layer. In this process a system of equations of motion is solved simultaneously with the energy balance equation for the turbulence in the differential form. In order to close the system, use is made of certain constants which are determined from the actual wind profile.

With such a construction of the problem it seems desirable to break the troposphere above the boundary layer into individual layers, each with a characteristic wind velocity profile, and to solve the posed problem for these layers.

References

1. Zavarina, M. V. and Yudin, M. I. Utochneniye i ispol'zovaniye chisla Richardsona dlya vyyavleniya zon boltanki samoleta (More Accurate Determination and Application of the Richardson Number for the Detection of Airplane Turbulence Zones). Meteorologiya i Gidrologiya, No. 2, 1960.
2. Matveyev, L. T. Kolichestvennyye kharakteristiki turbulentnogo obmena v verkhney troposfere i nizhney stratosfere (Quantitative Characteristic of Turbulent Exchange in the Upper Troposphere and the Lower Stratosphere). Izvestiya AN SSSR, Ser. Geofizicheskaya, No. 7, 1958.
3. Monin, A. S. Turbulentnyy rezhim v prizemnom sloye vozdukh (Turbulent Conditions in the Air Layer Near the Level of the Ground). Informatsionnyy Sbornik GUGMS, No. 1, 1951.
4. Pinus, N. Z. Tropopauza i uroven' s maksimal'noy skorost'yu vetra (The Tropopause and the Maximal Wind Velocity Level). Meteorologiya i Gidrologiya, No. 3, 1961.
5. Shnaydman, V. A. O turbulentnosti v nekotorykh sloykh svobodnoy atmosfery (Turbulence in Certain Free Air Layers). Dissertation for the Degree of Physical and Mathematical Sciences, 1962.
6. Yurgenson, A. P. Isslegovaniye struktury turbulentnykh dvizheniy, vyzyvayushchikh boltanku sovremennykh samoletov (Studies of the Structure of Turbulent Motion which Causes Buffeting of Modern Airplanes). Meteorologiya i Gidrologiya, No. 10, 1960.
7. Andersen, A. D. Free-air turbulence. Journal of Meteorology, Vol. 14, No. 6, 1957.

TURBULENCE IN THE PROXIMITY OF JETSTREAMS

T. P. Krupchatnikova

ABSTRACT

Results of theoretical investigations into the problem of the characteristics of turbulence in jetstreams in the case of a variable coefficient of turbulent exchange in the vertical plane of the jetstream are presented. Solutions are given for equations of motion and energy balance of turbulence in a "narrow" jet. The formulas obtained make possible the construction of a vertical velocity profile of the wind in jetstreams and to calculate the thickness of the turbulent layer relative to the stream axis.

The method for calculating the turbulence characteristics proposed in this work is based on the theory developed by D. L. Laykhtman and V. A. Shnaydman (Ref. 2) and by D. L. Laykhtman and E. K. Byutner (Ref. 3).

The authors of Refs. 2 and 3 assume that the profile of geostrophic wind is a function of the altitude:

$$(u_g - u_{1g}) + i(v_g - v_{1g}) = f(z),$$

where u_{1g} , v_{1g} are velocity components of the geostrophic wind outside

of the turbulent layer where the velocity of the geostrophic wind is equal to the velocity of the true wind.

If the mean value of the coefficient of turbulent viscosity in a stream is equal to k , then the equation of motion may be written as

$$k \frac{d^2 \Phi}{dz^2} - 2i\omega_z [\Phi(z) - f(z)] = 0. \quad (1)$$

where

$$\Phi(z) = u + iv - u_{1g} - iv_{1g};$$

where ω_z is the vertical component of the angular velocity of the rotation of the earth at a given latitude.

Solving equation (1) and taking into account the boundary condition

$$\Phi|_{z \rightarrow \pm \infty} \rightarrow 0$$

these authors obtained

$$\Phi = \frac{a\sqrt{2i}}{2} \left[\int_z^{\infty} e^{-a\sqrt{2i}(\xi-z)} f(\xi) d\xi - \int_z^{-\infty} e^{a\sqrt{2i}(\xi-z)} f(\xi) d\xi \right], \quad (2)$$

where

$$a = \sqrt{\frac{\omega_z}{k}}$$

The following condition is imposed on the function $f(z)$:

$$\lim_{z \rightarrow \pm \infty} \int_z^{\infty} e^{a\sqrt{2i}(\xi-z)} f(\xi) d\xi = 0;$$

Formula (2) may be used for obtaining the turbulence characteristics in the case of any profile of geostrophic wind.

In Ref. 3 a case was considered for the presence of a sharp increase of the horizontal pressure gradient in a narrow altitude interval. The dependence of the horizontal pressure gradient on the altitude in this case may be approximated by the δ function:

$$\frac{1}{\rho l} \frac{\partial p}{\partial y} = b \delta(z), \quad \frac{1}{\rho l} \frac{\partial p}{\partial x} = 0,$$

where b is a constant. Then (2) will become

$$\Phi(z) = \frac{ab}{\sqrt{2i}} e^{-az} (i \sin az - \cos az) \quad \text{for } z \geq 0.$$

According to Ref. 3, the velocity modulus will have the following form:

$$c(z) - u_1 = \sqrt{(u - u_1)^2 + v^2} = \frac{ab}{\sqrt{2}} e^{-az},$$

$$c_0 = [c(z) - u_1]_{z=0} = \frac{ab}{\sqrt{2}},$$

Here u_1 is the wind velocity outside the stream.

If we neglect the dissipation of energy as heat and the diffusion of vortices, from the turbulent energy balance equation

$$\int_{-H}^H k \left[\left(\frac{du}{dz} \right)^2 + \left(\frac{dv}{dz} \right)^2 \right] dz = \int_{-H}^H k \frac{g}{T} \left(\gamma_a + \frac{\partial T}{\partial z} \right) dz, \quad (3)$$

the relationship for the thickness $2H$

$$\frac{\int_{-H}^H k \left[\left(\frac{du}{dz} \right)^2 + \left(\frac{dv}{dz} \right)^2 \right] dz}{\int_{-\infty}^{\infty} k \left[\left(\frac{du}{dz} \right)^2 + \left(\frac{dv}{dz} \right)^2 \right] dz} = 0.75 \quad (4)$$

and equation (2), it is possible to find the turbulence characteristics

$$H = \frac{\ln 4}{2\alpha}, \quad \frac{k}{\omega_z} = \frac{1.08}{\frac{a}{g c_0^2}}$$

where

$$\begin{aligned} \alpha &= \frac{1}{T} \left(\gamma_a + \frac{\partial T}{\partial z} \right), \\ c'^2 &= k a c_0 e^{-\alpha z}, \\ c'_{\max} &= \sqrt{\overline{k \omega_z c_0}} \end{aligned}$$

(c'^2 is the gustiness of the wind).

These characteristics were obtained, as indicated above, assuming constancy of the coefficient of turbulent exchange. This, however, is a greatly idealized problem.

In this article we make an attempt to calculate the turbulent parameters in jetstreams, assuming that the turbulence coefficient is not a constant, but that it varies exponentially with altitude

$$k = k_0 \begin{cases} e^{-\beta z} & \text{for } z \geq 0 \\ e^{\beta z} & \text{for } z \leq 0, \end{cases}$$

Here k_0 is the coefficient of turbulent exchange near the axis of the stream, and β is the parameter which characterizes the rate of change of k in the stream in the vertical direction.

We are considering a narrow stream with a sharp wind velocity maximum on the axis and we approximate the relationship of the horizontal pressure gradient as a function of altitude by the δ function

$$f(z) = b \delta(z).$$

In such a case the equation of motion with a variable k in complex form will become

$$\frac{d}{dz} k(z) \frac{d\Phi}{dz} - 2\omega_z i \Phi(z) = -2i\omega_z b \delta(z). \quad (5)$$

Equation (5) along the whole interval from $-\infty$ to $+\infty$, except for the zero point, is identical to the following equation

$$\frac{d}{dz} k(z) \frac{d\Phi}{dz} - 2\omega_z i \Phi(z) = 0. \quad (6)$$

with boundary conditions

$$\Phi|_{z \rightarrow \pm \infty} \rightarrow 0, \quad (7)$$

$$\Phi|_{z=+0} = \Phi|_{z=-0}. \quad (8)$$

The solution of equation (6) may be written in the following form

$$\Phi_1|_{z>0} = c_1 \sqrt{x} I_1(2\sqrt{mx}) + c_2 \sqrt{x} K_1(2\sqrt{mx}),$$

$$\Phi_2|_{z<0} = c_3 \sqrt{y} I_1(2\sqrt{my}) + c_4 \sqrt{y} K_1(2\sqrt{my}),$$

$$\text{here } x = e^{\beta z}; \quad y = e^{-\beta z}; \quad m = \frac{2a^2 i}{\beta^2};$$

Here $I_1(2\sqrt{mx})$ and $K_1(2\sqrt{mx})$ are Bessel's Functions of the first kind and of the first order (Ref. 1). Constants c_1 and c_3 are determined from

the conditions of equation (7). In order to fulfill these conditions it is necessary that

$$c_1 = c_3 = 0.$$

From the condition of equation (8) we find that $c_2 = c_4$. Then one may write that

$$\begin{aligned} \Phi_1 &= c \sqrt{x} K_1(2\sqrt{mx}) \text{ for } z > 0, \\ \Phi_2 &= c \sqrt{y} K_1(2\sqrt{my}) \text{ for } z < 0 \end{aligned} \quad (9)$$

In order for (9) to be the solution of equation (5), it must satisfy the following condition:

$$k \frac{d\Phi}{dz} \Big|_{z=+0} - k \frac{d\Phi}{dz} \Big|_{z=-0} = 2i\omega_z b.$$

For this it is necessary to assume that

$$c = \frac{ab\sqrt{2i}}{2K_0(2\sqrt{m})}$$

Then, the general solution of equation (5) will acquire the following form

$$\Phi(z) = \frac{ab\sqrt{2ix}K_1(2\sqrt{mx})}{2K_0(2\sqrt{mx})}, \quad (10)$$

where

$$x \begin{cases} e^{\beta z} & \text{for } z \geq 0 \\ e^{-\beta z} & \text{for } z \leq 0. \end{cases}$$

It was indicated above that

$$\Phi(z) = u + iv - u_{1s}.$$

In order to find the values of the wind velocity components we substitute variables

$$2\sqrt{m} = 2\sqrt{\frac{2a^2i}{\beta^2}} = \sigma\sqrt{i}$$

and take into account that according to Ref. 1

$$\begin{aligned} K_0(\sigma\sqrt{x}) &= \ker(\sigma\sqrt{x}) + i\operatorname{kei}(\sigma\sqrt{x}), \\ -\sqrt{i}K_1(\sigma\sqrt{x}) &= \ker'(\sigma\sqrt{x}) + i\operatorname{kei}'(\sigma\sqrt{x}), \end{aligned}$$

where $\ker(\sigma\sqrt{x})$ and $\operatorname{kei}(\sigma\sqrt{x})$ are Tompson's Functions.

Then (10) will become

$$\Phi = -\frac{ab\sqrt{2x}}{2} \frac{\ker'(\sigma\sqrt{x}) + i\operatorname{kei}'(\sigma\sqrt{x})}{\ker\sigma + i\operatorname{kei}\sigma}$$

from which, by separating the real and the imaginary parts, we find

$$\begin{aligned} u - u_1 &= -\frac{ab\sqrt{2x}}{2} \frac{\ker'(\sigma\sqrt{x})\ker\sigma + \operatorname{kei}'(\sigma\sqrt{x})\operatorname{kei}\sigma}{\ker^2\sigma + \operatorname{kei}^2\sigma}, \\ v &= \frac{ab\sqrt{2x}}{2} \frac{\ker'(\sigma\sqrt{x})\operatorname{kei}\sigma - \operatorname{kei}'(\sigma\sqrt{x})\ker\sigma}{\ker^2\sigma + \operatorname{kei}^2\sigma}, \\ c(z) - u_1 &= \frac{ab\sqrt{2x}}{2} \sqrt{\frac{\ker'^2(\sigma\sqrt{x}) + \operatorname{kei}'^2(\sigma\sqrt{x})}{\ker^2\sigma + \operatorname{kei}^2\sigma}}. \end{aligned} \quad (11)$$

In order to determine the turbulent exchange coefficient and the thickness of the turbulent layer we make use of equations (3) and (4).

After a few transformations these equations may be recognized

$$k \frac{dc^2}{dz} \Big|_{-H}^H = -\omega_z v_0 m, \quad (12)$$

$$(1 - e^{-\beta H}) = \frac{0.75 \omega_z v_0 b \beta}{k_0 g \frac{a}{\alpha}}, \quad (13)$$

where v_0 is the wind velocity along the stream axis. Substituting our expression for the wind velocity into equation (12), we finally obtain two equations for k and H :

$$\beta e^{4 \frac{a}{\beta} \left(1 - e^{\frac{\beta H}{2}}\right) - \frac{\beta H}{2}} \left(1 - 4 \frac{a}{\beta} e^{\frac{\beta H}{2}}\right) = -\alpha \sqrt{2} \psi(\sigma), \quad (14)$$

$$1 - e^{-\beta H} = \frac{1.07 a c_0^2 \beta \psi(\sigma)}{g \frac{a}{\alpha} \varphi^2(\sigma)}, \quad (15)$$

where

$$\begin{aligned} \varphi(\sigma) &= \sqrt{\frac{ker'^2 \sigma + kei'^2 \sigma}{ker^2 \sigma + kei^2 \sigma}}, \\ \psi(\sigma) &= \frac{kei' \sigma \cdot ker \sigma - ker' \sigma \cdot kei \sigma}{ker^2 \sigma + kei^2 \sigma}, \\ c_0 &= [c(z) - u_1]_{z=0} = \frac{ab \sqrt{2}}{2} \varphi(\sigma). \end{aligned}$$

In the calculations, the thickness of the turbulent layer for different values of β was found from equation (14) by the method of successive approximations. We limited ourselves to the second approximation.

We conducted certain calculations of the wind velocity from the obtained formula (11), for different values of β , i.e., taking into account the fact that k changes differently in going further away from the axis of the stream.

Since we cannot at the present time determine the value of β , due to insufficient experimental data, we conducted calculations at $\beta = 0$, $1/500$ and $1/1,000$. The whole interval of change in β was encompassed in these calculations.

Figure 1 shows wind velocity profiles for $k_0 = 250 \text{ m}^2/\text{sec}$, and $\beta = 0, 1/500$ and $1/1,000$.

As is apparent from the figure, the wind profiles in the case of variable k differ greatly from the wind profiles for constant k . The

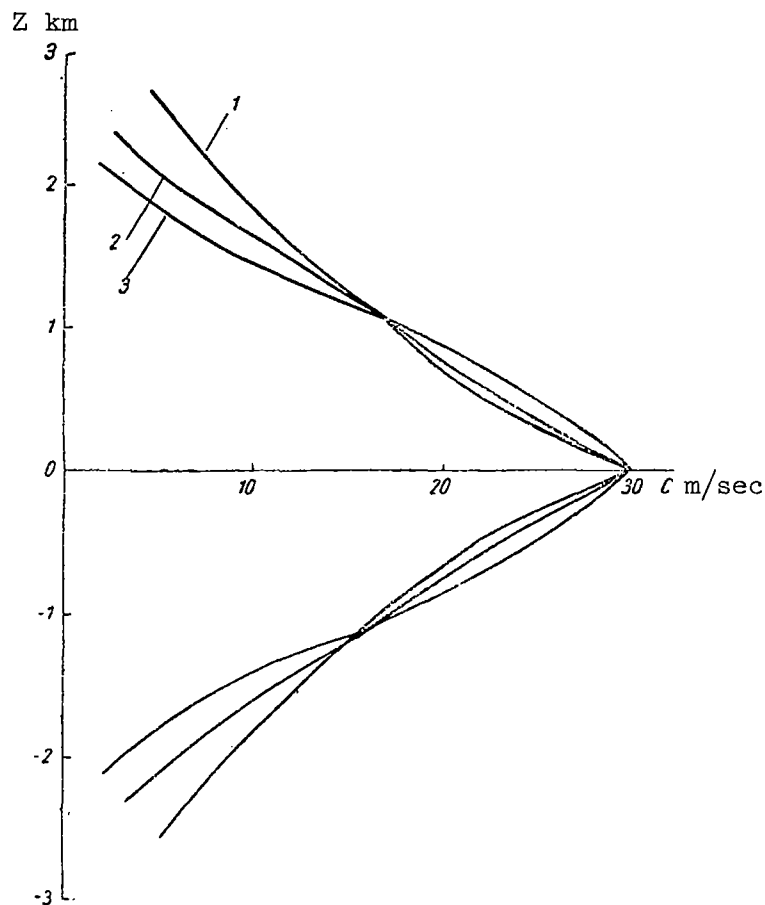


Figure 1. Wind velocity profiles in the jetstream when

$K_0 = 250 \text{ m}^2/\text{sec}$, and different values of β : 1, $\beta = 0$;

2, $\beta = 1/1,000$; and 3, $\beta = 1/500$

difference of values of $2H$ in the case of values of different k is also great. This is supported by the calculations which were conducted. Thus, for example, with a fixed value of $k = 250 \text{ m}^2/\text{sec}$, the magnitude of $2H$ when $\beta = 0$ comprises 2,720 m, and when $\beta = 1/500$, the value of $2H$ is 1,180 m.

In the future work must proceed in the direction of accumulation of the experimental data on the true distribution of turbulent exchange coefficient in streams.

The author expresses his deepest gratitude to Professor D. L. Laykhtman for his guidance in the course of this work.

References

1. Kuznetsov, D. S. Spetsial'nyye funktsii (Special Functions). Moscow, Gosizdat. "Vysshaya Shkola", 1962.
2. Laykhtman, D. L., Shnaydman, V. A. Kriterrii ustanovivsheysya turbulentnosti v struynykh techeniyakh (Stabilized Turbulence Criteria in Jetstreams). Meteorologiya i Gidrologiya, No. 12, 1960.
3. Laykhtman, D. L., Byutner, E. K. K voprosu o turbulentnosti v svobodnoy atmosfere (Free Air Turbulence). Trudy GGO, No. 127, 1962.

SOME RESULTS OF THE DETERMINATION OF TURBULENCE CHARACTERISTICS IN JETSTREAMS

V. D. Litvinova

ABSTRACT

A method for calculating turbulence characteristics in jetstreams from radiosonde data is presented. Data are given for the magnitude of vertical gusts and the turbulence coefficient in the turbulent zones of these streams.

D. L. Laykhtman and V. A. Shnaydman developed a theory for turbulence in a jetstream region (Refs. 2, 3), taking into account the vertical and horizontal temperature gradients outside the axis of this stream, and assuming that the horizontal pressure field is uniform and that turbulence is isotropic.

Turbulence in the jetstream zone results from the large horizontal temperature gradient, which creates a sharp peak in the profile of distribution of the geostrophic wind along the altitude. Because of the turbulence, the profile of geostrophic wind is smoothed; the extent of smoothing of the wind profile indicates the degree of turbulence of the atmosphere.

It follows from this theory that there should exist two turbulent layers with respect to the stream axis, one below the axis and one above the axis. This theoretical conclusion is supported by experimental data.

In Refs. 1 and 2, working formulas were obtained which made possible calculation of the magnitude of the pulsation of wind velocity c' , the thickness of the turbulent layer H , and the turbulence coefficient K .

For a wide stream, generally observed under real atmospheric conditions, these formulas are cumbersome; therefore, calculations are conducted by means of special nomograms, and even then only for that part of the jetstream which is located underneath the stream axis.

The calculations are conducted according to the following method. Using the data of the temperature-wind probing, the vertical wind-velocity profiles and temperature profiles are constructed, and from them one may find the following quantities:

- a) the value of the maximum wind velocity in the stream (c_m);
- b) the value of the wind velocity at the stream boundary (c_1);
- c) the distance in the vertical direction (z_1) from the axis of the stream to the point where the wind velocity equals $c_1 + \frac{c_0}{2}$; $c_0 = c_m - c_1$;
- d) the mean value of the absolute temperature (\bar{T}) in the lower half of the stream, i.e., at the point z_1 ;
- e) the mean vertical temperature gradient ($\bar{\gamma}$) in the lower half of the stream;
- f) an auxiliary quantity S , multiplied by 10^4 , and an auxiliary quantity A (from Tables 1 and 2);
- g) the area under the wind profile curve B_0 .

Table 1. Values of $S \cdot 10^4 = \frac{1}{\bar{T}} (\gamma_a - \gamma) \cdot 10^4$

\bar{T}	$\bar{\gamma}$										
	-0,1	0	+0,1	+0,2	+0,3	+0,4	+0,5	+0,6	+0,7	+0,8	+0,9
210	0,524	0,477	0,429	0,381	0,333	0,286	0,238	0,190	0,143	0,095	0,047
220	0,500	0,455	0,409	0,364	0,318	0,273	0,227	0,182	0,136	0,091	0,045
230	0,478	0,435	0,391	0,348	0,304	0,261	0,217	0,174	0,130	0,087	0,043
240	0,458	0,417	0,375	0,334	0,292	0,250	0,208	0,167	0,125	0,083	0,041
250	0,440	0,400	0,360	0,320	0,280	0,240	0,200	0,160	0,120	0,080	0,040
260	0,423	0,385	0,346	0,308	0,269	0,231	0,192	0,154	0,115	0,077	0,038

Commas represent decimal points throughout these tables.

The best results were obtained for those jetstreams in which the velocity drop c_0 was not less than 25 m/sec, and observations have shown that such cases are not very frequent.

In 1962 Shnaydman made certain modifications in the method of calculating turbulence characteristics, and made some simple and convenient nomograms. As before, one calculates the values of c_0 , z_1 , γ , \bar{T} , and then a new quantity, \tilde{z} , is introduced. This latter quantity is the distance which is equal to the difference in altitudes of maximum wind velocity and the point where the wind velocity is equal to $c_1 + \frac{c_0}{10}$.

As before, knowing the magnitude of \bar{T} and $\bar{\gamma}$, the magnitude of S and A are calculated by means of special tables. Further calculations are conducted using the two nomograms shown in Figure 1. In this figure the ordinate represents the values of A and the sloping curves represent the values of the magnitude of \tilde{z} . Knowing the magnitude of A and \tilde{z} , one finds on the abscissa the values of the thickness of the turbulent

layer H and quantities $\log \frac{K}{\omega_z}$, where K is the value of the turbulence coefficient and ω_z is equal to $\omega \sin \phi$ (here ω is equal to $7.29 \cdot 10^{-1} \text{ sec}^{-1}$, the angular velocity of the earth, and ϕ is the latitude of the location). Following this, the value of the velocity of gust c' is calculated:

$$c' = \sqrt{KVgS}. \quad (1)$$

The layers with superadiabatic vertical temperature gradients are unstable, thus favorable conditions prevail for the development of turbulence. The velocities of the vertical air gusts in such cases are

$$c' = H\sqrt{-gS}. \quad (2)$$

For a "narrow" stream, for which $\tilde{z} < 2$, the velocity of vertical gusts is equal to

$$c' = \sqrt{\frac{4\omega_z c_0^2}{\pi V g \beta}} \quad (3)$$

and the thickness of the turbulent layer is

$$H = 1.3 \frac{c_0}{\sqrt{gS}} \quad (4)$$

A basic advantage of the new method of calculation is that turbulence characteristics may be calculated for practically all jetstreams.

In addition, it is not necessary to calculate the area under the axis of the stream from the wind velocity profile. This operation previously required a considerable amount of time.

It may also be possible to carry out certain simplifications of the calculations of turbulence characteristics, associated with interpolation of quantities S and A , which are very time-consuming. For this purpose, from the experimental data we determined the frequency of occurrence of such quantities as the mean temperature of air (\bar{T}),

Table 2. Values of Quantity A

c_0	$S \cdot 10^4$						
	0,04	0,06	0,08	0,10	0,12	0,14	0,16
16	-6,816	-6,631	-6,504	-6,408	-6,328	-6,262	-6,204
20	-7,000	-6,824	-6,700	-6,602	-6,523	-6,456	-6,398
22	-7,082	-6,906	-6,782	-6,684	-6,606	-6,538	-6,480
24	-7,158	-6,983	-6,858	-6,760	-6,682	-6,614	-6,556
26	-7,227	-7,052	-6,926	-6,829	-6,750	-6,683	-6,625
28	-7,292	-7,116	-6,991	-6,894	-6,815	-6,748	-6,690
30	-7,352	-7,176	-7,051	-6,954	-6,874	-6,808	-6,750
32	-7,408	-7,232	-7,108	-7,011	-6,931	-6,864	-6,806
34	-7,461	-7,285	-7,160	-7,064	-6,984	-6,917	-6,859
36	-7,510	-7,335	-7,209	-7,113	-7,033	-6,966	-6,908
38	-7,557	-7,381	-7,257	-7,160	-7,080	-7,013	-6,955
40	-7,602	-7,426	-7,301	-7,203	-7,125	-7,058	-7,000
45	-7,704	-7,528	-7,403	-7,306	-7,226	-7,160	-7,102
50	-7,796	-7,619	-7,495	-7,398	-7,319	-7,252	-7,194
55	-7,879	-7,703	-7,578	-7,481	-7,402	-7,335	-7,277
60	-7,954	-7,778	-7,653	-7,556	-7,477	-7,410	-7,351
65	-8,024	-7,848	-7,723	-7,625	-7,546	-7,479	-7,421
70	-8,088	-7,912	-7,787	-7,690	-7,611	-7,544	-7,486
75	-8,148	-7,972	-7,847	-7,750	-7,670	-7,604	-7,545

c_0	$S \cdot 10^4$								
	0,18	0,20	0,25	0,30	0,35	0,40	0,45	0,50	0,54
16	-6,152	-6,103	-6,010	-5,937	-5,864	-5,806	-5,756	-5,710	-5,677
20	-6,347	-6,300	-6,204	-6,125	-6,058	-6,000	-5,949	-5,903	-5,870
22	-6,429	-6,384	-6,286	-6,208	-6,140	-6,082	-6,032	-5,986	-5,953
24	-6,505	-6,460	-6,362	-6,284	-6,216	-6,159	-6,108	-6,062	-6,028
26	-6,574	-6,528	-6,432	-6,352	-6,286	-6,227	-6,176	-6,131	-6,097
28	-6,639	-6,593	-6,496	-6,417	-6,350	-6,292	-6,241	-6,195	-6,162
30	-6,699	-6,653	-6,556	-6,477	-6,410	-6,351	-6,300	-6,255	-6,222
32	-6,755	-6,709	-6,612	-6,533	-6,466	-6,408	-6,358	-6,312	-6,278
34	-6,808	-6,762	-6,666	-6,586	-6,520	-6,461	-6,410	-6,364	-6,331
36	-6,857	-6,811	-6,714	-6,635	-6,569	-6,511	-6,460	-6,413	-6,380
38	-6,904	-6,860	-6,762	-6,682	-6,616	-6,557	-6,506	-6,461	-6,427
40	-6,949	-6,903	-6,806	-6,727	-6,660	-6,602	-6,550	-6,506	-6,471
45	-7,051	-7,006	-6,911	-6,829	-6,763	-6,704	-6,653	-6,608	-6,574
50	-7,143	-7,079	-7,000	-6,921	-6,854	-6,796	-6,744	-6,699	-6,664
55	-7,226	-7,180	-7,083	-7,005	-6,937	-6,879	-6,828	-6,782	-6,748
60	-7,301	-7,255	-7,158	-7,079	-7,012	-6,954	-6,903	-6,857	-6,824
65	-7,371	-7,325	-7,228	-7,149	-7,082	-7,023	-6,973	-6,926	-6,893
70	-7,434	-7,389	-7,292	-7,213	-7,146	-7,088	-7,037	-6,991	-6,958
75	-7,495	-7,449	-7,352	-7,272	-7,206	-7,148	-7,097	-7,051	-7,018

the mean vertical temperature gradient ($\bar{\gamma}$), and the velocity gradient (c_0).

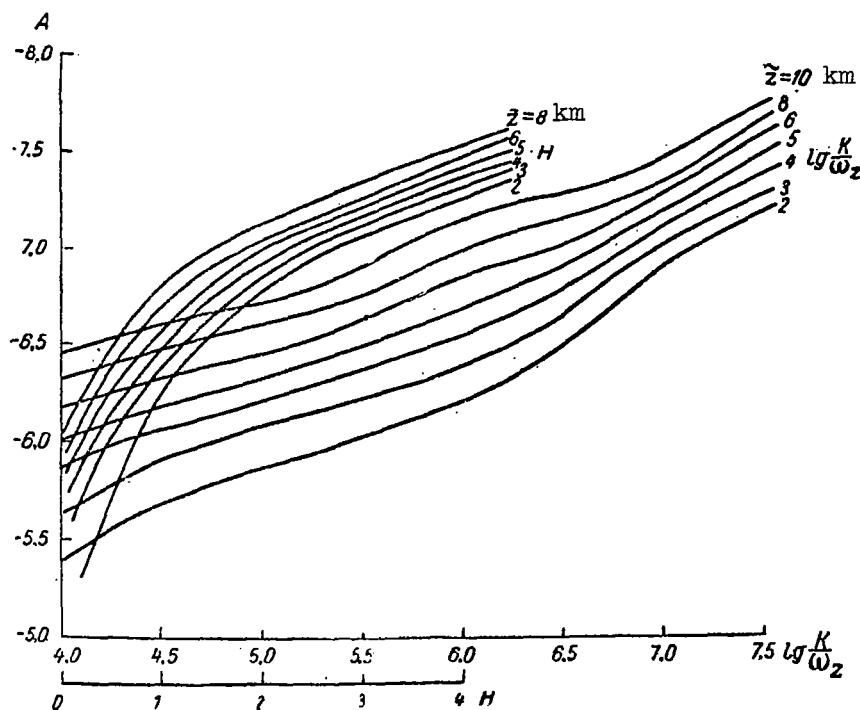


Figure 1. Nomogram for the determination of $\log \frac{K}{\omega_z}$ and H

It was found that the values of \bar{T} lie most often in the 215-245°C range. It was also found that $\bar{\gamma}$ lies within the 0.6-0.8°/100 m range and c_0 lies within the 20-40 m/sec range. This makes possible the

compilation of more detailed auxiliary tables for the indicated \bar{T} , $\bar{\gamma}$ and c_0 limits. This will result in a significant saving of time in cal-

culatation. For this purpose, both of our nomograms for calculation of $\log \frac{K}{\omega_z}$ and of H are represented on the same graph (Figure 1).

In order to calculate the repetition of the velocity gradient (c_0) and the turbulence characteristics (c' , H , K), we made use of the yearly cycle data obtained with a radiosonde equipped with shift-measuring attachments. The data were taken in the city of Dolgoprudnoye. There were 326 launchings in all; in 77 cases jetstreaming was observed. For calculating turbulence characteristics, 72 cases were used (in five cases the wind profile was quite washed out, and it was not possible to make calculations).

It was later found that of these 72 cases there were 12 cases with a velocity drop c_0 of 15-20 m/sec, 24 cases with a drop of 21-30 m/sec, 21 cases with a drop of 31-40 m/sec, 12 cases with a drop of 41-50 m/sec and only 3 cases with a drop of $c_0 > 50$ m/sec.

The observation data in jetstreams were also used for calculating such important turbulence characteristics as the velocity of gusts (pulsation velocity) and turbulence coefficient.

In the calculation of the frequency of occurrence of the wind gust velocities c' , it was found that in 11 cases the values of c' were less than 0-1 m/sec, in 33 cases they were within the 1-2 m/sec range, in 22 cases within the 2-3 m/sec range, and in 6 cases they exceeded 3 m/sec. Consequently, the magnitudes of gust velocities most frequently occur within the 1-3 m/sec range.

We obtained the following values for the turbulence coefficient K : 39 values within the 1-300 m^2/sec range, 16 within the 300-600 m^2/sec range, 15 within the 600-900 m^2/sec range, and 2 values exceeding 900 m^2/sec .

It is apparent that in 54 percent of the cases, the magnitude of the turbulence coefficient is less than 300 m^2/sec . During the analyses of conditions for which the values of K were larger than 300 m^2/sec , it was found that for 23 out of 33 cases with large K , the velocity drop c_0 was from 30 to 50 m/sec.

Thus, the sharper the profile of the jetstream and the greater the velocity gradient from the axis to the periphery, the more turbulent is the stream.

References

1. Ariel', N. Z., Byutner, E. K. Metodika opredeleniya kharakteristik turbulentnosti v struynykh techeniyakh (A Method for Determining Turbulent Characteristics in Jetstreams). Meteorologiya i Gidrologiya, No. 11, 1962.
2. Laykhtman, D. L., Shnaydman, V. A. Kriterii ustanovivsheysya turbulentnosti v struynykh techeniyakh (Stabilized Turbulence Criteria in Jetstreams), Meteorologiya i Gidrologiya, No. 12, 1960.
3. Pinus, N. Z., Shmeter, S. M. Atmosfernaya turbulentnost' vyzyvayushchaya boltanku samoletov (Atmospheric Turbulence Which Causes Airplane Tossing). Moscow, Gidrometeoizdat, 1962.

APPLICATION OF A THERMOANEMOMETER ON AN AIRCRAFT

N. K. Vinnichenko

ABSTRACT

Construction of an aircraft thermoanemometer, which was developed on the basis of a stationary thermoanemometer set-up is described. Methods for introducing corrections, processing oscillograms and determining errors of the apparatus are considered. Some test results are also presented.

Review of the Existing Methods for Measuring the Pulsation of Stream Velocity

It is necessary to investigate the pulsations of wind in order to solve a number of questions which occur in the physics of the atmosphere. The pulsations of wind (and temperature) play a deciding role in the processes of thermal and moisture exchange in the atmosphere, in the formation of clouds, in transformation of the blocking and other "special" layers of the atmosphere, etc. Mesoinhomogeneities in the wind field have an important role in the conditions of aircraft flight.

The fundamental investigations of the pulsation characteristics of the wind field, to the present time, were primarily conducted in the layers near the ground (at the Institute of Physics of the Atmosphere, Academy of Sciences, USSR, Central Geophysical Observatory imeni A. I. Voyeykova). In recent years these investigations also began in the lower troposphere (Institute of Physics of the Atmosphere, Academy of Sciences, USSR; Institute of Applied Geophysics, Academy of Sciences, USSR).

Some time previously the necessity arose for study of turbulence in the upper troposphere, and even in the stratosphere, which is associated primarily with the flying conditions of the various aircraft at these altitudes.

In order to investigate regularities in the upper troposphere and the lower stratosphere, quite successful use was made of various types of aircraft. Almost all measurements conducted with the use of aircraft encounter well-known physical and methodological difficulties.

Therefore, direct measurements of wind pulsation from an aircraft are very rare, and the appropriate apparatus exists only as experimental models. It is true, however, that measurements of the vertical pulsations of the wind velocity from shifts of the aircraft have been conducted for some time, and have achieved a high level of technical sophistication.

However, the measurement of the turbulent wind pulsation from these shifts greatly narrows the spectrum of the investigated gusts, as in this case the probe is the aircraft itself. Therefore, methods for the direct measurement of turbulent gusts from an aircraft have been in development for quite some time.

There exist several well-known methods for measuring the pulsation of the wind velocity component, which in principle are applicable to the aircraft (or, are now in use). These methods include:

1. Determination of the pulsation of wind velocity from the pressure pulsations in the dynamic line of the Pitot tube (Ref. 5); in the most advanced stage of development, this instrument is known as an inclinometer (Ref. 8).
2. The use of an ultrasonic anemometer to measure the change in the velocity of the propagation of sound in the stream as a function of the velocity of the stream (Ref. 2).
3. The use of a high frequency gas discharge anemometer to measure the change in discharge parameters as a function of the velocity of the incident stream (Ref. 7).
4. The use of an ionization anemometer to measure the stream velocity from the time of transfer of the ionic cloud from the radiator to the detector.
5. The Doppler navigation system, which measures the true velocity of the aircraft (with respect to the earth) from the shift of the frequency of the direct and the reflected radar signals from the surface of the earth (Doppler Effect); the difference between the ground and the airspeed of the aircraft gives the true wind (Ref. 6).
6. The use of a thermoanemometer to measure the changes of the conduction of heat from a heated filament as a function of the rate of the oncoming stream (Ref. 4).

Each of the indicated methods is described in specialized literature, and there is no need to discuss them here. However, it is interesting to conduct a comparison of these methods in terms of the most general and the most significant of these characteristics. In the author's opinion, these characteristics are:

1. The number of measured stream components¹ (X, Y, Z);

¹The term "stream" here means the airstream which is incident to the moving aircraft. The X-axis is placed in the direction of the motion of the plane, the Z-axis is vertical and the Y-axis is perpendicular to the XZ plane.

2. The dependence of the output quantity on the stream velocity;
3. The frequency range;
4. The resolving ability in terms of dimensions; and finally
5. Significant limiting conditions.

These characteristics have been compiled in the Table (Figure 1).


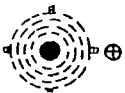
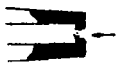
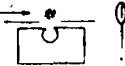


Method		Characteristics of the method				
		1	2	3	4	5
Inclinometer		3 x, y, z	$u = K\sqrt{X}$	0 - 100 c	~ 1 cm	Without limitations
Ultrasonic anemometer		2 y, z	$u = KX$	0 - ~ 10 kc	~ Several cm	Noise, vibrations, large particles
High frequency discharge	10 - 100 mc 	2 x, z	$u = KX^2$	$0 \rightarrow \infty$	~ Several mm	Dampness, electric field, large particles
Ionization anemometer		1 x	$u = KX$	$0 \rightarrow \infty$	~ Several cm	Without limitations
Doppler system		2 x, y	$u = KX$	0 - 0.01 c	~ Several mm	Mountains, water
Thermoanemometer		1 x	$u = \sqrt{A B \sqrt{x}}$	0 - 50 kc at 100 m/sec	~ 1 mm	Large particles, dust

Figure 1. A table for comparison of the characteristics of different methods for measuring the pulsation of wind velocity

We immediately note that the Doppler navigation system differs drastically from all other methods of measurement of stream velocity and its pulsations. In this case, the large scale pulsations of the wind "drag away" the aircraft and thus change its true ground speed. Because of the large momentum of modern heavy aircraft, this method does not permit recording of wind pulsations which are smaller than 1 km.

Great possibilities are offered by the high frequency, gas-discharge anemometer; the probe itself is relatively simple and the frequency range is practically unlimited. The idea for such a probe was expressed recently (Ref. 7), and the terrestrial tests were conducted on a model of such dimensions. The greatest objection to the use of this method on the aircraft is that the unscreened discharge will create strong interferences in radio communication between the aircraft and the earth.

The ionization anemometer also has an excellent frequency characteristic and there is a simple relationship between the output quantity and the stream velocity. The complexity of this method lies in the fact that the ion "packet" on the way from the emitter to the receiver will be greatly washed out. This considerably impairs the recording of the moment of passage of the "packet". Terrestrial tests of such an instrument have thus far given no hope for its successful use on an aircraft.

The ultrasonic anemometer was successfully tested on the IL-14 aircraft by staff members of the Institute of Physics of the Atmosphere, Academy of Sciences, USSR, in 1961-1962. It is difficult now to predict what kinds of problems may occur upon installation of this instrument on high-speed aircraft.

The inclinometric method attracted investigators for a long time by the simplicity of the external probe and the possibility of the use of this instrument under the most severe atmospheric conditions, especially in strong clouds¹. Good quality construction of such an instrument requires high experimental competence as transducers of pressure pulsation must be located close to the measuring equipment (i.e., with short lead tubes). The inclinometer was created in the Laboratory for Cloud Investigation of the Central Aerological Observatory (CAO), and successfully tested in 1962 on the IL-14 aircraft (Ref. 5).

Finally, we shall deal in detail with the possibility of the use of the thermoanemometric method on an aircraft. To the present time, thermoanemometers were used only for measurements in the layers near the ground (Ref. 4). The main difficulties in the use of the thermoanemometer on an aircraft are: first, the not completely established technology of the production of probes (probes could not stand high stream velocity); and, second, unrefined electronic measuring apparatus which do not permit recording of high-frequency pulsations of stream velocity.

In 1961, the Laboratory for Atmospheric Dynamics began the development of the aircraft variation of the thermoanemometric apparatus on the

¹It should be noted that only the inclinometer permits the measurement of all three stream velocity components.

basis of the stationary thermoanemometer made by the company, "Disa Elektronik" (Denmark), designed for measurements in wind tunnels.

The Principles of Thermoanemometric Method of Measurement

The principle of operation of the thermoanemometer is sufficiently well known. Therefore, we shall provide here only the basic relationships which will be used in the future.

The relationship between the velocity of gas and the heat losses of a cylindrical wire, located across the stream, was found by L. V. King (Ref. 3):

$$Q = l(T_w - T_0)(K + \sqrt{2\pi K \rho C_p d U}), \quad (1)$$

where Q is the loss of heat per unit time, l is the length of the wire, T_w is the temperature of the wire, T_0 is the temperature of the medium,

K is the thermal conductivity of the medium, ρ is the density of the medium, C_p is the heat capacity of the medium, d is the diameter of the wire, and U is the velocity of the stream.

This equation was derived assuming that the gas is incompressible and that it proceeds by gravity flow.

If one were to consider that $Q = 0.24 V^2/R_w$, where V is the voltage applied across the wire and R_w is the resistance of the wire at temperature T_w , then equation (1) may be rewritten in the following form

$$V^2 = a + b \sqrt{U}, \quad (2)$$

where a and b are constants at constant T_w , T_0 and ρ .

The dependence which is expressed by equations (1) and (2) is preserved within a broad range of Reynolds Numbers: $0.1 \leq Re \leq 10^5$.

Equation (2) was obtained for static conditions. Under dynamic conditions, i.e., in the presence of the pulsation of the velocity of the stream, the working quality of the thermoanemometer will depend on the time constant of the probe. This time constant with accuracy down to the constant coefficient is equal to

$$\tau = \frac{m C}{K + C \sqrt{U}}, \quad (3)$$

where m is the mass of the wire, C is the specific heat capacity of the wire, U is the velocity of the stream and K is a constant. From expression (3) it may be seen that the time constant of the probe increases with the increase of the heat capacity of the wire and decreases with the increase of the speed of the stream. Consequently, during the measurement of the pulsation of the velocity of the stream at high frequency, it is necessary to incorporate two contradictory requirements--high strength of the wire and very small dimensions (which would insure low heat capacity).

If the thermoanemometer probe is placed on a stand aboard an aircraft, and the probe wire is placed perpendicular to the direction of the flight of the plane, then the thermoanemometer will be measuring the air velocity of the plane (i.e., the speed of the plane with respect to the air), and its pulsation. This is based on the following:

Let us connect a system of coordinates with the center of gravity of a horizontally flying aircraft in such a way that the Z-axis will be directed vertically, the X-axis being the direction of flight and the Y-axis perpendicular to the XZ plane. Let us locate the thermoanemometer in such a way that the direction of its wire coincides with the Y-axis. Then the thermoanemometer will measure (at a given moment) the magnitude of any velocity vector located in the XZ plane (i.e., perpendicular to the wire of the probe). Any vector \vec{U} , lying in the XZ plane, may be separated into U_x and U_z components, the first of which, U_x , is the instantaneous

airspeed of the plane and the second, U_z , corresponds to the vertical wind gust. It is clear that the mean value of U_x is equal to the mean airspeed of the plane $|\vec{V}|$, and the mean value of U_z is, generally speaking, equal to 0.

Let us assume that a gust of wind acts on the aircraft in the X direction, equal to ΔU in amplitude, and of such a magnitude that the plane is virtually unaffected by it. The thermoanemometer will then measure the velocity equal to $(|\vec{V}| + |\Delta\vec{U}|)$. If the plane were subjected to a gust of wind in the Z-direction, also equal to ΔU , then the thermoanemometer would measure the velocity equal to $(\vec{V} + \Delta\vec{U})$, the absolute magnitude of which is equal to

$$\sqrt{|\vec{V}|^2 + |\Delta\vec{U}|^2} - |\vec{V}|$$

The pulsation of the velocity in the first case is equal to $|\Delta\vec{U}|$, and in the second case it is equal to

$$\sqrt{|\vec{V}|^2 + |\Delta\vec{U}|^2} - |\vec{V}|$$

Let us compare these pulsations by finding their ratio:

$$\frac{\sqrt{|\vec{V}|^2 + |\Delta\vec{U}|^2} - |\vec{V}|}{|\Delta\vec{U}|} = \sqrt{\frac{|\vec{V}|^2}{|\Delta\vec{U}|^2} + 1} - \frac{|\vec{V}|}{|\Delta\vec{U}|}. \quad (4)$$

Equation (4) approaches zero as $\frac{|\vec{V}|}{|\Delta\vec{U}|}$ approaches infinity. This indicates

that in the case of a large mean air velocity, the thermoanemometer will measure only the pulsation of air velocity (along the X-axis) and will be almost insensitive to the vertical gusts (along the Z-axis). For example, one may calculate that for a vertical gust with a 5 m/sec amplitude, the thermoanemometer will register a pulsation of only 0.18 m/sec, if the mean flight speed is 65 m/sec (aircraft IL-2).

It should be remembered that pulsations of the airspeed of an aircraft result not only from wind gusts at a given flight altitude, but also from the characteristics of the aircraft itself (for example, an instability in engine performance, the pilot's actions which change the angles of inclination, banking of the aircraft, etc.). However, modern aircraft have a large mass and therefore develop extremely large momenta (of the order of seconds). Therefore, one may consider that during careful flying, the pulsation of the speed of the aircraft due to the above causes will be so insignificant that it is outside the bounds of our interest. For this reason, it is possible to measure the projection of the pulsation of the air velocity upon the direction of flight as the difference between the pulsation of the airspeed and its mean value.

It should be noted that measurement of the projection of pulsation of velocity upon the direction of flight will vary greatly in different directions of flight of the aircraft with respect to the direction of the wind at the given altitude. Consequently, during flight experiments, it is necessary to fix accurately the course of the plane with respect to the mean wind direction. Only then will it be possible to find accurately the projection of the pulsation of the wind velocity that was measured.

Block Diagram of the Instrument

The "Disa" thermoanemometer, used by us as the basic instrument in the development of an airborne type of thermoanemometer, is a stationary instrument which was developed especially for accurate measurements in wind tunnels. It consists of a probe and a measuring section with visual measuring instruments. The instrument operates on 110-220 v, 50 cps, ac.

During the development of the airborne variation of such an instrument, it was necessary to solve three basic problems:

(1) the construction of a stand for mounting the probe on the fuselage of the aircraft that would enable the automatic removal of the probe into a protective shield during takeoff and landing, and when approaching clouds (this protection is necessary as the filament may break in dirty air);

(2) the construction of a power supply which would operate from the airplane circuit (26 v, dc); and,

(3) the development of a recording circuit for the measured parameters.

Automatically removable stand. None of the external instrument probes we used up to this time required the development of a system for automatic removal of the probe inside a shield, and we had no experience in constructing similar systems. It is true, however, that there are many hydraulic and electromechanical systems which are used for different purposes on aircraft. The idea of such systems should be used by us, although as far as the devices themselves are concerned, it is not possible to make use of them because of their bulk and complexity.

Many laboratory and flight experiments were conducted in the development of an automatic stand which would satisfy all of the desired requirements¹.

Figure 2 shows the automatic stand for the thermoanemometer probe.

The advantages of this stand include its relatively small mass (2.6 kg), its high mechanical strength (the stand was designed to be mounted on the TU-104 airplane), and the simplicity and reliability of its internal construction. The stand may be mounted on any aircraft, including those which are hermetically sealed.

Power supply. It has already been mentioned that the stationary thermoanemometer is powered from a commercial line (110-220 v, 50-60 cps). In order to use the instrument on an aircraft it was necessary to develop a power system that would operate from the available circuit (26 v, dc). It is known that the majority of power rectifier circuits of electronic instruments normally operate on 400 cps circuits, if the stabilization system is not of the ferro-resonance type. Consequently, in order to power the measuring section of the thermoanemometer it is possible to use the aircraft converters of the MA or PO type and the appropriate power rating, which convert 26 v, dc into 115 v, 400 cps. Here, however, we met with one difficulty. One of the dc amplifiers on the measuring section of the thermoanemometer uses zero stabilization

¹

The construction of the stand was developed by the engineer K. M. Uskov.

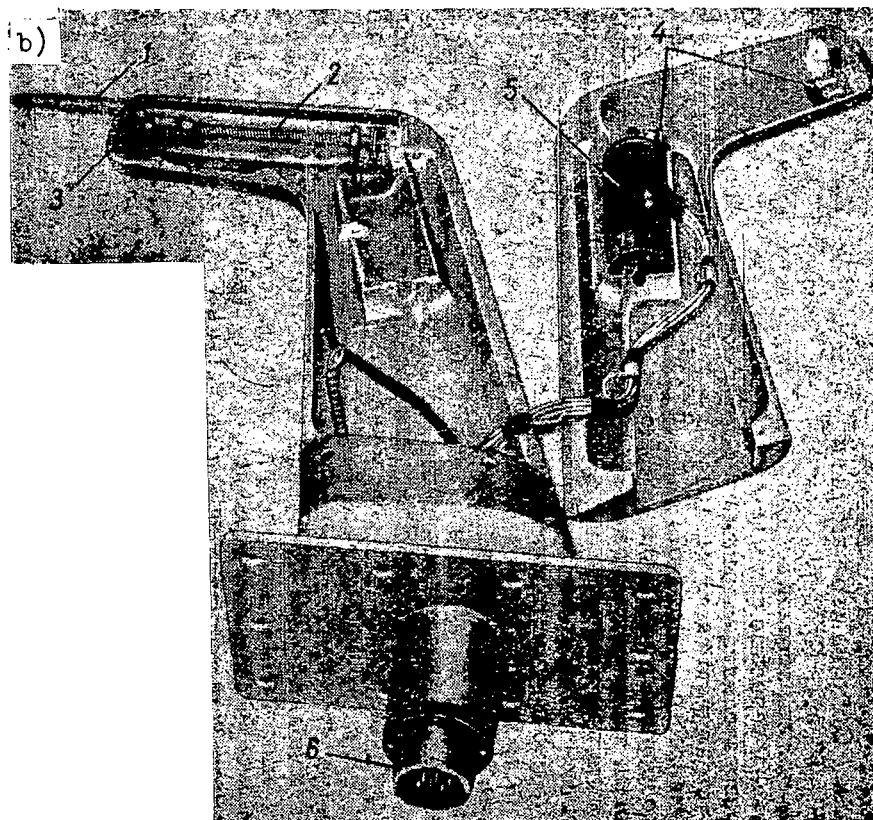
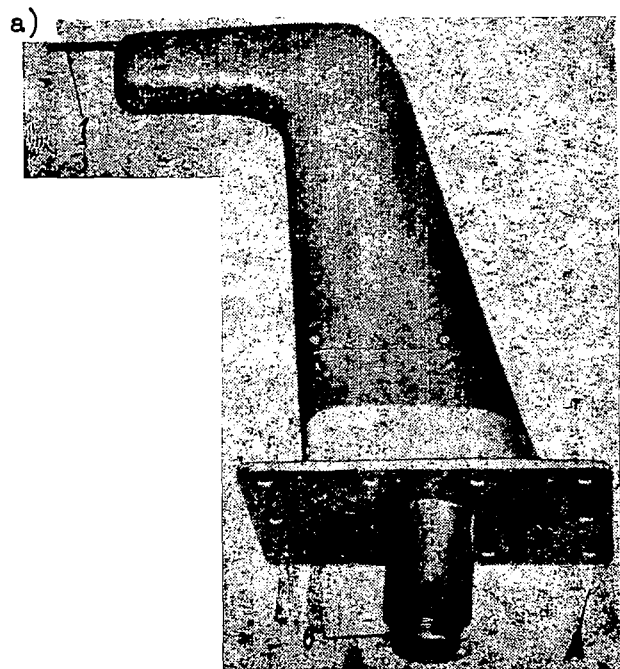


Figure 2. Automatic stand. a), assembled; b) inside view. 1, probe; 2, movable carriage; 3, shield for the opening; 4, end switches; 5, electric motor; 6, hermetic fitting

by means of a vibrating converter. Its winding is fed from the filament circuit (6.3 v, 50-60 cps). It was found that the "points" of the vibrating converter cannot operate at 400 cps. At the same time it is not possible to use the aircraft type, 400 cps vibration-type converters because the vibrating converter of the thermoanemometer has two points. Therefore, it was necessary to construct a separate power supply for the vibrating converter which changed 26 v, dc to 6.3 v, 50-60 cps. Similar solid state circuits, containing high-gain transformers were described in Ref. 1. The converter generates square-wave pulses of 50 cps and 6.3 v amplitude. The frequency and amplitude of the pulses is sufficiently stable and independent of the parameters of the triodes, but is completely determined by the magnetic properties of the transformer. The vibrating converter powered from such a circuit operates normally.

Recording circuit. The output of the measuring section of the thermoanemometer produces a pulsating voltage, the mean value of which (~ 9 v) corresponds to the mean airspeed of the aircraft (~ 65 m/sec) and the pulsations result from the fluctuation of air velocity.

It is apparent that voltage with such a large constant component cannot be fed directly onto a sensitive galvanometer. Consequently, the instrument was modified with a balancing unit which includes two cathode followers (working and balancing), a potentiometer of the balancing unit and a visual null point detector.

The aircraft-type recorder K-12-21 was used for recording the pulsations of air velocity. This recorder contains high sensitivity galvanometer vibrators and high speed photographic paper which enables a good resolution of the recording.

Description of the operation of the instrument. The thermoanemometer, which is used in the described apparatus, is a constant-temperature thermoanemometer as opposed to the more frequently used constant-current thermoanemometers.

In the constant-current thermoanemometer circuit, a constant current is passed through the probe. This current is independent of the flow velocity. Changes of the resistance of the probe, corresponding to the fluctuations of the stream velocity, will cause changes in the voltage drop across the filament in the probe. The most sensitive modern probes have time constants of not less than one millisecond. Therefore, the natural amplitude-frequency characteristic of the probe may be flat only up to frequencies of 100-200 cps. This is certainly insufficient for measuring the spectrum of turbulence. In order to extend the upper frequency limit, use is made of a compensating amplifier with an inverse amplitude-frequency characteristic in respect to the probe. Thus, one obtains a flat response of the instrument up to the

frequencies which are much higher than the natural characteristic of the probe. It is, however, necessary to note that the natural time constant τ is a function of the mean stream velocity (see formula (3)). Therefore, the amplitude-frequency characteristic of the compensating amplifier must change upon the change of the mean stream velocity. This is certainly very inconvenient.

The basic advantage of the constant temperature thermoanemometer is the fact that it is possible to increase significantly the upper frequency limit which may be recorded by the instrument without distortion. The inability of the probe to record the high frequency pulsations is due to its heat capacity. It should be noted that the heat capacity is present directly in formula (3) only because the probe that operates with constant current must change its internal energy (its temperature) in connection with changes of stream velocity. In the constant-temperature thermoanemometer, the resistance of the probe and, consequently, its temperature are maintained constant for all stream velocities. Because this is true the role of the heat capacity of the probe is then significantly lowered. Thus, we obtain an increase of the upper frequency limit of measurement several times over that of circuits with constant current.

Figure 3 shows a block diagram of the aircraft-type thermoanemometer unit in which it is easy to observe the principle of operation of the instrument and the functions of individual sections.

Let the automatic stand with the thermoanemometer probe 1 be in a constant velocity stream, and let the calibrated bridge a of the measuring unit 2 be balanced.

Let us now assume now that the stream velocity changes. The resistance of the probe will immediately change, the bridge a will become unbalanced, and the unbalanced signal will be perceived by the amplifiers b, c and d, which will change the current in the bridge in such a way that the resistance of the probe will again become equal to the controlled resistance in the leg of the bridge. The voltage applied to the bridge will be measured by the visual instrument M_2 , the readings of

which are the measure of the mean stream velocities. At the same time, a signal from the outputs of amplifiers b, c and d is fed to the series of low e and high f frequency filters, which enables one to obtain at the output (jack i) a definite frequency band of the pulsation of the stream. The effective value of the velocity pulsations is recorded by a thermoelement M_1 , with visual display through the ac amplifier g.

The output signal from jack i of the measuring unit 2 proceeds to the auxiliary dc amplifier 5, the output signal of which is fed to the balancing circuit 6. By means of a balancing circuit, the constant

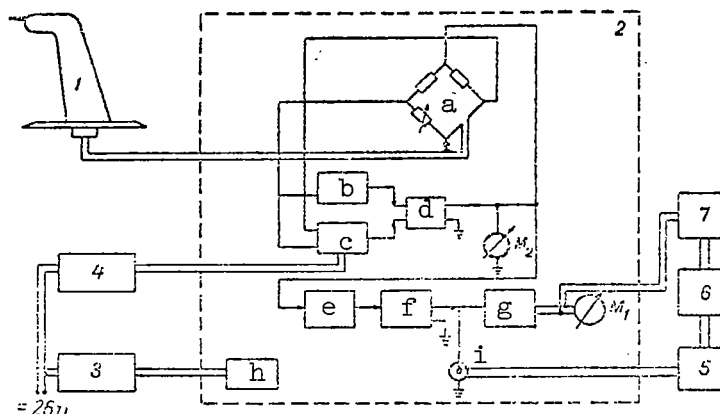


Figure 3. Block diagram of the aircraft-type thermoanemometric unit. 1, automatic stand with probe; 2, measuring unit; a, calibrated bridge; b, dc preamplifier; c, ac preamplifier; d, dc amplifier; e, low frequency filter; f, high frequency filter; g, ac amplifier; h, stabilizing rectifier; i, output jack; 3, transformer MA-250; 4, power supply for vibration converter; 5, dc amplifier; 6, balancing unit; 7, K-12-21 recorder

component of the output signal is compensated out and its pulsations are fed to the sensitive vibrator of the recorder K-12-21. In addition, one of the vibrators of the recorder records the effective value of the pulsations of the stream velocity in parallel with the visual thermo-electric instrument.

It is necessary to discuss in somewhat greater detail the operation of the feedback amplifiers b, c and d. Amplifier b is a dc preamplifier, the zero point of which is stabilized by means of a vibrating converter. Amplifier c is an ac preamplifier and amplifier d is a final dc amplifier. Such circuits insure low dc drift, i.e., the longtime stability of the amplifier significantly exceeds the stability obtained by means of ordinary dc amplifiers. This system of amplifiers is one which primarily determines factor F , which in turn indicates the magnitude of the increase of the upper limit of the measured frequencies as compared with the same limit of the natural frequency of the probe:

$$F = 2SR_w \frac{R_w - R_0}{R_0}, \quad (5)$$

where S is the sensitivity of the system of amplifiers b, c and d (in ma/v), R_w is the resistance of the probe at operating temperature, and

R_0 is the resistance of the probe at the temperature of the medium.

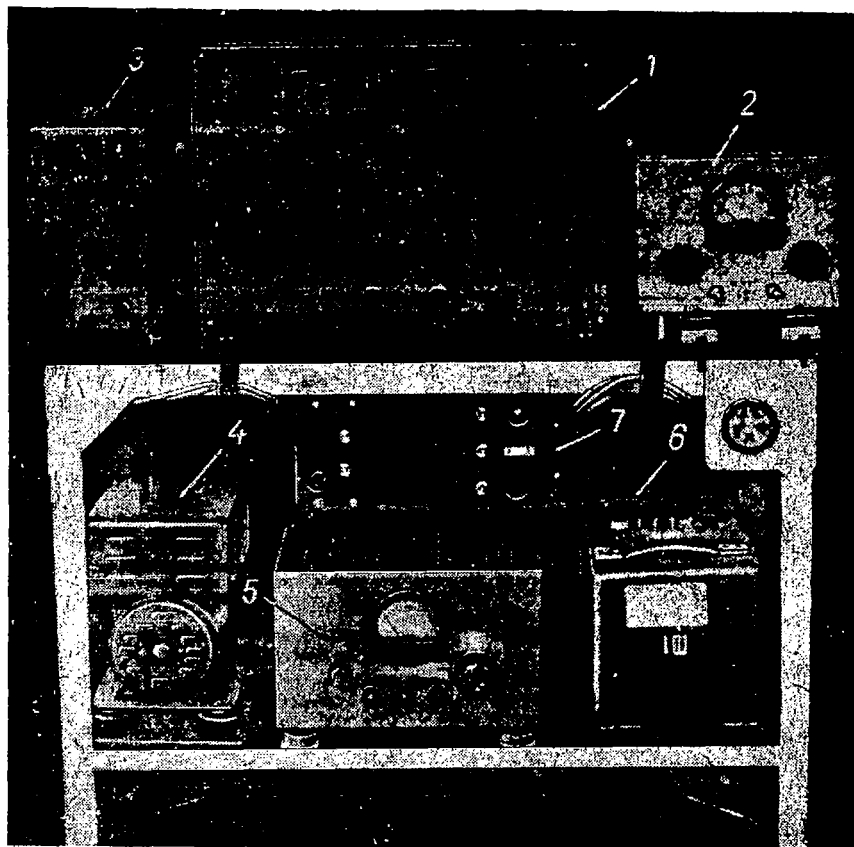


Figure 4. Rack for thermoanemometric unit. 1, measuring block; 2, balancing block; 3, dc amplifier; 4, MA-250 transformer; 5, stabilizing rectifier; 6, K-12-21 recorder; 7, control panel

The block diagram (Figure 3) also shows the stabilized rectifier h of the measuring block 2, which is fed from 3--the airplane transformer MA-250 and the power supply 4 for the vibrating converter of the amplifier b.

Now let us cite the principal technical characteristics of the aircraft-type thermoanemometer unit.

1. The thermoanemometer probe is made of platinized tungsten wire, 5μ in diameter and 1 mm in length.
2. The probe operates at stream velocities up to 150 m/sec at pressure of 1 atm in very clean air.

3. The natural time constant of the probe is 1 m/sec.
4. The upper frequency limit (at 3 db level) is 50 kc at the mean stream velocity of 100 m/sec.
5. The sensitivity is 20 mv per 1 m/sec when the stream velocity is 100 m/sec.
6. The dc drift is $\pm 25 \mu v$.
7. The accuracy of the reading of the effective pulsation values is 2 percent.
8. The maximum recording sensitivity is 8 cm/sec per 1 mm.
9. The upper frequency limit of the recording is 10 cps.
10. The time required to remove the probe automatically into the protective shield is 10 sec.
11. The power consumption is 500 w.
12. The unit weighs 60 kg.

It becomes immediately apparent that we record not even one thousandth of the frequency band which may be encompassed by the instrument. The fact of the matter is that our initial purpose was to check out the operation of the unit as a whole and to improve on certain theoretical calculations of instrumental parameters.

Figure 4 shows the mounting table of the aircraft-type thermoanemometer installation.

Correlation of Measuring Data

Formula (2) relates uniquely the output voltage of the measuring unit with the velocity of the oncoming stream on the probe. The correlation of data would have been very simple (although the relationship was nonlinear), if the parameters in a and b in formula (2) remained constant.

However, the comparison of formulas (1) and (2) indicates that

$$u = R_w l (T_w - T_0) K \quad (6)$$

and

$$b = R_w l (T_w - T_0) K^{3/2} S^{1/2} C_p^{1/2} d^{1/2} (2\pi)^{1/2}. \quad (7)$$

In expressions (6) and (7), the quantities T_w , l , d and R_w are constants for a specific probe at any stream parameters. However, the quantities T_0 , K , S and C_p are variables which are functions of temperature (T_0) and the air pressure. It is clear that during measurements in wind tunnels the changes of the temperature and the pressure are generally so small that the correction to quantities a and b is very slight. During measurement in the layer near the ground, the changes of the pressure and, especially, temperature are much greater than during measurements in wind tunnels. The correlation method and the introduction of corrections to measurements in the layer near the ground have been thoroughly described in the work of S. I. Krechmer (Ref. 4). If the measurements are conducted in an airplane, then the temperature correction and the pressure correction naturally increase so much that these corrections must be very carefully taken into account.

Let us substitute the well-known expressions for K , S and C_p in terms of the temperature and the pressure in formulas (6) and (7). Then, with accuracy which is comparable to the accuracy of the constant, we obtain

$$a = R_w l \frac{(T_w - T_0) T_0^{1/2} (1 + 2 T_0 10^{-4})}{T_0 + 124}, \quad (8)$$

$$b = R_w l d^{1/2} \frac{(T_w - T_0) T_0^{1/4} (1 + 2 T_0 10^{-4}) P^{1/2}}{(T_0 + 124)^{1/2}}. \quad (9)$$

Let us write the expressions (8) and (9) in the form

$$a = A \Phi_1(T_0), \quad (10)$$

$$b = B \Phi_2(T_0, P), \quad (11)$$

where $A = R_w l$, $B = R_w l d^{1/2}$ and represent constants for any particular probe and

$$\Phi_1(T_0) = \frac{(T_w - T_0) T_0^{3/2} (1 + 2 T_0 10^{-4})}{T_0 + 124}, \quad (12)$$

$$\Phi_2(T_0, P) = \frac{(T_w - T_0) T_0^{1/4} (1 + 2 T_0 10^{-4}) P^{1/2}}{(T_0 + 124)^{1/2}} \quad (13)$$

change as a function of temperature (Φ_1 , Φ_2) and pressure (Φ_2), and are independent of the probe parameters.

Apparently for correct correlation of measurement data it is necessary to know the values of constants A and B for each probe, and to construct theoretically the correction functions Φ_1 and Φ_2 . The constants

A and B cannot be determined accurately by calculations, and thus they are found experimentally from the result of multiple tearing of each probe. Calculations of the values of functions Φ_1 and Φ_2 in the 220°-

320°K temperature range and in the 200-800 mm Hg pressure range were conducted according to formulas (12) and (13).

After all of the quantities and functions which enter formula (2) have been determined, we may correlate the obtained recordings with some degree of accuracy. After processing electrometeorograms, knowing the true temperature and pressure at any given altitude, we can find the values of functions Φ_1 and Φ_2 . The readings of instrument M_2 in

the measuring unit (Figure 3) are also known. Accordingly, from formula (2) we can calculate the mean airspeed at the given altitude taking formulas (10) and (11) into account:

$$U_{\text{mean}} = \left(\frac{V^2 - A \Phi_1}{B \Phi_2} \right)^2. \quad (14)$$

Although the relationships of voltage across the filament and the velocity is nonlinear, it is possible to show that in the case of a sufficiently large mean stream velocity, the correlation of the velocity pulsations may be carried out according to linear relationships.

Let us assume that the mean airspeed of the aircraft is 65 m/sec. Then, from formula (2), it is possible to find the slope of the curve:

$$V = f(U) = \sqrt{A \Phi_1 + B \Phi_2} \sqrt{U} \quad (15)$$

at the point $U = 65$ m/sec, and to replace equation (15) by a linear equation

$$V = V_{65 \text{ m/sec}} + V'_{65 \text{ m/sec}} U, \quad \text{where} \quad V'_{65 \text{ m/sec}} = \left[\frac{df(u)}{dU} \right]_{U=65 \text{ m/sec}} \quad (16)$$

Calculations show that when the pulsation amplitude is 5 m/sec, the error which occurs because of the use of formula (16) instead of (15) does not exceed 2.5 percent. It is clear that this error will increase with the amplitude of pulsation, and will decrease with the increase of the mean airspeed. The possibility of using the linear relationship (16) simplifies very significantly the processing of data on the recorded pulsation.

Measurement Errors

Calculation of the errors of measurement of the mean stream velocity and its pulsations is not complex in principle, but it is quite cumbersome. Therefore, we limit ourselves only to the main points on which the calculations were based, and we also present final magnitudes of errors.

Let us start from the systematic error of the instrument. It occurs during the measurement of the mean stream velocity because we do not know accurately the temperature of the heated filament T_w , which enters formulas (10) and (11) for Φ_1 and Φ_2 . By means of the available instruments we cannot measure the temperature coefficient of the filament from its resistance with sufficiently high accuracy. Considering the magnitude of the error in determining the resistance of the calibration break through a (Figure 3), and assuming that the absolute value T_w is $\sim 300^\circ\text{C}$, we obtain the absolute value $\Delta T_w \sim 7^\circ\text{C}$. Then, calculating maximum errors of Φ_1 and Φ_2 , which result from the error in T_w determination, we finally obtain the maximum absolute error in the determination of the mean air velocity to be as high as 10 m/sec (if the absolute value of the mean velocity is 65 m/sec). This is a very large error, but because it is systematic it may be taken into account. This may be done through multiple comparison of the indications of the thermoanemometer with indications of Pitot tube at different altitudes. Such a comparison will make possible the determination of the magnitude of the systematic error and thus, also, the error in the determination of T_w .

In order to evaluate the random errors in the determination of the mean velocity in its pulsation, it is necessary to take into account the following factors which have an effect on the total error of the determination of velocity:

1. the random error in the determination of Φ_1 and Φ_2 due to inaccuracy of the determination of air temperature and pressure by means of electrometeorograph;
2. the random error in reading the voltage from the instrument M_2 of the measuring unit (Figure 3);
3. the random error in the determination of the ordinate of the curve on the recording.

Taking into account all of these errors, we obtain the maximum relative error in the determination of the pulsation of velocity as ~ 12 percent. The obtained error is extremely large even for the statistical analysis of the material. One may see from calculations that almost one-half of this error results from the inaccuracy in reading the bridge voltage from the instrument M_2 . This error may be significantly

decreased by the use of high sensitivity potentiometric recorders. However, the most important factor in lowering the total error is to increase the accuracy of measurement of meteorological parameters by means of the electrometeorograph.

Some Results of Flight Tests of the Instrument

The main purpose of flight tests of the instrument was to verify the operation of the assembly as a whole. It was also necessary to test different variations of the automatic stands for probes, and to determine the systematic error in the determination of the mean air velocity.

Flight tests were conducted in three stages in 1960-1962 on the aircraft IL-2.

In addition to the already described thermoanemometric apparatus, the aircraft was equipped with a Central Aerological Observatory electrometeorograph and instruments for the measurement of the pulsation of temperature and shifts of the plane.

The flight methods were the usual for any pulsation measurements. The measurements were conducted during flights on horizontal levels at altitudes from 50 to 5000 m. The duration of passes comprised 7-10 minutes. In the course of each pass, the pilot carefully maintained his altitude and the number of rpms of the engine, which helped to minimize the effects of instability of the aircraft itself on the accuracy of the measurements.

Two tests of the first stage were conducted in the winter of 1960-1961 in the vicinity of Vnukovo. The third stage was conducted in April-May, 1962 in the Simferopol' region.

The tests show that the aircraft thermoanemometric apparatus is completely operative. During tests, slight modifications were made in the circuitry of the measuring and recording apparatus. The greatest modification was in the construction of automatic stands (as a result of tests the final version of the stand is shown in Figure 2).

It became clear that far from the clouds (even in such low altitudes of 30-50 m) the air is sufficiently clean since the filament did not

break once. However, we noticed that the filament malfunctioned when the aircraft was flying near clouds, although it appeared visually that it was still in clear air. It is natural to assume that cloud particles may be found a significant distance from the visually apparent cloud.

During the tests it was also found that the recording always contained pulsations with a frequency of from 8 cycles and higher, and amplitudes which significantly exceed the amplitudes of all other frequencies. The analysis of the measurement data showed that this was caused by the vibrations of the aircraft structure on which the stand and the probe were rigidly mounted. Apparently, such vibrations of the probe may be eliminated only through the use of extremely complex shock absorbing joints. One may assume, however, that the vibration frequencies of the aircraft structure are within a very narrow frequency band (this, naturally, requires a thorough verification). If this is so, then it will be possible to eliminate this frequency vibration by use of a band filter and still to be able to obtain a sufficiently complete picture of the spectrum of velocity pulsations.

In order to determine the systematic error in the determination of the mean airspeed, markers were made at several altitudes from the velocity of 165 to 235 km/hr. After a detailed study of the electrometeorograms, comparisons of the velocity of the mean airspeed were made--those obtained by means of a Pitot tube and those obtained by means of the thermoanemometer. It was found that the thermoanemometer increases the speed, on the average, by 5 m/sec, and scattering around this value is small. One may say that the values of Φ_1 and Φ_2 were calculated correctly in principle.

It was not the purpose of this article to discuss a small amount of material on the horizontal pulsations of wind velocity obtained during the tests of the apparatus. Rather, it is only possible to say that we observed a relationship between the magnitudes of the pulsation of velocity and the shifts of the aircraft.

Pulsations of the velocity with the amplitude of 3-4 m/sec lead to shifts with amplitudes of $\pm 0.4-0.5$ g.

Conclusions

As a result of tests of an airplane thermoanemometer unit, it was convincingly shown that the airborne thermoanemometer may be used for measuring atmospheric turbulence.

In considering the future for the application of the described method of measuring wind pulsation, it is again necessary to compare it with

already existing methods (in particular with the inclinometer). The thermodynamic method has two serious drawbacks: it is inapplicable in a slightly contaminated atmosphere and in clouds; and, with this method it is possible to measure only one (i.e., horizontal) component of wind velocity. These drawbacks reduce the area of applicability of this method. However, the study of turbulence in a clear sky (incidentally, this is the most dangerous type from the aviation standpoint) is in itself sufficiently important. As far as the second drawback is concerned, the modern theoretical concepts regarding the structure of turbulence enable us, with the knowledge of the characteristics of one of the wind components, to make a judgment regarding the characteristics of the other two. This method also has an important advantage, i.e., the frequency characteristic of the instrument enables recording of extremely small disturbances even on a high speed aircraft. It makes this method applicable for measuring a sufficiently broad turbulence spectrum.

In order to utilize the indicated advantages to the fullest extent, it is even necessary to conduct a spectral study of signals on an aircraft or to change to such a system of recording (possibly magnetic) that would enable one to conduct the operational correlation on the ground.

The development of an automated "recording-processing" system will make possible the application of the described apparatus to sensitive measurements in the turbulent atmosphere.

References

- Zhuravlev, A. A. and Mazel', K. B. *Preobrazovateli postoyannogo napryazheniya na tranzistorakh* (Transistorized Converters of Direct Current). Moscow, Gosenergoizdat, 1960.
- Zubkovskiy, S. L. *Chastotnyye spektry pul'satsiy gorizontal'noy komponenty skorosti vetra v prizemnom sloye vozdukha* (Frequency Spectra of the Pulsations of the Horizontal Wind Velocity Component in the Atmospheric Layer Near the Ground). *Izvestiya AN SSSR*, No. 10, *Seriya Geofiz.*, 1962.
- King, L. V. *Konvektsiya tepla iz nebol'shikh tsilindrov v potoke zhidkosti* (Convection of Heat from Small Cylinders in a Stream of Fluid). London, *Transact. Roy. Phil. Soc., Ser. A*, Vol. 214, 1914.
- Krechmer, S. I. *Metodika izmereniya mikropul'satsiy skorosti vetra i temperatury v atmosfere* (A Method for Measuring Micropulsations in the Wind Velocity and Temperature of the Atmosphere). *Trudy Geofizicheskogo Instituta AN SSSR*, No. 24 (151), 1954.
- Pakhomov, L. A. *Samoletnaya apparatura dlya izmereniya vektora vetra* (Airborne Apparatus for Measuring Wind Velocity Vector). *Trudy TsAO*, No. 41, 1962.

6. Sytina, N. V. Avtonomnyye dopplerovskiye radionavigatsionnyye pribory (Autonomous Doppler Type Radionavigational Instruments). Sovetskoye Radio, 1957.
7. Khazen, A. M. Primeneniye vysokochastotnogo elektricheskogo razryada v aerodinamicheskikh issledovaniyakh (The Use of High Frequency Electrical Discharge in Electrodynamic Investigations). Promyshlennaya Aerodinamika, No. 19, Measurement of Airstreams, Oborongiz, 1960.
8. Bulletin of the American Meteorological Society, Vol. 43, No. 10, pp. 566-568, October, 1962.

Translated for the National Aeronautics and Space Administration by
John F. Holman and Co. Inc.

"The aeronautical and space activities of the United States shall be conducted so as to contribute . . . to the expansion of human knowledge of phenomena in the atmosphere and space. The Administration shall provide for the widest practicable and appropriate dissemination of information concerning its activities and the results thereof."

—NATIONAL AERONAUTICS AND SPACE ACT OF 1958

NASA SCIENTIFIC AND TECHNICAL PUBLICATIONS

TECHNICAL REPORTS: Scientific and technical information considered important, complete, and a lasting contribution to existing knowledge.

TECHNICAL NOTES: Information less broad in scope but nevertheless of importance as a contribution to existing knowledge.

TECHNICAL MEMORANDUMS: Information receiving limited distribution because of preliminary data, security classification, or other reasons.

CONTRACTOR REPORTS: Technical information generated in connection with a NASA contract or grant and released under NASA auspices.

TECHNICAL TRANSLATIONS: Information published in a foreign language considered to merit NASA distribution in English.

SPECIAL PUBLICATIONS: Information derived from or of value to NASA activities. Publications include conference proceedings, monographs, data compilations, handbooks, sourcebooks, and special bibliographies.

TECHNOLOGY UTILIZATION PUBLICATIONS: Information on technology used by NASA that may be of particular interest in commercial and other nonaerospace applications. Publications include Tech Briefs; Technology Utilization Reports and Notes; and Technology Surveys.

Details on the availability of these publications may be obtained from:

SCIENTIFIC AND TECHNICAL INFORMATION DIVISION
NATIONAL AERONAUTICS AND SPACE ADMINISTRATION
Washington, D.C. 20546